INVESTIGATION OF MOLECULAR AND CELLULAR MECHANISMS UNDERPINNING THE NEUROTOXICITY OF HOMOCYSTEINE AND ITS METABOLITES IN MODELS OF NEURODEGENERATION

Lisa Strother

A Thesis Submitted for the Degree of PhD
at the
University of St Andrews

2018

Investigation of molecular and cellular mechanisms underpinning the neurotoxicity of homocysteine and its metabolites in models of neurodegeneration

Lisa Strother

University of
St Andrews

CONTENTS

LIST OF FIGURES

ACKNOWLEDGEMENTS

First and foremost, I would like to thank Dr Gayle Doherty, initially for giving me this opportunity and her never ending support, patience and guidance ever since. She has been such an inspiration and a terrific mentor, I have been incredibly lucky to have a supervisor from whom I have learned so much. She was always there to offer me assistance and knew when I needed a push, her help and guidance has been amazing from beginning to end. I could not have asked for a better supervisor.

I would also like to thank all my colleagues at the university in the psychology and neuroscience department, the school of biology and the school of physics. The guidance and training I received from everyone has been invaluable in the completion of this thesis. A special thank you to Dr Gareth Miles for assistance in my electrophysiological experiments and his guidance as my second supervisor. Additionally, my fellow students for their emotional support and unfailing friendship, they have made this process an enjoyable one even though the challenging times.

My biggest thank you is to my wonderful parents, throughout my life they have never once let me believe that there was anything I was not capable of. They have always supported anything I chose to pursue. Their love, support and encouragement has brought me to this moment and the completion of this process would not have been possible without them. I cannot thank you both enough. You are my inspiration.

My final thank you goes to Mark, my fiancé and best friend. He has been by my side throughout this whole process, he has been there for me during every difficult moment, every time I wanted to give up and he pulled me through. Your endless love, encouragement and belief in me is the reason I have completed this thesis. I am eternally grateful to you for everything and I am incredibly lucky to have such a wonderful person like you by side every day.

I would like to dedicate this thesis to my wonderful Grandma, I know the submission of this thesis would have made her incredibly proud, we both had a deep love of books, and now, I would like to dedicate this one to her.

Funding

This work was supported by the Wellcome Trust ISSF studentship 105621/Z/14/Z; and the 600th anniversary scholarship

Research Data/Digital Outputs access statement

Research data underpinning this thesis are available at [DOI https://universityofstandrews907-my.sharepoint.com/personal/ls205_st-andrews_ac_uk/_layouts/15/onedrive.aspx]

ABSTRACT

Elevated levels of homocysteine (HCy) are a known risk factor in several disease states (1). HCy has several other metabolites, homocysteine thiolactone (HCy-T) and homocysteic acid (HCA). Whilst HCy-mediated neurotoxicity has been extensively studied, the underlying mechanisms of HCy-T and HCA mediated neuronal damage remain largely unknown. This thesis aims to explore the underlying mechanisms, triggered by HCy and metabolites which result in neuronal cell death, and may be appropriate targets for future research on disease-modifying interventions in neurodegenerative disorders. As ageing is the greatest risk factor for neurodegeneration, a novel model of human neuronal ageing was established, permitting investigation of the pathways triggered by HCy in ageing.

Using SH-SY5Y cells, a novel differentiation protocol was established and categorised, once fully differentiated, these cells were shown to be fully functional neurons and could be maintained for a month in culture. Using a range of concentrations of HCy and HCy-T, the concentration cell death occurs at was determined using crystal violet and lactate dehydrogenase assays. Mechanisms of toxicity were determined using pharmacological intervention at the NMDA receptor, nitric oxide scavengers and antioxidants. Using a combination of immunocytochemistry, live cell imaging and ELISA, alterations in markers of cell damage could be examined.

The results showed HCy and HCy-T have distinct mechanisms of toxicity. Whilst both are neurotoxic, HCy directly acts via the NMDA receptor, however HCy-T appears to be less potent. Additionally, HCy-T caused a greater increase in reactive oxygen species generation than HCy, and each metabolite also displayed distinct mitochondrial network abnormalities. Finally, using the long-term culture methods, the chronic effects of HCy, HCy-T and HCA were examined. However, extensive cell death was apparent at low doses in all metabolites

therefore no definitive mechanisms could be determined. This culture method was deemed not appropriate for toxicity experiments.

DECLARATIONS

Candidate's declaration

I, Lisa Strother, do hereby certify that this thesis, submitted for the degree of PhD, which is approximately 36,420 words in length, has been written by me, and that it is the record of work carried out by me, or principally by myself in collaboration with others as acknowledged, and that it has not been submitted in any previous application for any degree.

I was admitted as a research student at the University of St Andrews in September 2013.

I received funding from an organisation or institution and have acknowledged the funder(s) in the full text of my thesis.

Date Signature of candidate

Supervisor's declaration

I hereby certify that the candidate has fulfilled the conditions of the Resolution and Regulations appropriate for the degree of PhD in the University of St Andrews and that the candidate is qualified to submit this thesis in application for that degree.

Date Signature of supervisor

Permission for publication

In submitting this thesis to the University of St Andrews we understand that we are giving permission for it to be made available for use in accordance with the regulations of the University Library for the time being in force, subject to any copyright vested in the work not being affected thereby. We also understand, unless exempt by an award of an embargo as requested below, that the title and the abstract will be published, and that a copy of the work may be made and supplied to any bona fide library or research worker, that this thesis will be electronically accessible for personal or research use and that the library has the right to migrate this thesis into new electronic forms as required to ensure continued access to the thesis.

I, Lisa Strother, confirm that my thesis does not contain any third-party material that requires copyright clearance.

The following is an agreed request by candidate and supervisor regarding the publication of this thesis:

Printed copy

No embargo on print copy.

Electronic copy

No embargo on electronic copy.

Date Signature of candidate

Date Signature of supervisor

Underpinning Research Data or Digital Outputs

Candidate's declaration

I, Lisa Strother, understand that by declaring that I have original research data or digital outputs, I should make every effort in meeting the University's and research funders' requirements on the deposit and sharing of research data or research digital outputs.

Date Signature of candidate

Permission for publication of underpinning research data or digital outputs

We understand that for any original research data or digital outputs which are deposited, we are giving permission for them to be made available for use in accordance with the requirements of the University and research funders, for the time being in force.

We also understand that the title and the description will be published, and that the underpinning research data or digital outputs will be electronically accessible for use in accordance with the license specified at the point of deposit, unless exempt by award of an embargo as requested below.

The following is an agreed request by candidate and supervisor regarding the publication of underpinning research data or digital outputs:

No embargo on underpinning research data or digital outputs.

Date Signature of candidate

Date Signature of supervisor

LIST OF ABBREVIATIONS

ABTS	2,2'-azino-bis (3-ethylbenzothiazoline-6-sulphonic acid)
AD	Alzheimer's disease
ADMA	Asymmetric dimethylarginine
ALS	Amyotrophic lateral sclerosis
AMPA	α-amino-3-hydroxy-5-methyl-4-isoxazolepropionic acid
AP5	D-2-amino-5-phosphonopentanoate
APP	Amyloid precursor protein
ATP	Adenosine Triphosphate
AU	Arbitrary units
Aβ	Amyloid beta
BACE	β-secretase
CBS	cystathione β synthase
COMT	Catechol-O-methyl-transferase
CPTIO	2-4-carboxyphenyl-4,4,5,5-tetramethylimidazoline-1-oxyl-3-oxide
CREB	cAMP response element binding protein
CVD	Cardiovascular disease
Cyc	Cytochrome c
DAF2-DA	4,5-Diaminofluorescein diacetate
DAPI	Diamino-2-phenylindole
DDAH	Dimethylarginine dimethylaminohydrolase

DMEM	Dulbeccos modified eagle medium
DMSO	Dimethyl sulfoxide
DNPH	2,4-Dinitrophenylhydrazine
EAA	Excitatory amino acids
EAAT	Excitatory amino acid transporter
ECACC	European collection of cell cultures
eNOS	Endothelial nitric oxide synthase
ERK	Extracellular signal-regulated kinase-1
ETC	Electron transport chain
FCS	Foetal calf serum
GABA	Gamma amino buteric acid
HCA	Homocysteic acid
HCy	Homocysteine
HCy-T	Homocysteine thiolactone
hHCy	Hyperhomocysteinemia
HNE	4-hydroxynonenol
HRP	Horseradish peroxidase
ICC	Immunocytochemistry
iNOS	Inducible nitric oxide synthase
LDH	Lactate dehydrogenase
LTP	Long term potentiation
MAPK	Mitogen activated protein kinase
MAT	Methionine adenosyltransferase
MCI	Mild cognitive impairment

mGluR	Metabotropic glutamate receptor
MI	Myocardial infarction
MMSE	Mini mental state examination
MnTbap	Manganese (III) tetrakis (4-benzoic acid) porphyrin chloride
mPTP	Mitochondria permeability transition pore
MPTP	1-methyl-4-phenyl-1,2,3,6-tetrahydropyridine
MRI	Magnetic resonance imaging
MTHFR	Methytetrahydrofolate reductase
MTT	3-(4,5-dimethylthiazol-2-yl)-2,5-diphenyltetrazolium bromide
MTTHR	Methytetrahydrofolate reductase
NBF	Neutral buffered formalin
NMDA	N-methyl-d-aspartate
nNOS	Neuronal nitric oxide synthase
NO	Nitric oxide
NOS	Nitric oxide synthase
OCD	Obsessive compulsive disorder
OHDA	6-hydroxydopamine
PARP	Poly ADP ribose polymerase
PBS	Phosphate-buffered saline
PBS-T	Phosphate-buffered saline with 0.1%Tween 20
PD	Parkinson's disease
PI3K	Phosphatidylinositol-4,5-bisphosphate 3-kinase

POMS	Profile of mood states
PON 1	Paroxonase 1
PP2A	Protein phosphatase 2A
PS1	Presenelin 1
PSS	Perceived stress scale
RA	Retinoic acid
ROS	Reactive oxygen species
SAH	S-adenosyl homocysteine
SAM	S-adenosyl methionine
SR2	Serum replacement 2
SSRI	Selective serotonin reuptake inhibitor
SVZ	Subventricular zone
T2DM	Type 2 diabetes mellitus
TBS	Tris buffered saline
TBS-T	Tris buffered saline containing 0.1% Tween 20
TH	Tyrosine hydroxylase
tHCy	Total homocysteine
UK	United Kingdom

CHAPTER 1: INTRODUCTION AND BACKGROUND

1.1 INTRODUCTION

Elevated levels of homocysteine (HCy) are a known risk factor in several disease states; and it has been shown that HCy-reducing therapies may be beneficial to health (1). This thesis aims to explore the underlying mechanisms, triggered by HCy, which result in neuronal cell death. Specifically, this work aims to highlight pathways activated following metabolic conversion of HCy to the metabolite Homocysteine thiolactone (HCy-T), which may be appropriate targets for future research on disease-modifying interventions in neurodegenerative disorders. As ageing is the greatest risk factor for neurodegeneration, a novel model of human neuronal ageing was established, permitting investigation of the pathways triggered by HCy in ageing.

1.1.1 Homocysteine metabolism

HCy is a sulphur-containing non-protein amino acid that is a natural product of methionine metabolism (2). Dietary consumption is considered the principle source of methionine, mainly derived from meat products , eggs and fish (2).

The rate of generation and removal of HCy is controlled by two metabolic pathways; transsulferation and remethylation (figure 1.1). The formation of S-adenosyl methionine (SAM) from methionine and adenosine triphosphate (ATP) is catalysed by methionine adenosyltransferase (MAT) (3). SAM is the body's primary methyl donor and is required for DNA methylation and protein synthesis. However, in the presence of elevated levels of methionine, SAM is converted to S-adenosyl homocysteine (SAH) with the aid of methyltransferase. SAH is then broken down to form HCy and adenosine, adenosine is the hydrolysed to for L-HCy, and as SAH can compete with SAM for binding sites, methylation reactions become impaired (4) (figure 1.1).

To prevent the build-up of damaging levels of HCy, it is converted to either methionine or cysteine. In the remethylation pathway, HCy acquires a methyl group, which can be derived

from one of two sources. Firstly, betaine can be converted to N,N-dimethylglycine releasing a methyl group in a reaction that is vitamin B12 independent (4). Alternatively, in a vitamin B12-dependant pathway, HCy is remethylated by the addition of a methyl group from the conversion of 5-methyltetrahydrofolate to tetrahydrofolate, which occurs as part of the folate cycle (figure 1.1) (2). In the transsulfuration pathway, HCy is condensed with serine, catalysed by cystathione β synthase (CBS) using vitamin B6 as a cofactor, to form cystathione which is then cleaved to α-ketobutyrate and cysteine (5). Cysteine is a precursor of glutathione, the predominant redox buffer, meaning it is important with respect to oxidative stress (4).

Figure 1.1 Homocysteine Metabolism

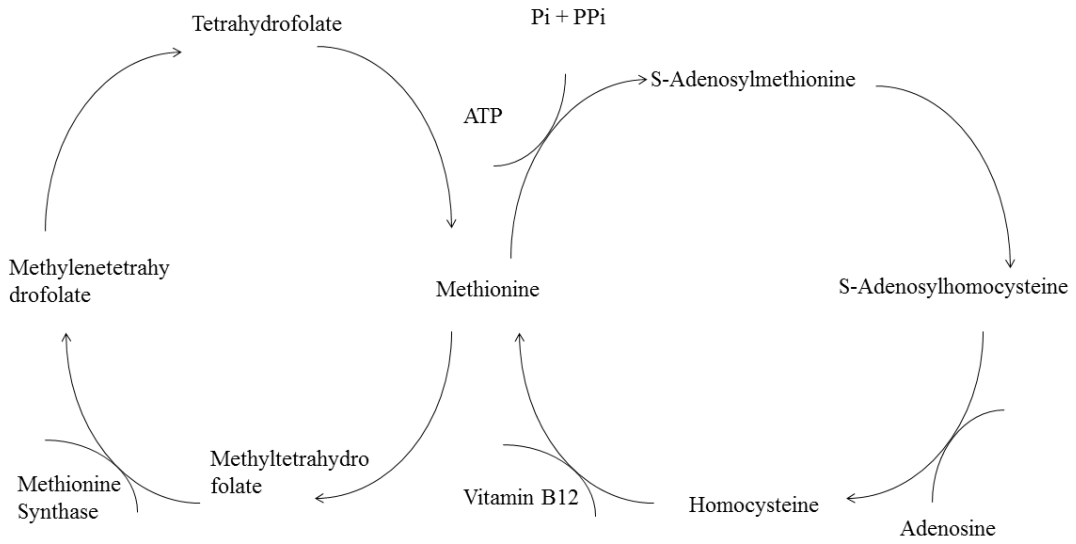

The above diagram illustrates the process by which homocysteine is metabolised and excreted from the body under normal circumstances. Methionine is derived from the diet; this is then catalysed by ATP to form S-adenosylmethionine, which is the predominant methyl donor in the body and is responsible for most cellular repair systems. This can then be converted to s-adenosylhomocysteine which is responsible for incorporating homocysteine into proteins. This is then converted to homocysteine and can be condensed to cysteine in a vitamin B6 dependant manner and excreted in the urine. Alternatively, homocysteine can be converted back to methionine for usage by the means of entering the folate cycle. THF = tetrahydrofolate, SAM = S- adenosylmethionine, SAH = adenosylmethionine, B6 = vitamin B6, B12 = vitamin B12.

1.1.2 Genetic Risk Factors for elevated homocysteine

Physiologically normal levels of HCy range in the blood between 4 and 10µM, with mild elevation considered as 16-30 µM; intermediate elevation as 31-100µM; and severe elevation at over 100µM (6). Hyperhomocysteinemia (hHCy) is defined as the state wherein an individual presents with levels over 16µM in the blood. The state of homocysteinuria (wherein an individual presents with homocysteine in the urine) typically exists when levels exceed 100 µM in the blood, and is most commonly due to homozygous mutation in the 1 carbon metabolism cycle genes such as methytetrahydrofolate reductase (MTHFR) (3,7). Heterozygosity for these mutations can lead to moderate HCy elevation, especially in individuals with a diet that is low in folate and/or vitamin B12 (8). Intermediate elevation of HCy has been linked with methionine adenosyltransferase (MAT) I/III deficiency, which

results in a reduction in the conversion in methionine to SAM (9). In addition, genetic mutations resulting in vitamin B12 or folate deficiency, thus impairing the conversion of HCy, are a genetic cause of hyperhomocysteinemia (10–12).

1.2 NON-GENETIC FACTORS DETERMINING HOMOCYSTEINE ELEVATION

A number of lifestyle factors can contribute to elevated HCy; including dietary vitamin B12 and folate intake (13,14), coffee consumption (15), alcohol consumption and the use of certain medications. These will be discussed in more detail below.

1.2.1 Influence of gender on homocysteine levels

Males have higher levels of HCy than pre-menopausal females, although HCy in post-menopausal females is higher; this is most likely due to hormonal differences between the genders (16). Although there is little research to date, it has been shown that testosterone levels have no effect on HCy (17,18). Therefore, it is more likely that the gender differences observed are due to oestrogen concentrations rather than testosterone. Oestrogen supplementation via hormone replacement therapy is effective in lowering HCy levels in post-menopausal women (19) supporting the hypothesis that HCy levels are hormonally modulated. This is thought to be due to oestrogens ability to enhance CBS, therefore increasing the conversion of HCy to cysteine. In addition, it has been demonstrated that 17β estradiol (levels of which are typically higher in females) directly applied to murine macrophage cells (RAW 264.7 cells) can attenuate the oxidative stress induced by direct application of HCy (20), suggesting that not only is oestrogen capable of lowering HCy levels, it can also attenuate the oxidative stress and damage generated by high levels of HCy (18).

1.2.2 Influence of diabetes on homocysteine levels

HCy concentrations have been found to be higher is those with certain endocrine disorders such as diabetes. The association between HCy and diabetes has been extensively studied, during

pregnancy high HCy has been associated with gestational diabetes which has been observed in many cohorts (21,22). Furthermore, high HCy has been identified as risk factor for the development of Type 2 Diabetes Mellitus (T2DM) in those with prior diagnosis of gestational diabetes (23). This has been suggested to be as result of the increased circulating levels of glucose influencing HCy metabolism and methylation. Although during pregnancy it is recommended that women commence taking folate supplementation it is also this that has been correlated with increased incidence of gestational diabetes, as has reduced vitamin B12 levels (24). Although much of the research has focussed on gestational diabetes the same has been investigated for type 1 and type 2 diabetes, although whether elevated HCy is associated with insulin resistance is debated. With tracking of HbA1c, a measure of how well the diabetes is being controlled, a positive correlation exists between poor long term glycaemic control and elevated HCy (25). However, *in vivo,* HCy has been shown to increase insulin resistance, one proposed mechanism for this is that HCy-T causes in increase in ROS, this in turn inhibits insulin receptor tyrosine kinase activity and therefore decreasing PI3K activity and inhibiting glycogen synthesis (26,27).

1.2.3 Influence of pregnancy on homocysteine levels

HCy levels have been shown to be lower in pregnant women than non-pregnant women (28), giving further credence to the hypothesis that hormonal factors are at play in determining HCy levels. HCy levels have been shown to be significantly decreased in the first trimester of pregnancy in particular (29), although the impact of certain public health measures advising women to make lifestyle changes at this time should be borne in mind.

Guidance from the UK Department of Health encourages women to begin folate supplementation prior to conception and during early pregnancy to prevent neural tube defects (such as spina bifida) (30,31), and given the role of folate in HCy metabolism (figure 1.1), it is perhaps unsurprising that a reduction in HCy levels is observed in this population.

Similarly, other common lifestyle modifications during pregnancy may contribute to lower levels of HCy being observed. For example, guidance to reduce or abstain from alcohol and caffeine consumption (to be discussed in more detail below) as part of the current UK guidance (29) could also play a role. It is worth noting, however, that whilst pregnancy is generally associated with a reduction in HCy levels, elevated HCy during pregnancy has been associated with adverse outcomes such as the development of autism spectrum disorders and neural tube defects (32). Neural tube defects are the most common congenital defect which are caused by failure of neural tube closure *in utero* which can result in a range of outcomes from anencephaly to spina bifida (33). Furthermore, in women with gestational diabetes (34), HCy levels are often elevated (34). This, in turn, has been shown to increase the risk of miscarriage and low birth weight (30). Indeed, even in the absence of underlying metabolic aberrations such as diabetes, elevated levels of HCy have been correlated with low birth weight and slowed foetal growth (23). Finally, the risk of pre-eclampsia has also been positively correlated with elevated HCy and low folate levels (20). Together these data reinforce the detrimental effects of hHCy on pregnancy outcomes.

1.2.4 Influence of ageing on homocysteine levels

HCy levels have been shown to increase with advancing age (36), and the literature outlines several mechanisms by which this is thought to occur. These are further exacerbated in post-menopausal females by hormonal factors, as previously discussed in section 1.2.1.

Vitamin B deficiency is more common with advancing age (36), in part due to the increased incidence of atrophic gastritis, which results in reduced absorption of vitamin B12 from the diet (37). This lower vitamin B12 level contributes to elevation in HCy levels (figure 1.1).

Similarly, a reduction in appetite (commonly associated with increasing age) (28) can result in increased HCy, due to reduced vitamin intake. This is due to various factors such as a reduction

in gastric emptying with age, resulting in earlier satiety, in turn resulting in reduced food intake overall. Age-related impairment of taste and smell are thought to make eating less appealing (28), thus reducing intake. In addition, the increased use of certain medications (such as proton pump inhibitors) can result in a reduction in taste and smell (38).

1.2.5 Influence of caffeine intake on homocysteine levels

Several authors have shown a strong positive association between caffeine consumption and elevated levels of HCy (36). Caffeine is an antagonist of vitamin B6, and can therefore down-regulate the transsulfuration pathway, thereby inhibiting the breakdown and excretion of HCy, thus increasing its levels (39). Caffeine is also an antagonist at adenosine receptors however there is no evidence that this has an effect on HCy levels. Coffee consumption has been shown to significantly increase HCy levels in people with no pre-existing cardiovascular disease from 11.2 ± 5 micromol/L for no consumption and 12.7 ± 4 micromol/L for >500 ml/day consumption (40). Similarly, it has been shown that caffeine consumption in capsule form, or through consumption of caffeinated beverages (such as coffee), can increase HCy levels, with coffee increasing HCy more than the equivalent caffeine concentration from the capsule (41). This is potentially due to other components in coffee which may also increase HCy levels.

However, the precise relationship between caffeine intake and HCy is far from clear, with data from cohort studies highlighting benefits of moderate caffeine consumption in cognitive decline or impairment (34, 35), and in reducing systolic and diastolic blood pressure, as well as potentially reducing the likelihood of developing hyperhomocysteinemia (43) (as defined in section 1.1.2). These have been observed predominantly through studies examining coffee consumption either measured as cups per day or in milligrams. One postulation regarding the effects of the consumption of caffeinated beverages and whether they lead to positive or negative effects on HCy levels is due to their content of phenolic acids (43,44). Phenolic acids, or polyphenols, are known to be the most abundant of the antioxidants that can be obtained

through the diet, and are widely found in caffeinated drinks (43). The exact interplay between polyphenol content of caffeinated drinks and HCy levels is unclear with some investigators reporting no effect and others reporting an increase due to the role of polyphenols as acceptors of methyl groups during the metabolism of methionine to HCy, which can lead to elevation of HCy levels (45–47). Conversely, the antioxidant activity of polyphenols has been linked to a decrease in total homocysteine (tHCy) in AD patients (48). Other potentially confounding factors are also apparent, with many authors examining the effects of caffeine on HCy using different beverages prepared in different ways (44). This could potentially explain the differing conclusions amongst studies, regarding the potential health benefits/risks of caffeine consumption. Ultimately, increased caffeine, in the majority of published studies, is associated with an increase in HCy levels (40,47,49).

1.2.6 Influence of alcohol on homocysteine levels

Many authors have studied the effects of alcohol consumption on HCy levels, and predominantly, strong positive correlations exist between alcohol consumption and HCy levels (50–52). For example, two weeks of consuming 24g of ethanol per day (either as vodka or red wine) was shown in one study to increase total homocysteine (tHCy) levels in healthy male participants by 3% and reduce B vitamin levels by 5%, suggesting a possible mechanism underpinning alcohol-mediated HCy elevation (51). A reduction in folate levels was also seen within the vodka intervention group as 4.81 to 4.36ng/ml and 4.94 to 4.63ng/ml in the red wine intervention group (51).

However, just as with caffeinated beverages, the effects of alcohol on HCy levels have been reported to be either an increase or decrease, depending on the frequency, amount and type of alcohol consumed. It has been demonstrated that when all other lifestyle factors, such as smoking, were controlled, exclusive whisky drinkers had significantly increased tHCy levels by 2µM (53). In the case of tequila, 30 days of daily administration of 30ml before a meal

revealed no acute increase in HCy but levels of HCy were increased after 30 days (51) suggesting a chronic effect. Therefore, it can be suggested that daily alcohol intake over a chronic period causes a decrease in either vitamin B12 and/or folate, or the ability of the body to absorb them, thus increasing HCy levels. Conversely, moderate and regular alcohol consumption (in the form of red or white wine) in obese participants lowered HCy levels, compared to obese subjects who drank no alcohol at all, or drank alcohol very infrequently (54,55). These individuals also had higher folate levels than those who did not drink (56). It has been well documented that there are beneficial effects of beer on HCy levels, thought to be due to many beers containing B vitamins and folate (53). Conversely, wine does not contain folate or any B vitamins essential to the HCy metabolism cycle. However some wines contain betaine which could serve as a methyl donor to convert HCy back to methionine (52).

Taken together this shows that whilst excessive alcohol consumption, and purer forms (such as spirits) can increase HCy, moderate beer and wine consumption may be effective in reducing HCy, as they contain components such as antioxidants which are known to be effective in countering increases in HCy levels. Thus, alcohol consumption *per se* increases HCy levels but specific drinks may have a differential effect depending upon other components of the beverage.

1.3 MALADAPTIVE EFFECTS OF HCy FOR HEALTH

1.3.1 Evidence for a role of homocysteine in cardiovascular disease

Moderately elevated HCy levels are associated with increased risk of developing cardiovascular disease (CVD) (57). Longitudinal experiments have attempted to determine if HCy is a true risk factor for CVD or a marker of disease presence (58). Several trials have shown that HCy-lowering treatments are ineffective at preventing the risk of a myocardial infarction (MI) in patients who have pre-existing hypertension (40). However data obtained

from hospital patients has shown that increases of 10μM HCy from the normal range increased the risk of a MI by 20% (60). In addition, individuals with moderate elevations of HCy are at a higher risk of atherosclerosis (42), a pathological process which commonly leads to CVD, MI and stroke (57). This is thought to be in part due to effects of HCy on the vasodilator, nitric oxide (NO), the mechanisms of which will be discussed in section 1.4.8.

1.4 HCy IN NEURODEGENERATIVE DISORDERS

1.4.1 Homocysteine increases the risk of developing psychiatric disorders

Elevated levels of HCy have been associated with schizophrenia and other affective disorders (44) such as depression (63). Elevated HCy levels correlate positively with objective measures of low mood (a key clinical feature of depression) (64): the Profile of Mood States (POMS) and Perceived Stress Scale (PSS) (46), suggesting an association between elevated HCy and low mood. It was shown that in healthy young adults, vitamin B12 and folate supplementation can have a positive effect on mood as assessed by these measures, as a reduction in scores was noted after administration of a multivitamin and that HCy levels decreased (46). It should be noted however that in this trial a multivitamin was used therefore other compounds could have been responsible for the effect seen.

Nutritional deficiencies are thought to play a role in the development of psychiatric disorders (66–69), as many nutrients obtained from the diet are crucial to the generation of neurotransmitters, deficiencies in which play a role in the neuropathology of a range of disorders, including obsessive compulsive disorder (OCD) and depression (68,69). Common nutritional deficiencies seen in those with psychiatric disorders include omega 3 fatty acids and B vitamins which act as precursors for key neurotransmitters such as dopamine, noradrenaline and serotonin (70,71).

This suggests, it is possible that dietary supplementation to reduce HCy by increasing B vitamin and folate concentrations could be used to elevate low mood and potentially treat psychiatric disorders, such as depression. This could be possible by changing the treatment process from using drugs or drugs alone, such as reuptake inhibitors, which are commonly used to treat a range of disorders (72,73), to instead harness the body's own endogenous neurotransmitter production. Furthermore, this has been shown to be an effective co-treatment for obsessive compulsive disorder (OCD) in mice assed using the marble burying test, although mood was not enhanced when dietary supplementation was given in combination with fluoxetine, a selective serotonin reuptake inhibitor (SSRI) (74).

Whilst it has been shown that elevated HCy has been associated with deficiencies in neurotransmitters including serotonin, noradrenaline and dopamine (69), potentially suggesting a role of elevated HCy itself, some authors dispute this. It has been reported that reversing this effect was achieved by the consumption of a multivitamin containing B vitamins (65). To date, it has not been possible to ascertain to what degree HCy itself or other potentially confounding factors (such as the nutritional deficiencies outlined above) contribute to neurotransmitter deficiency in the pathology of psychiatric disorders.

Many authors discussed the HCy hypothesis which states that HCy is capable of causing cerebral vascular disease and neurotransmitter deficiency, and this in turn causes the low mood associated with elevated HCy (75). Throughout the literature the hypothesis has been commonly reported, and whilst elevated HCy appears to be associated with low mood, the mechanism may not be entirely B vitamin-dependent.

Several studies have also implicated elevated HCy in the pathology of schizophrenia (62,76,77), and the role of elevated HCy in schizophrenia is distinct from other mood disorders discussed above, as HCy is capable of activating the GABAergic and glutamatergic systems,

contributing to the pathology of the disorder (78). HCy is a known partial agonist at the NMDA receptor (to be discussed in more depth in section 1.4.5) and impairment of NMDA receptor signalling is known to be common in schizophrenia (79) and is thought to play a key role in many of the symptoms of schizophrenia (79). This was suggested as a potential mechanism from a nested case-control study of a large birth cohort which showed that elevated maternal HCy levels in the third trimester were associated with a two-fold increase in the risk of the development of schizophrenia for the offspring (78).

Genetic mutations within the MTHFR gene has been implicated in the pathology of schizophrenia. Higher levels of HCY have been found amongst first degree relatives within families with a history of schizophrenia, higher than in families without such a history (80). Furthermore, a positive correlation exists between elevation in HCy levels and the severity of negative symptoms of schizophrenia (negative symptoms include low mood and depression) (81).

1.4.2 Mild cognitive impairment and Alzheimer's disease

Elevated HCy has been identified as an independent risk factor for several neurodegenerative disorders and has also been implicated in the development of mild cognitive impairment (MCI), a precursor to the development of dementia in some individuals (82). For instance, within the elderly African-Caribbean population increasing severity of MCI, as determined by a battery of 11 psychometric tests, was significantly associated with elevated HCy levels as gathered from unfasted venous samples (75). Further to this, a double blind randomised control trial showed that administration of B vitamins, folate or a multivitamin improved the memory of those with MCI, as determined by scores on the Mini Mental State Examination (MMSE), a quantitative measure of cognitive function (83). Indeed a number of small scale studies have suggested that in those with MCI, HCy-lowering therapies were effective in improving memory test performance scores (56).

Cystathione beta synthase (CBS) mutant mice which have high levels of HCy mimicking that of hHCy in humans, develop severe mental retardation and premature death in homozygous mutants and heterozygous show impaired LTP and reduced cognitive abilities. The introduction of a high folate diet reduced the memory impairment by aiding the conversion of HCy back to methionine (85). Additionally, when wild type mice that were fed diets deficient in folate showed reduced performance in both spatial and cognitive tasks (86). Furthermore, it has been shown that the induction of elevated HCy through diet causes a reduction in the firing capacity in slice cultures in electrophysiological experiments as determined by analysing the input-output relationship in the CA1 region of the hippocampus. LTP was induced by a theta tetanus and this showed increased HCy impaired the mechanism of LTP, which is a crucial factor for memory formation (86).

Alzheimer's disease is a progressive neurodegenerative disease and the most common form of dementia which commonly affects those over the age of 65, the life expectancy post diagnosis is on average 7 years, at present there is no disease modifying treatments. The key hallmark pathologies of AD include neurofibrillary tangles and amyloid beta plaques within the brain causing progressive memory impairment (87–89). HCy is a risk factor for AD as concentrations above 14μM double the risk of developing AD and therefore a thorough and comprehensive understanding of the molecular mechanisms of HCy-mediated neurotoxicity offers the potential for novel drug developments for preventing or treating AD. There have been several trials examining the role of HCy-lowering therapies for treating AD and for preventing the development of AD in those with mild cognitive impairment (MCI) (90). A combination of high dose vitamin B12, B6 and folic acid was successful in reducing the rate of brain atrophy by 30% (as measured by serial Magnetic Resonance Imaging (MRI) scans) coupled with a reduction in cognitive decline in those with MCI over a period of 2 years (measured using the MMSE) compared to a placebo group (90). However, other clinical trials using HCy-lowering

therapies were less successful when treatment had been commenced after the diagnosis of AD revealing that therapeutic interventions to modulate HCy levels may be most effective as preventative measure than a treatment (82, 83).

HCy can also exacerbate amyloid β (Aβ) and tau neurofibrillary tangle formation once the disease process has commenced. The toxicity of the soluble form of amyloid β (Aβ) is enhanced in the presence of elevated HCy (92,93), demonstrating a role of HCy in accelerating the pathological processes driving AD. Additionally, HCy impairs the methylation of key promoter regions of the presenilin 1 gene, resulting in its overexpression (67). This leads to an increase in levels of the presenilin 1 enzyme which cleaves the amyloid precursor protein (APP) peptide alongside β-secretase (BACE) as part of the amyloidogenic pathway, which can result in accumulation of toxic Aβ1-42, a key pathology of AD (66). Furthermore, HCy can also downregulate protein phosphatase 2A (PP2A), due to impaired methylation, which results in hyper-phosphorylation of tau leading to the formation of tau tangles (68, 69), another key hallmark pathology of AD (96). Thus, modulation of the key pathways linked to AD pathology may explain why elevated HCy is damaging to patients with symptomatic AD. However, these findings do not explain why HCy is a risk factor for the initiation of the disease, and this would benefit from being the focus of future research.

1.4.3 Parkinson's disease

Parkinson's disease (PD) is a progressive neurological disorder which is characterised by degeneration of the pars compacta region of the substantia nigra (70). The substantia nigra is a region of the brain predominantly comprised of dopaminergic neurons and as such, the commonest treatment for PD is with Levodopa (L- DOPA) therapy, a dopamine precursor to replace the loss of DA (98). This is an effective treatment but can provoke unwanted side effects such as dyskinesia which is characterised by uncontrollable movement (99). Although an effective treatment, L-DOPA increases HCy levels. The main metabolic fate of L-DOPA is

O-methylation leading to the formation of 3-O-methyldopa, in a reaction catalysed by catechol-O-methyl-transferase (COMT) with SAM acting as a methyl donor (100). The donation of a methyl group from SAM leads to the formation of SAH, which in turn is hydrolysed to produce HCy. This leads to high levels of homocysteine in the plasma of L-DOPA-treated patients (100). A positive correlation exists between homocysteine levels and performance on the UPDRS (unified Parkinson's Disease rating scale) revealing that hHCy can increase the rate of disease progression (100). In models of PD, administration of L-DOPA and the subsequent increase in HCy is associated with reduced neurogenesis within the subventricular zone (SVZ) of the adult brain (101) which is mediated via the NMDA receptor then activation of the ERK pathway (to be discussed in more depth in section 1.4.5). Furthermore, in empirical induction of PD symptoms in rodents using 1-methyl-4-phenyl-1,2,3,6-tetrahydropyridine (MPTP) and 6-hydroxydopamine **(**OHDA), dietary-induced hHCy exacerbated the neurotoxicity of both reagents although it was not neurotoxic in its own right (72). Thus, reducing HCy levels in PD patients (particularly those on L-DOPA therapy) may benefit patients by slowing down the progression of the disease and increasing the threshold to neuronal death.

1.4.4 Stroke

Stroke refers to a disturbance in neurological function caused by an interruption to the blood supply to a particular vascular territory within the brain (102). It can be broadly divided into two subtypes: haemorrhagic and ischaemic, accounting for 15% and 85% of strokes respectively (103). Haemorrhagic strokes occur secondary to haemorrhages within the brain parenchyma, and will not be discussed further, as they are not within the remit of this research. Ischaemic stroke occurs when the blood supply to an area of the brain is interrupted due to vascular occlusion of blood vessels (95).

Meta-analyses have shown that several polymorphisms associated with hyperhomocysteinuria significantly increased the risk of developing an ischaemic stroke (104) and also increase the

risk of recurrent stroke (72). Longitudinal data has revealed that levels of HCy in patients who went on to have ischaemic strokes were elevated both before and after the event, revealing that hHCy is a prospective risk factor for ischaemic stroke. It remains unclear whether a correlation between HCy levels and severity of stroke symptoms exists (77, 78). However, it has been demonstrated that patients with higher HCy concentrations had a higher mortality 2 years after their stroke (107). Increased activation of NMDA receptors after an ischaemic stroke in rats contributes to neuronal cell death and results in increased oxidative damage (98, 102) which will be discussed in more detail in section 1.4.7. As the NMDA receptor is also activated by HCy, this suggests that HCy could exacerbate post-stroke damage (108). However, trials using NMDA receptor antagonists have been unsuccessful to date in reducing symptoms post ischaemic stroke, this is postulated to be in part due to a short therapeutic window for intervention. It is thought that these have been unsuccessful to date as ischaemic injury occurs immediately after the stroke occurs, therefore intervention with NMDA receptor antagonists would be effective if administered prior to the stroke. As a result it is unlikely that NMDA receptor antagonists would be likely to effect outcome however may be effective in the treatment of a second event, although ongoing research for variations of current NMDA channel blockers is in progress (82).

In addition to HCy, excitatory amino acids (EAA) have been implicated in the pathogenesis of ischaemic stroke. Elevated levels of glutamate and glycine in particular are shown in ischaemic stroke, and are correlated with the severity of the ischaemic infarct in mice (81). As will be discussed later in section 1.5.3, HCy and glycine are partial agonists of the NMDA receptor, HCy binds at the glycine binding site of the NMDA receptor and during ischaemia, both can enhance NMDA receptor activity and therefore exacerbate the disease process of an ischaemic stroke once it has begun. During the acute phase of an ischaemic stroke, the level of glycine increases rapidly and remains high for a sustained period, with glycine levels continually rising

in ongoing ischaemia (110). Therefore, research is currently underway into the therapeutic potential of NMDA receptor glycine binding site antagonists rather than glutamate binding site antagonists (111). HCy is a partial agonist of the glycine binding site in addition to being an agonist at the glutamate binding site (112). As levels of glycine are elevated during a stroke, an additional increase in HCy during stroke has the potential to exacerbate the stroke severity in terms of neuronal cell death. Thus after an ischaemic stroke, if HCy binds the glutamate site and glycine binds the glycine site this can trigger excitotoxicity at lower levels of HCy (113). Together these findings reveal that the complex interplay of HCy with the NMDA receptor warrants further investigation to fully elucidate the best therapeutic strategies for intervention in stroke patients presenting with confounding hyperhomocysteinemia.

1.5 MECHANISMS OF HOMOCYSTEINE TOXICITY

1.5.1 Overview of toxicity

In addition to being a risk factor for the initial onset of neurodegeneration, elevated levels of HCy may accelerate the rate of degenerative decline (114). There is an established link between elevated HCy levels and reduced cognitive function (115), atrophy of AD-linked brain regions (116) and mild cognitive impairment (MCI) which can progress to dementia within 4-6 years in around 42% of patients (117). There are many proposed mechanisms by which HCy may be neurotoxic, these include: direct activation of NMDA receptors and downstream signalling, calcium mishandling (86), oxidative stress and damage (87), impaired methylation (76) and inflammatory processes (88).

Many of the existing studies in relation to the neurotoxic effects of HCy have limitations. Specifically, the use of supraphysiological doses of HCy to obtain a neurotoxic effect raise questions as to the relevance of the results. For instance 1mM and 5mM were used to induce cell death in cerebellar granule cells and up to 25mM PC12 cells (89,90), with those linked to

homocysteinuria rather than hyperhomocysteinemia used in cerebellar granule neurons (123) and hippocampal and cortical neurons (113,114). Nonetheless, toxic responses to 25μM HCy have been reported in cerebellar purkinje neurons (124) suggesting that physiologically valid models of HCy-linked neurodegeneration can be established.

In vivo rodent models of elevated HCy generally take one of two forms: 1) a genetic model of chronically elevated HCy or 2) induction through diet (93, 94). These may offer a more valid insight into the maladaptive effects of HCy on the brain but also have limitations in the number of techniques that can be applied in a whole organism situation. Whilst the advantage of studying the whole organism as one entity is appealing, genetically modified models of chronically elevated HCy have the disadvantage that there are several resultant defects, such as increased CVD that can reduce the lifespan of the model and make experimentation challenging. Following dietary induction of hyperhomocysteinemia it can be difficult to determine and control the circulating levels of HCy in the model organism as a proportion will be excreted or converted- often unpredictably. In both cases, monitoring of the exact concentration of HCy can be problematic.

1.5.2 Homocysteine thiolactone

HCy thiolactone (HCy-T) is a reactive thioester that is generated as a result of elevated HCy in an error-editing reaction in methanol tRNA synthase (127). Unlike HCy, HCy-T is cyclic in structure. It reacts with amino groups of lysine residues resulting in the addition of peptide bound HCy groups (homocysteinylation) (96) and by increasing oxidative stress (129). A diagnosis of T2DM results in a 65% increase in the risk of developing AD, and HCy-T can inhibit insulin receptor signalling, as discussed in section 1.2.2. HCy-T causes an increase in ROS generation which inhibits phosphorylation of insulin receptor tyrosine kinase, and therefore PI3K and glycogen synthase kinase (GSK3β) thus disturbing insulin signalling. This may be of relevance to the current study as there is a clearly established link between elevated

HCy, Alzheimer's disease and T2DM (130). HCy-T has been shown to induce apoptosis in several cell types; in pancreatic β cells, exposure to HCy-T resulted in signs of early apoptosis after 18 hours (99). Rat H19-7 hippocampal cells exhibit reduced proliferation in a reduced folate environment, with enhanced apoptosis and alterations to vascular transport, cell polarity and synaptic plasticity also seen (132). These are related to homocysteinylation of key neuronal proteins because of reduced homocysteine-thiolactonase (the enzyme that hydrolyses HCy-T to HCy) activity (100). Homocysteinylation of the 42 amino acid form of the Aβ peptide that is linked to AD increases neurotoxicity by stabilising soluble oligomeric forms of the peptide, enhancing its propensity to aggregate (134). However, the finding that the activity of homocysteine thiolactonase is reduced in AD patients (133), implies that homocysteinylation of neural proteins can contribute to alterations of differentiation, vesicular transport, and plasticity in neuronal cells *in vivo* (132). Final evidence for a potential role for HCy-T in AD comes from the observation that mutations in Paroxonase 1 (PON1) lead to enhanced cell and tissue damage by HCy, as this enzyme is crucial for inactivating HCy-T, further linking HCy-T to HCy-mediated cell damage (135). This occurs because PON1 is able to reduce oxidative stress and hydrolyse HCy-T, this ability to neutralise oxidative stress and reduce HCy-T means that the process of homocysteinylation is no longer possible (136).

1.5.3 Homocysteine directly activates the NMDA receptor

The NMDA receptor is the main excitatory system in the nervous system (137). The main physiological agonists of the receptor are glutamate and co-agonists for the receptor are glycine and D-serine (138). Activation of the NMDA receptor is required for optimal neuronal function and plays an important role in learning and memory (139). However, excessive or insufficient activation can activate cell death pathways due to an increase in intracellular calcium and the generation of reactive oxygen species (ROS), this can be in the form of apoptosis or necrosis (140). The receptor itself is comprised of four subunits. Each receptor is a complex of two

GluNR1 subunits and a combination of GluNR2 and GluNR3 subunits (141). The subunit composition is an important determinant of the function of the NMDA receptor and is thought to depend on anatomical location within the brain. For example, the predominant form of the receptor in the hippocampus and cortex contains GluN2A and GluNR2B subunits (142,143).

Direct activation of synaptic NMDA receptors is required for neuroprotection (144), this occurs by the activation of PI3K and Akt to switch off cell death signalling and by the activation of CREB to increase pro-survival signalling (136). However, activation of extrasynaptic receptors can induce cell death pathways as these are activated by lower stimuli, therefore overactivation is more likely (144). Furthermore, extrasynaptic activation causes inhibition of CREB and activation of cell death signalling via FOXO. Another potential explanation for the divergent cell viability response to receptor activation is that the synaptic and extrasynaptic receptors may be comprised of distinct subunit combinations, underpinning their differing physiological function. Synaptic receptors predominantly contain two GluNR1 subunits and two NR2B subunits whereas extrasynaptic predominantly contain predominantly GluN2A subunits (145). The extrasynaptic receptors require a reduced stimulus to mediate a response and can be activated by low tonic levels of NMDA, whereas the synaptic receptors require a greater and more direct activation (146). The composition of NMDA receptor subunits also varies with anatomical localisation. In rodents GluN2A/B containing receptors are predominantly expressed in the forebrain whereas GluNR2C are predominantly expressed in the cerebellum (111).

HCy has been shown to directly activate the metabotropic group subtype of glutamate receptors, included mGlu1 and mGlu5 and AMPA/kainate receptors (69). 24 hours after a 30 minute exposure to 20mM HCy, primary cerebellar granule cells exhibited a 60% reduction in cell viability, and this was ameliorated by the co-application of channel blockers antagonists of mGlu1, mGlu6 (96).

It is believed that HCy toxicity is primarily mediated by the NMDA receptor (148–152), as HCy is an agonist at the glutamate binding site of the NMDA receptor and a partial agonist at the glycine site (112). Calcium imaging and patch clamp recordings have revealed that the ability of HCy to illicit a response at the NMDA receptor was approximately 30% less than that of NMDA itself (112). However, this may have been a result of its competing antagonistic actions at the glycine binding site. In retinal ganglion cells, increasing the concentration of glycine from 1μM to 50μM and co-application of HCy was as effective as NMDA at evoking currents in whole cell patch clamp experiments (149). Furthermore, this depolarisation was sufficient to remove the magnesium block, the resultant increase in neuronal calcium influx matched application of NMDA when HCy was administered in the presence of excess glycine in cortical neurons (112). This reinforced the hypothesis that the antagonist actions of HCy at the glycine co-agonist site were the cause of its apparent reduced potency in comparison to NMDA. In support of this, when NMDA receptor channel blockers were applied, there was no longer a reduction in cell viability in response to HCy (112). Thus HCy-mediated cell death can be blocked with competitive and non-competitive antagonists of the NMDA receptor. Non-competitive NMDA receptor antagonist, Mk801 causes a full block of the receptor in a use dependant manner, this drug only work when the channel is opened through depolarisation. Competitive antagonists D-AP5 complete for the glutamate binding site of the NMDA receptor and memantine which is a low affinity and voltage dependant antagonist (112). Indeed, blockade of the receptor with Mk801 in rat cerebellar granule cells was sufficient to ameliorate cell death induced by HCy and resultant calcium influxes associated with NMDA receptor activation (113), revealing that this receptor is central to HCy-mediated neurotoxicity.

1.5.4 Homocysteine preferentially activates GluN2A subunits: implications for downstream signalling

When HCy binds the NMDA receptor it predominantly does so at the glutamate binding site, but the resultant downstream signalling is distinct from that triggered by glutamate (153). HCy preferentially activates the GluN2A-containing extrasynaptic receptors whereas glutamate excitotoxicity is primarily mediated via the GluN2B subunit (151). HCy has been shown to activate the ERK/MAPK signalling pathway which is an integral component to determining the fate of the cell. The magnitude and duration of the signal determines whether pro-cell survival or cell death signals are initiated, (figure 1.2). Whilst HCy and glutamate activate the same downstream signalling pathways, HCy-mediated phosphorylation of ERK elicits an immediate response which reduces to baseline then increases again reaching a maximal level after 6 hours (151,154). Glutamate, however, only causes an increase in phosphorylation of ERK for 2.5 minutes and this effect is not sustained (151,154). The sustained activation of ERK mediated by HCy renders ERK phosphorylation to trigger cell death rather than cell survival pathways (151).

As a result of phosphorylation of ERK, cAMP response element binding (CREB), a key cell survival transcription factor is activated leading to the promotion of cell survival pathways. In contrast, the sustained ERK phosphorylation in response to HCy elicits only transient CREB activation, as a negative feedback mechanism results in dephosphorylation of CREB, thereby shutting off cell survival signals (155). This effect can be eliminated by that addition of ERK blockers, further reinforcing the hypothesis that HCy-mediated sustained ERK activation is central to HCy-mediated cell death.

Figure 1.2 Signalling pathways activated by NMDA receptor activation via Glutamate or Homocysteine

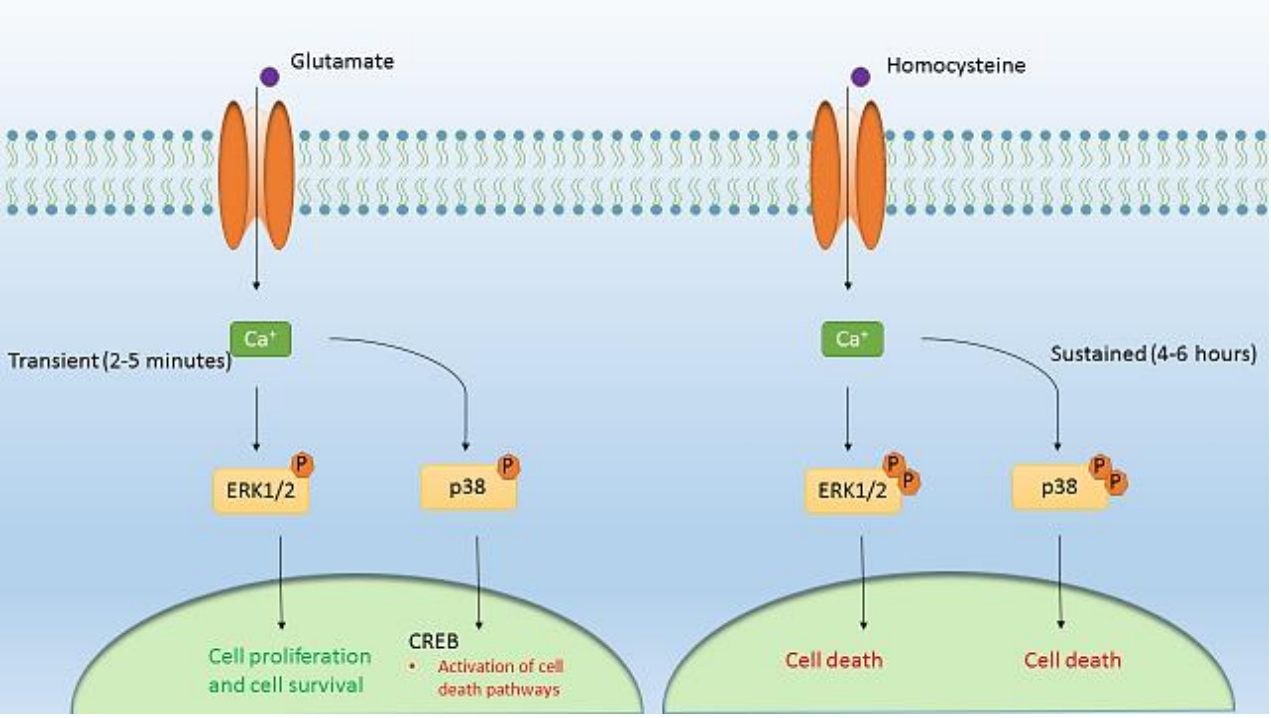

Figure 1.2 shows the downstream signalling that occurs upon activation of the NMDA receptor when glutamate is bound as compared to when HCy is bound. When glutamate binds this causes an increase in calcium influx into the cells, followed by phosphorylation of ERK and p38, within 2 to 5 minutes. However, when HCy binds this phosphorylation occurs within the first 5 minutes and is maintained for a period of 5-6 hours. Ca^{2+} = calcium, CREB = cAMP response element binding, ERK 1/2 = Extracellular Signal-regulated Kinase-1/2.

1.5.5 Homocysteine increases levels of intracellular calcium

Glutamate excitotoxicity causes a rise in intracellular calcium through activation of the NMDA receptor (156). Using fluorescent dyes such as Fluo-3 (which binds to calcium), it has been shown that HCy also causes a dose-dependent increase in intracellular calcium levels (86), which can be enhanced by co-application of glycine (104). It is clear that HCy-mediated calcium increases are dependent on HCy activity at NMDA receptors and metabotropic glutamate receptors, as they can be blocked by either the addition of non-competitive NMDA receptor antagonists (149), or the competitive NMDA receptor antagonist D-2-amino-5-phosphonopentanoate (AP5) (157). Blockade of the metabotropic glutamate receptors prevents

intracellular calcium increase in response to HCy (158) and calcium transients in both neuronal and cardiovascular tissue (157,159). Ultimately, in neurons, increases in intracellular calcium can lead to increases in oxidative damage, which leads to cell death (160). However, blockade of the NMDA receptor does not fully ameliorate the generation of ROS (86). Furthermore, in cerebellar granule neurons, HCy application did not result in an increased uptake of calcium (150). Therefore, it can be concluded that HCy can increase intracellular calcium levels in most neuronal cell types, which can be ablated by the application of antagonists of NMDA receptors, but there are other mechanisms of ROS generation and HCy toxicity that require elucidation by further research.

1.5.6 Nitric oxide in neuronal function

Nitric oxide (NO) is a key neuromodulator and in the periphery acts as a non-adrenergic and non-cholinergic transmitter and has effects such as vasodilation and muscle relaxation (161). Nitric oxide is generated by nitric oxide synthase (NOS) of which there are 3 forms: neuronal NOS (nNOS), endothelial NOS (eNOS) and inducible NOS (iNOS) (162). In the brain NO has many important functions: for example, it plays an important role in long term potentiation (LTP) and therefore is important in synaptic plasticity (163). An increase in NMDA receptor activation leads to an increase in intracellular calcium and a subsequent increase in NOS activity and NO release, which then upregulates cGMP to aid glutamate release (161), leading to further NMDA receptor activation. NOS is commonly found in close proximity to the NMDA receptor in neurons at the post synaptic density (PSD) (134). Depending on the conditions present, NO can either be neuroprotective or neurotoxic. When there is excessive glutamate activation or mitochondrial dysfunction superoxide is generated which reacts with NO to form the potent oxidant peroxynitrite (149). NO is also capable of nitrosylating proteins such as PKC, leading to dysfunction and NO has also been linked to damaging DNA which leads to poly ADP ribose polymerase (PARP) activation (165). Furthermore, NO can bind with

complex 1 and 2 of the mitochondrial electron transport chain, inhibiting it (166), thus NO mediates many potentially damaging cellular pathways.

HCy application results in an increase in NO and scavenging NO in neurons can prevent cell death induced by HCy (149) . There appears to be a significant overlap in the way that NO and HCy induce neuronal cell death, and thus it has also been suggested that inhibition of NO can ameliorate the effects of HCy toxicity (129, 130). HCy inhibits dimethylaminohydrolase (DDAH) thus modulating the activity of asymmetrical dimethyl arginine (ADMA), which is an endogenous inhibitor of eNOS. DDAH degrades and inhibits ADMA to form l-citruline and methylamine (161,167). Thus, when HCy post-translationally inhibits DDAH, this enzyme can no longer block the activity of ADMA and eNOS activity is increased and as such HCy modulates NO, but in an indirect manner. This effect is independent of NMDA receptor activation (12,169). In addition, HCy increases the expression of iNOS and can therefore increase NO release and nitrosylative stress and ROS (170). This has negative effects on the vasculature and blood brain barrier, which is exposed to oxidative damage as a result. iNOS is also widely expressed in neurons, astrocytes and glia (171–173) in addition to the endothelial cells of the blood brain barrier and thus HCy-mediated iNOS activation can directly upregulate nitrosylative stress and ROS expression within the central nervous system.

It is well established that NO can modify tyrosine residues on proteins (nitrotyrosinylation) which can be used as a biomarker of NO activity within cells (136). In cerebral microvascular endothelial cells, HCy signals via mGlu5 to activate iNOS leading to increased bioavailability of intracellular NO and accumulation of nitrosylatively-modified tyrosine residues (3-nitrotyrosine (3-NT))(159). 3-NT elevation is observed in a number of neurodegenerative conditions such as Alzheimer's disease, Parkinson's disease and amyotrophic lateral sclerosis (174–176). In addition a positive correlation has been exhibited between plasma HCy and 3-NT-modified proteins in schizophrenia (177). Thus HCy-mediated NO release can increase the

expression of a biomarker associated with neurodegeneration indicating that this pathway warrants fuller investigation in models of neurodegeneration.

In addition to modification of tyrosine residues, NO can interact with cysteine through a process known as cysteine S-nitrosylation. NO acts directly act on the NMDA receptor via S-nitrosylation (135), to reduce excitotoxicity, with one study isolating a key region (cysteine 399) of the GluN2A subunit which is S-nitrosylated and this causes a reduction in the resultant calcium influx (178). This implies that since HCy preferentially activates the GluN2A subunit, NO could potentially inhibit HCy-mediated toxicity at the NMDAR via reducing the intracellular calcium. This further underlines the complexity of the data relating to the actions of HCy at NMDAR and its effects on NO, and the need, therefore, for further research into these highly interconnected pathways.

Figure 1.3 Activation of nitric oxide and reactive oxygen species upon NMDA receptor activation

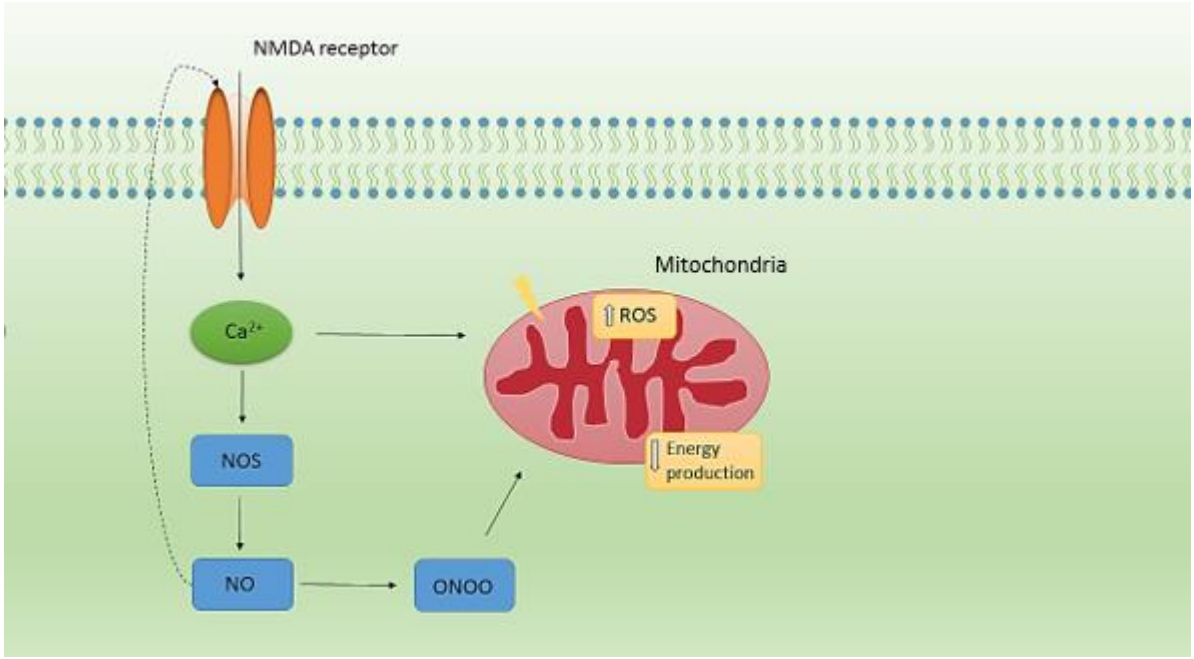

Figure 1.3 shows that the resultant increase in intracellular calcium upon activation of the NMDA receptor causes activation of NOS (nNOS, iNOS and eNOS), which in turn causes an increase in NO and therefore an increase in peroxynitrite (ONOO). This directly inactivates several complexes of the mitochondrial respiration chain and further increases the generation of ROS, which causes further damage to the cell. In addition to activation of the NO pathway, calcium itself causes an increase in the generation of ROS as the mitochondria can act to buffer excess calcium influx into the cell. NOS = nitric oxide synthase, nNOS = neuronal nitric oxide synthase, iNOS = inducible nitric oxide synthase, eNOS = endothelial nitric oxide synthase, ONOO = peroxynitrite, ROS = reactive oxygen species. Ca^{2+} = calcium.

1.5.7 The role of mitochondria in energy balance

Mitochondria are the intracellular organelles responsible for the generation, processing and supply of energy. They are highly active in cells which have high energy demands, such as neurons (179), and are structurally comprised of an inner and outer membrane with intramembrane space and matrix. In the matrix lies the mitochondrial DNA (mtDNA), which has the capacity to generate proteins required for the maintenance of the mitochondrial machinery (180). The inner membrane contains all of the required components for the electron transport chain (ETC) with 5 main components, complexes I-V, which utilise H^+ ions to generate ATP (181). During ATP generation, H_2O is also generated as well as highly reactive free radicals, which generate hydrogen peroxide. This can be converted back to water by glutathione peroxidase and catalase (181). However, this system has the capacity to generate hydroxyl radicals which can cause oxidative damage to DNA, RNA and proteins and cause lipid peroxidation as discussed in further detail in section 1.4.11. Furthermore, this means that the mtDNA is also susceptible to damage by hydroxyl radicals due to its proximity to the site of radical generation which forms the basis of one of main theories of cellular ageing. Further research has implicated mitochondrial dysfunction in several neurodegenerative diseases, particularly Parkinson's disease (PD) (182) and Alzheimer's disease (177).

For optimal cellular energy requirements to be met, there must be an adequate number of mitochondria, and this is achieved by two processes: mitochondrial fission and mitochondrial fusion. The mitochondrial outer membrane fuses with that of another mitochondria in the

process of fusion which is required for mitochondrial repair (183). Alternatively, the mitochondria can undergo fission: the process of splitting one mitochondria into two mitochondria to allow the generation of more cellular energy (183). These processes are usually in a constant balance with one another and are tightly controlled by an array of fission and fusion proteins (183).

1.5.8 Homocysteine, oxidative stress and mitochondrial dysfunction

Intracellular calcium levels are tightly regulated as excessive calcium influx can lead to subsequent damage to the mitochondria, and the mitochondria can act as a buffer when calcium levels are high (137). However, once the buffering capacity has reached maximal levels there is resultant increase in ROS generation, oxidative stress and finally cell death (185). When extrasynaptic NMDA receptors are activated by chronic glutamate elevation, high levels of calcium influx into the cell and mitochondrial dysfunction is observed (186). Excessive calcium has been found in conjunction with mitophagy and mitochondrial loss which has been reported in Parkinson's disease models extensively (187). When the mitochondria are no longer able to buffer excess calcium, it effluxes out of the cell bypassing the conventional pathways for the excretion of calcium, in a process known as the mitochondria permeability transition pore (mPTP) (188). Under conditions of cellular stress, activation of the NMDA receptor can cause opening of the mPTP and causes a reduction in ATP generation due to disruption of the electron transport chain (189). Even though HCy also signals via the NMDAR, there is little evidence to date regarding the actions of HCy on the mitochondria.

Studies using retinal ganglion cells from cystathionine β synthase (CBS) deficient mice have suggested that HCy may alter mitochondrial fusion and fission proteins thereby affecting the mitochondrial network (190). This study showed that HCy increases the levels of mitochondrial fission protein Fis1 (190). Similarly, mitochondrial fission genes are upregulated in a yeast model of HCy imbalance (177). Thus, HCy may increase mitochondrial number

through upregulation of mitochondrial fission. Similarly, it has been reported that activation of the NMDA receptor can result in an increase in mitochondrial fission, which is NO-mediated through S-nitrosylation and thus activation, of the pro-fission protein DRP1. In circumstances where there is a reduction in mitochondrial fusion protein OPA1 in response to oxidative stress, there is a downstream upregulation of NMDA receptors (191). Together these data show that a vicious cycle exists whereby oxidative stress leads to dysregulation of mitochondrial dynamics. This can lead to upregulation of the NMDA receptor which in turn could exacerbate oxidative stress via increased intracellular calcium.

Figure 1.4 Mechanisms of mitochondrial fusion and fission

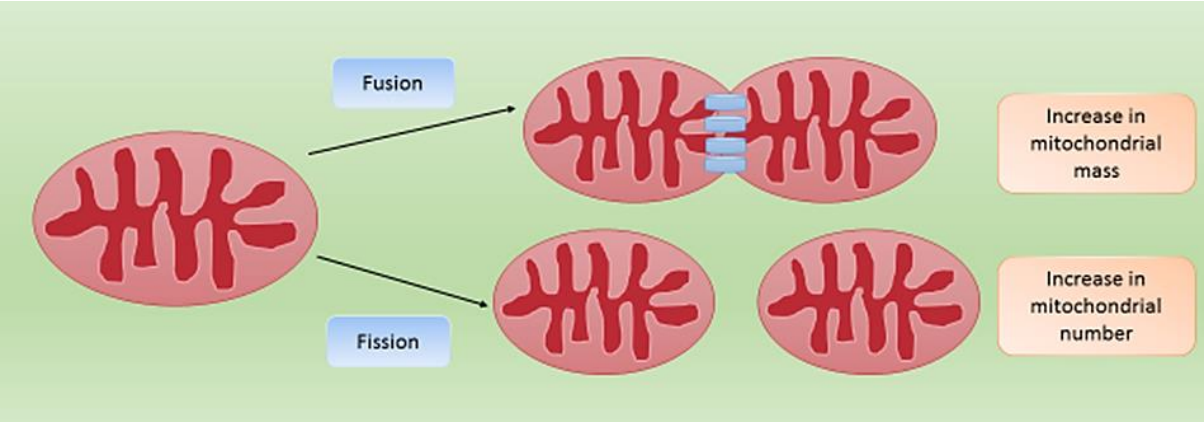

Figure 1.4 shows the mitochondria are highly dynamic organelles and upon changes in cellular stress and requirements the mitochondria can adapt to the surrounding environment. If a mitochondrion becomes damaged, the process of mitochondrial fusion may be activated and therefore an undamaged mitochondrion may share its components to repair and support, this creates a network of mitochondria with increased mitochondrial mass. If the energy demands of the cell increase it is also possible for fission to occur and thereby create more mitochondria to support the energy demands of the cell.

As HCy has a very pronounced effect on the NMDA receptor, it can be postulated that HCy would at the least affect the mitochondria indirectly due to cellular influx of calcium. The mitochondrial membrane potential in rat cortical neurons has been shown to be impaired in response to HCy exposure (185). In cardiac cells, a more in depth analysis of the effects of hHCy was achieved by looking at the enzymatic activity of each of the complexes of the mitochondrial respiration chain, showing that hHCy caused the activities of complexes III and

IV to be reduced (192). This study showed that cardiac cell contractility was reduced, coupled to enhanced lipid peroxidation in response to alterations in the activity of these complexes of the respiration chain (182)

Oxidative stress occurs in cells when the balance between generation of reactive oxygen species overthrows the cellular capacity to combat ROS (180). Oxidative stress has been reported to be present in AD up to 10 years prior to the onset of symptoms (193). The brain has high requirements for oxygen and therefore generates high levels of ROS as a by-product of normal metabolism (193). HCy is an oxidising agent in its own right but the exact nature of how HCy contributes to oxidative stress remains to be determined (77).

Several studies have examined the role of ROS, RNS and oxidative damage in response to elevated HCy, and it is known that HCy can cause oxidative damage to mitochondrial DNA (194) and impair mitochondrial function (119). In astrocytes, the mitochondrial membrane potential is impaired in response to HCy exposure (195). Furthermore, HCy can induce oxidative stress when it is condensed to form cysteine; a precursor of glutathione, which in the reduced form, is one of the main antioxidants and is also used as a measure of antioxidant capacity in the cell (77). HCy can also cause uracil misincorporations into DNA and can cause lipid peroxidation (114). Together these findings suggest that HCy-mediated oxidative damage may be a major contributing factor to the pathology of neurodegenerative disease.

The aims of this thesis are to establish to what extent HCy metabolite, HCy-T contributes to neuronal cell death and how the mechanisms of this compare to HCy. The areas of particular interest are the effects on the NMDA receptor, this has been well characterised for HCy so whether this is the same for HCy-t is important to determine. Then what role oxidative stress and mitochondrial dysfunction plays in cell death induced by these metabolites. Finally, to

establish a culture system which can support long term application of HCy and metabolites to determine the effects of subclinical concentrations of these in culture.

CHAPTER 2: MATERIALS AND METHODS

2.1.1 MATERIALS

Unless otherwise stated all chemicals were obtained from Sigma Aldrich, UK and laboratory consumables were obtained from VWR, UK.

2.2.1 Culture of SH-SY5Y Neuroblastoma Cells

The SH-SY5Y human neuroblastoma cell line was obtained from European Collection of Cell Cultures (ECACC). These cells were originally derived from the SK-N-SH cell line which was sub-cloned three times to SH-SY, SH-SY5 and finally to the SH-SY5Y line. The cells were obtained from ECACC on dry ice, and upon collection, the cells were warmed to 37ºC in a water bath and mixed with 25ml of pre-warmed 10% FCS medium (Dulbecco's modified eagle medium (DMEM) containing 10% v/v foetal calf serum (FCS, Fisher Scientific, UK), 4.5g/l D-glucose, 0.584 g/l L-glutamine and 3.7 g/l sodium bicarbonate). Cells were seeded in a T75 tissue culture flask and placed into a 5% CO_2 incubator until confluent. Once confluent, the cells were detached from the base of the flask by trypsinisation using 0.001% w/v trypsin (Worthington's, USA) in calcium and magnesium free phosphate buffer solution (PBS) and replaced in the incubator until cells had rounded and lifted from the flask surface. The cells were then resuspended in pre-warmed 10% FCS medium.

2.2.2 Cryopreservation of stocks for future use

Following trypsinisation, a 10µl aliquot of the cell suspension was mixed with 10µl of trypan blue dye to assess the viability of the cells prior to cryopreservation and to determine cell number. Cells were counted using a haemocytometer to obtain a 1,000,000 cells/ml suspension for cryopreservation. If more than 5% of the cells stained blue, indicating a reduction in cell viability, they were discarded. The number of cells in four corner squares of the haemocytometer containing 16 squares was counted and the average was taken per square. This dilution with trypan blue solution was accounted for by doubling the number of cells counted per square, and haemocytometer volume and the number of cells per ml was calculated and

appropriate dilutions were made. The media containing the cells for cryopreservation were transferred to a falcon tube (5ml for T25 flasks and 10ml for T75 flasks) and placed in Boeco u-32r centrifuge and centrifuged at 2500RCF for ten minutes at 37°C. All supernatant was removed, and the cells were then suspended in a mixture of 90% FCS and 10% dimethyl sulfoxide (DMSO) and frozen at -80°C until required. To reanimate following cryopreservation, cells were warmed in a water bath for 1 minute and suspended in 20ml pre-warmed 10% FCS medium and transferred to a T75 flask. All medium was removed from the flask and replaced 48 hours later to prevent cell damage from residual DMSO presence.

2.2.3 Plating cells for experimentation

The cells were grown at 37°C in a humidified atmosphere of 5% CO_2 and 95% air and allowed to grow to 70-80% confluence before trypsinising from the culture flask and plating in appropriate sized plates or dishes. The cells were left for at least 48 hours to settle prior to treatment. To differentiate to a neuronal phenotype, cells were incubated with 1% FCS medium (DMEM supplemented with 1% v/v foetal calf serum, 4.5g/l D-glucose, 0.584 g/l L-glutamine and 3.7 g/l sodium bicarbonate) containing 10µM retinoic acid (RA) for 5 days with medium renewal every 48 hours. This medium was removed, and the cells were maintained in defined SR-2 medium (DMEM containing 18µM 5-fluorodeoxyuridine (5-FDU), 2% v/v serum replacement-2 (SR2) 4.5g/l D-glucose, 0.584 g/l L-glutamine and 3.7 g/l sodium bicarbonate) for at least one week before treatment. The addition of the mitotic inhibitor 5-FDU ensures that minimal undifferentiated cells remained in culture by eliminating cells that remain within the cell cycle. The media was then replenished every 48 hours.

Table 1: Plating densities of the SH-SY5Y neuroblastoma cells utilised in this study

Dish/Plate	Density	Coverslip size
35mm	$1.5X10^5$	22mmX22mm
60mm	$5\ X10^5$	22mmX22mm
24 well plate	$5X10^4$	13mmX13mm
96 well plate	$1\ X10^4$	NA

2.2.4 Measures of cell viability – Lactate Dehydrogenase Assay

Cell membrane integrity was assessed using a lactate dehydrogenase (LDH) assay which measured the release of intracellular LDH from cells whose membrane permeability had been compromised (196). At the end of the experiment, an aliquot of the medium for each experimental condition was removed and centrifuged at 13,000 rpm to remove cell debris or any floating undifferentiated cells. 50µl of the aliquoted media was then added to a 96 well plate. LDH mixture (iodonitrotetrazolium chloride 26% w/w, phenozine methosulphate 6.7% w/w, and β-nicotinamide adenine dinucleotide hydrate 67% w/w) was added to a buffer containing 0.2M tris(hydroxymethyl)aminomethane (tris) and 0.5% v/v lactic acid. 0.1% v/v triton X-100 was added to the final solution and once thoroughly dissolved, this mixture was added at an equal volume to the media. The reaction was allowed to progress until a red colour developed and the absorbance was read at 490nm on BioHit BP plate reader. A blank value from media alone which had not been in contact with the cells was obtained. This blank reading was subtracted from the readings obtained for the experimental conditions.

2.2.5 3-(4,5-dimethylthiazol-2-yl)-2,5-diphenyltetrazolium bromide (MTT) assay

(3-(4,5-dimethylthiazol-2-yl)-2,5-diphenyltetrazolium bromide) (MTT) is a yellow tetrazole which forms purple formazan crystals in the presence of actively respiring cells (197), and is

commonly used as an assessment of cell viability. The assay measures mitochondrial activity and readings vary according to respiration rate or the activity of NADPH enzymes, which are a key component of the conversion. This was considered when interpreting the results of the study.

100ng/ml MTT solution in PBS was added to cells at a 1:1 v/v ratio to give a final concentration of 50ng/ml. The cells were then returned to the incubator for 1-4 hours with frequent checks, and the reaction was terminated when the formation of the formazan crystals was visible under brightfield microscopy. All medium was removed, and the cells and crystals were solubilised in 50µl of DMSO (for wells of 96 well plates) or 500µl (for 24 well plates). Once the crystals had fully dissolved the plate was then read on the BioHit BP plate reader at 570nm. A selection of wells containing only media, and no cells, were measured to determine the background (blank)reactivity of the reaction components with the culture media as above and this value was subsequently subtracted from the sample values for analysis.

2.2.6 Crystal violet assay

Post treatment, the cells were fixed in neutral buffered formalin solution (NBF; 0.4% w/v disodium hydrogen phosphate, 0.65% w/v sodium dihydrogen phosphate, 37-40 v/v% formaldehyde solution and deionised water) for 15 minutes. This solution was removed, and the cells were washed 3 times for 5 minutes in PBS. The PBS was removed and 100µl of solution containing 5% v/v from a stock crystal violet acetate solution (0.1% v/v), 5% v/v of 100% ethanol and 90% v/v deionised water was added to each well including a row of wells which had not contained any cells to serve as a blank. This solution was left for 30 minutes to allow for the dye to penetrate the cells and gain sufficient staining, then washed for a minimum of 5 times in PBS and until no purple dye remained visible in the PBS solution. The PBS was then removed and 100µl DMSO added to 96 well plates and 500µl added to 24 well plates to dissolve the cells and release the purple dye. The absorbance of the resultant solution was read

at 570nm on BioHit BP plate reader. The blank value was subtracted from each treatment group and all data normalised to control to estimate of cell number.

2.2.7 Determination of cell number by DAPI labelling

Diamino-2-phenylindole (DAPI) is a cell permeable dye used for fluorescent staining of DNA and cell nuclei. DAPI fluoresces blue upon binding to the minor groove of double stranded DNA. These factors make DAPI an ideal cell dye for cell counting and counterstaining. Cells were grown on coverslips (as is detailed in table 1) and after experimentation were fixed in NBF for 15 minutes. The cells were then washed three times in PBS for 5 minutes each wash. 500ng/ml DAPI in PBS was added for 15 minutes. The cells were then mounted in mounting medium (1% w/v N-propyl gallate, 80%v/v glycerol and 19% v/v PBS). Images were obtained on a Zeiss AxioImager MR2 microscope using either 40X or 63X magnification ex/em360⁄460. 5-10 images per condition per coverslip were obtained. To prevent observer bias, the images were split into folders and renamed by an impartial party. The number of cells in each field of view were counted and data inputted into a spreadsheet. The folders were then converted back by the impartial party to reveal the conditions.

2.2.8 Immunocytochemistry

Cells were treated for the appropriate time then fixed with NBF and washed three times in PBS. Nonspecific binding of the secondary antibody was then blocked by the addition of a 10% v/v heat inactivated horse serum in PBS for 30 minutes. This was then removed, and the cells were washed twice in PBS and once in PBS containing 0.1% v/v tween 20 to permeabilise where appropriate. The cells were then incubated in a solution containing the primary antibody diluted in PBS (see table 2 for dilutions). This was incubated overnight at 4°C. The next day the primary antibody was washed off with PBS, three times for five minutes and a fluorescently tagged secondary antibody was added at a 1:200 dilution in PBS containing 0.1% v/v tween 20. The fluorescent tag was either FITC or Texas red depending upon the research application,

and this was incubated for 2 hours in the dark at room temperature. The secondary antibody was selected based on the species in which the primary antibody was grown, for example if a mouse monoclonal antibody was used as the primary then an appropriate secondary was required as the secondary to bind the primary. This was then washed off three times in PBS for five minutes and where appropriate, counterstained with DAPI for 15 minutes. The cells were then mounted using a mountant containing 1% propyl gallate w/v, 80% glycerol v/v and 19% PBS v/v. This was then sealed onto a glass microscope slide using nail polish and the nail polish allowed to dry prior to imaging. Images were obtained using the Zeiss AxioImager MR2, on either 40X or 63X magnification with 5-10 images per condition per coverslip obtained. Where appropriate, the fluorescence intensity was taken from the image using the Zeiss software, Zen 2 blue edition, and the relative fluorescence intensity was calculated as per cell. This was achieved by taking the sum intensity from the image obtained directly from the Zeiss software, the images were then coded as described above and the number of cells staining positive for DAPI were counted. If the cells were on the edge of the image, then they were only counted if more than 50% of the cell was visible in the image. The sum intensity was then divided by the number of cells counted. The mean intensity per cell was then divided by the mean intensity per cell in the untreated group and multiplied by 100 to give a change in percentage for each treatment group.

Table 2

Antibody	**Concentration**
Mouse α βIII tubulin (genscript)	1:1000
Mouse α Tyrosine hydroxylase (sigma)	1:500
Mouse α 4-hydroxynonenol (abcam)	1:500
Rabbit α Synapsin I (sigma)	1:1000

2.2.9 MitoTracker Red Staining

MitoTracker is a cell permeable rhodamine-based dye which stains mitochondria red in live samples. The ability of the MitoTracker to enter the mitochondria is dependent on the mitochondrial membrane potential and is a useful tool for examining the effects of treatments on the mitochondrial network (198). The method described for examining the network structure of the mitochondria is based on 4 criteria (198). The mitochondria were characterised (using the criteria of Wappler) (198) as:

- Normal: i.e. well dispersed and defined throughout the cells

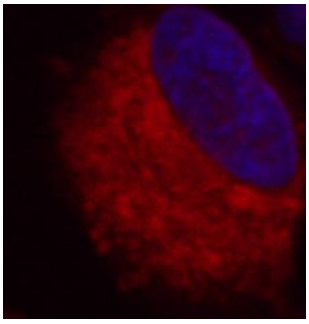

- Rounded: where the mitochondria cluster together and give the appearance of clustering or swelling

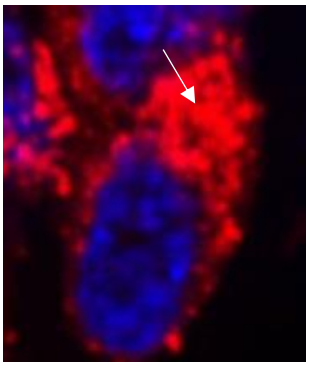

- Highly interconnected: where they form string-like networks.

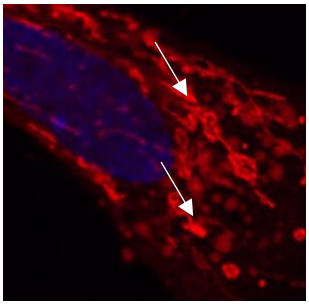

- Lacking in mitochondrial staining: in this case there is either a loss of mitochondria or as this dyes ability to stain mitochondria is dependent on the mitochondrial membrane potential, there has been an alteration in the mitochondrial membrane potential.

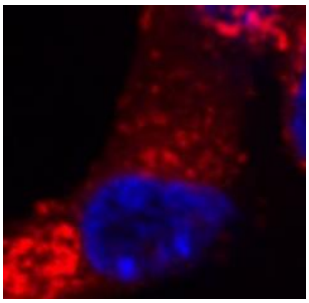

Cells for MitoTracker red staining were grown in 24 well plates containing 13mm diameter boroscillate glass coverslips. At the end of the culture period cell medium was removed and replaced with pre-warmed DMEM containing 100nM of MitoTracker dye and the cells returned to the incubator for 45 minutes. The cells were then washed twice in pre-warmed medium and then fixed in NBF for 15 minutes and washed 3 times for 5 minutes in PBS. It should be noted that MitoTracker staining persists after fixation. The cells were then counterstained with DAPI as described above and mounted using mounting medium or CitiFlour mountant (VWR). The coverslips were then sealed with nail polish and imaged using the Zeiss AxioImager abs/em 581/644 nm 63X magnification with 5-10 images taken per coverslip and a minimum of three separate cultures for each condition. The morphology of the mitochondrial network was then characterised according to the criteria of Wappler as outlined.

The images were then collated and grouped by treatment; the number of cells containing each morphology per field of view was then noted. This was presented as a proportion of the total number of cells per field of view. This was then averaged by each coverslip imaged then by the number of individual coverslips per batch of cells giving the final number of experiments. The data was then presented for each treated batch of cells as a comparison and proportion of untreated or control cells.

2.2.10 DAF2-DA staining

DAF2-DA is a live cell dye that fluoresces green when bound to nitric oxide (NO). After entering the cell, the DAF2-DA is transformed to DAF2 by cellular esterases. This is a widely used method for measuring NO generation in cells (199).

Cells were incubated for 15 mins with 1µM DAF2-DA and then fixed in NBF and mounted post treatment as described above (section 2.2.8). It should be noted that DAF-2DA staining persists following formaldehyde fixation. 5-10 images per coverslip per condition were taken from a minimum of 3 cultures established on separate occasions. Images were taken using the same exposure time so that alterations in fluorescent intensity could be detected. The images were taken at 63X objective on the Zeiss AxioImager at abs/ em 495nm/515nm microscope. The images were then collated and grouped by treatment. The sum intensity of each image was taken directly from Zeiss software; the number of cells from each image was then counted. The total intensity per field of view was then divided by the number of cells to give the average intensity per cell. The data for this was then collated by treatment and by experiment. The images from cells which had received no treatment were presented as the untreated control and all treatments were normalised to untreated control.

2.2.11 Mitochondrial Membrane Potential

Alterations in the mitochondrial membrane potential can be indicative of cellular wellbeing. It has been widely reported that loss of mitochondrial membrane potential is altered in several disease states (200,201). Mitochondrial membrane potential was determined using the dye JC1. This dye is a cationic carbocyanine dye which can accumulate in the mitochondria. At low concentrations the dye exists as a monomer and therefore emits green fluorescence, and under these circumstances the mitochondria are depolarised. At high concentrations the dye exists as an aggregate and will emit a red fluorescence, under these conditions the mitochondria are considered to be hyperpolarised (202). This gives an indication of the mitochondrial membrane potential as green emission is indicative of depolarised mitochondrial membrane potential and red is indicative of a hyperpolarised mitochondrial membrane, a normal membrane potential is approximately -140mV at rest (203).

A JC1 dye kit for mitochondrial staining was used and the manufactures guidelines were followed. Stock solutions of the JC1 dye were prepared in DMSO to be used at a final concentration of 5 µM and stored at -20^{o}C until required. 50µl of the stock solution was added to 8 ml of deionised water (dH_20) and vortexed. 2ml of staining buffer was added and left at room temperature for 2 minutes. This solution was then mixed at a 1:1 ratio with pre-warmed culture medium and added to the cells which had been seeded onto coverslips in 24 well plates and treated for the appropriate time, according to the experiment conducted. The cells were then returned to the incubator for 20 minutes and live imaged using the Zeiss AxioImager ex/em 514/529 on the rhodamine and FITC channels. 5-10 images were taken at X40 and X63 for each coverslip for each condition using cultures established on at least 3 separate occasions. The total number of cells per field of view was counted, as was the number of cells displaying predominantly green fluorescence and the number displaying a mixture of green and red. The totals of both red and green cells were divided by the total number of cells. The data for this

was then collated by treatment and by experiment. The images from cells which had received no treatment were presented as the untreated control and all treatments were presented as a proportion of this. This was presented as a proportion of the total number of cells per field of view.

2.2.12 H_2DCF-DA

To detect the generation of reactive oxygen species in live samples the dye H_2DCF-DA was used. This dye is a cell permeable dye that binds reactive oxygen species and fluoresces green (204).

Cells were grown on boroscillate glass coverslips in 24 well plates and treated as appropriate. After treatment 10µM H_2DCFDA was added to the culture media and the cells were returned to the incubator for 45 minutes. The coverslip was then removed, and the cells were imaged live using the Zeiss AxioImager MR2 Ex/Em: 485/520 nm. 10 images were taken on X40 magnification per coverslip per condition and on cultures established on at least 3 separate occasions. For each experiment the exposure time was constant so that any changes in fluorescent intensity could be accurately determined. The images were then collated and grouped by treatment. The sum intensity of each image was taken directly from Zeiss software; the number of cells from each image was then counted. The total intensity per field of view was then divided by the number of cells to give the average intensity per cell. The data for this was then collated by treatment and by experiment. The images from cells which had received no treatment were presented as the untreated control and all treatments were normalised to untreated control.

2.2.13 Protein extraction

Cells were grown on either 35mm or 60mm dishes (see table 1 for densities). After treatment, all medium was removed from cells and stored at -20^{o}C for future use in LDH assays to

determine whether there were any effects on cell viability, which could confound the analysis of protein expression. Cells were washed in PBS followed by a 5-minute incubation in extraction buffer containing PBS, 0.1% v/v triton X-100 and 1% v/v protease inhibitor cocktail, the volume was determined by cell density. Cells were carefully scraped from the bottom of the dish with a cell scraper. All solutions were transferred to a 1ml tube and centrifuged at 13000 RPM for 10 minutes at room temperature. The supernatant was then transferred to a fresh tube and saved as the soluble fraction, the pellet also saved as the insoluble fraction. This was stored at -80°C and small aliquots of the soluble fraction were saved at -20°C to avoid freeze thawing the samples.

2.2.14 Protein concentration determination

The concentration of protein in extractions was determined using a Bradford assay. A range of concentrations (0.001 – 100mg/ml) of bovine serum albumin were used to produce a standard curve. 10µl of the soluble fraction of each protein sample was mixed with 10µl 1M sodium hydroxide to solubilise the protein, and 500µl of Bradford reagent (0.025% w/v brilliant blue, 40% v/v methanol, 7% v/v acetic acid in deionized water) This was then loaded into a 96 well plate and read and 570nm on the BioHit BP plate reader and protein concentration was determined by comparison with the standard curve. The standards were plotted as a scatter graph and a trend line added. The r and x^2 were then added and if the x^2 was less than 0.94 then this was discarded as it was determined that there was an error in the preparation of the standards. The absorbance from each of the samples was then calculated based upon the standards and this was calculated as per the calculation from the trendline form the Bradford assay. This was standardised and diluted as appropriate for western blotting and ELISA.

2.2.15 Subcellular fractioning

To examine the effects of homocysteine on mitochondrial proteins for ELISA the mitochondria were extracted. This was achieved by a differential centrifugation method by which organelles

of the cell can be fractioned out by centrifuging at different speeds and temperatures. An alternative mitochondrial extraction kit was initially tested and compared to the centrifugation method and a better yield was obtained with this method rather than the kit, and therefore this method was used for these experiments.

The cells were grown on 60mm dishes (see table 1) and treated as appropriate. All cell medium was removed from the dishes and cells were suspended in ice cold extraction buffer (0.3 M mannitol, 0.1% w/v BSA, 0.2mM EDTA, 10mM HEPES adjust to pH 7.4 with KOH and/or HCl followed by addition of 1% v/v protease inhibitor cocktail-l). Cells were scraped off the bottom of the culture dish using a cell scraper and transferred to a dounce homogeniser and thoroughly homogenised on ice with approximately 15 strokes. The supernatant was transferred to a fresh tube and centrifuged at 1300g for 10 minutes at 4°C. The supernatant containing cell debris was discarded and the remaining pellet was resuspended in the extraction buffer (0.3M mannitol, 0.1% w/v BSA, 0.2mM EDTA, 10mM HEPES adjusted to pH 7.4) mixed and centrifuged again at 7000g for 10 minutes. This supernatant was saved as the cytosolic fraction and the pellet resuspended in the isolation buffer. This was then centrifuged again at 7000g for 10 minutes and the resultant pellet saved as the pure mitochondrial fraction. This was aliquoted and stored at -80°C until required.

To validate the purity of the samples a western blot was used to check the mitochondrial fraction for βIII tubulin to determine whether there was any contamination with cytosolic fraction.

2.2.16 Western blot analysis

Western blot is a commonly used method to detect changes in the protein expression within samples. Unlike some other methods of examining changes in protein expression such as ELISA, the western blot allows for a detailed output of the molecular weight of these proteins.

Protein samples were mixed at 1:5 ratio of protein sample buffer (2% v/w SDS, 20% glycerol v/v, 0.4mM Tris (pH8), 0.01% w/v bromophenol blue, 2% β mercaptethanol v/v, 0.075% EDTA w/v and deionised water). The sample buffer provided the samples with the weight and the charge to allow for free movement through the gel. The samples were then boiled at 96 °C for 10 minutes to denature the sample and expose the antibody binding sites. The samples were then loaded in a 10% SDS-polyacrylamide gel (NuSep) giving a final protein concentration per well of 20µg/µl as determined by the Bradford assay. The gel was then run using 1X running buffer (sigma T7777) prepared from a 10X running buffer stock in deionized water for electrophoresis, at 150V for 45 minutes with a standard protein ladder in one lane to allow determination of molecular weight. Once optimal separation of the ladder had occurred, the gel was then removed and placed into a sandwich for transfer. This comprised of 2 sponges, 2 pieces of electroblotting paper, the gel, a nitrocellulose membrane, 2 pieces of blotting paper then another 2 sponges. This was then loaded into a cassette and placed in the x cell blot module ™ gel rig with the gel facing the positive electrode so the protein transferred from the gel to the membrane for subsequent detection. This was run in 1X transfer buffer (sigma T4904) prepared from a 10X transfer buffer stock by a 1:10 dilution in Milli Q water containing 20% v/v methanol. On occasions where protein detection was weak, a PVDF membrane was used instead of the nitrocellulose, as it has a higher affinity for protein binding but must be soaked in ethanol prior to use. In all cases a wet transfer was used and ran at a constant 30V and 200mA for at least 90 minutes. After transfer, the membrane was removed and the quality of the transfer was checked by staining with Ponceau S solution containing 0.33% w/v ponceau S, 0.3% v/v acetic acid in deionised water, which will bind proteins on the membrane (199). If samples were visible, the dye was washed off with TBS until the membrane was clear. If this was unsuccessful, the blot was discarded as this is indicative of either no protein within the samples or a poor transfer. If no obvious error had been made, the samples were run again on the SDS

gel as described above, the gel was then removed and stained with coomassie blue (0.025% w/v brilliant blue, 40% v/v methanol, 7% v/v acetic acid and deionised water) which was left until bands appeared on the gel to check the quality of gel running and protein samples. This was then destained in 10% v/v acetic acid in deionized water and visualised using a chemidoc gel documentation system under the UV illumination for optimal visualisation of protein bands. If this showed positive staining after a negative Ponceau S stain this indicates that there was an issue with the transfer and if negative or very low, an issue with the samples themselves and new were obtained.

Immunodetection using specific antibodies (see table 3 for concentrations) was achieved by leaving the membrane overnight at 4°C in 5% w/v dried milk in TBS +0.1% v/v triton X-100. The membrane was then washed 3 times for 5 minutes in TBS containing 0.1% v/v triton X-100. Primary antibody binding was detected using an appropriate horseradish peroxidase (HRP) conjugated secondary antibody at 1:10,000 v/v in TBS-T and visualised using chemiluminescence ECL substrate (Pierce) using the GelDoc Imager it2 with Vision Works software. The intensity of the bands was determined using Image J software. This intensity was then transferred to a Microsoft Excel spreadsheet, data for treatment groups were presented as a percentage relative to untreated cell extractions. This was corrected using a western blot for the house-keeping protein α-tubulin as a loading control, which was selected as it gave a better signal as compared to β-actin and GAPDH is dysregulated in neurodegenerative disorders (193).

Table 3

Antibody	Concentration
Mouse α tubulin (sigma)	1:2000
Rabbit α APP (Genscript)	1:5000
Rabbit α pTau (ser262) (Genscript)	1:5000
Mouse α Nitrotyrosine (Santa Cruz)	1:250
Goat α VDAC (Santa Cruz)	1:1000

2.2.17 Oxyblot

To determine if the protein samples had been oxidatively modified the oxyblot assay was used to determine if carbonyl groups had been incorporated into proteins. This method shows whether protein samples have been oxidised by superoxide or other types of free radicals. In this assay, the carbonyl groups are derivatised by 2,4-Dinitrophenylhydrazine (DNPH) and then detected using DNP antibodies (199).

Protein samples were chemically denatured by the addition of 12% w/v SDS in deionized water for 15 minutes. The samples were then mixed with DNP residues and left for 20 minutes, and manufacturer supplied neutralisation buffer was then added to halt the reaction. 1X sample buffer was mixed with a mixture of manufacturer supplied standard proteins to serve as a molecular weight ladder. The samples are then loaded into a gel at 10µg/µl per well and the remainder of the assay was carried out as described for a western blot (see section 2.2.16). The primary antibody was added at a concentration of 1:600 and the secondary was added at 1:300. The intensity of the bands was determined using Image J software. This intensity was then transferred to an excel spreadsheet, data for treatment groups were presented as a percentage relative to untreated cell extractions.

2.2.18 ELISA

As a high throughput method of detecting changes in protein samples, ELISA assay coupled to a representative western blot was carried out. This was initially optimised to determine the best method to be used.

Parameters trialled to optimise ELISA:

- Coating Buffer – PBS, commercially prepared coating buffers, range of dilutions for sample in PBS
- Coating Time - 4 hours at room temperature, overnight at room temperature, overnight at 4ºC
- Primary antibody - range of concentrations for all, overnight at 4ºC, 37 ºC, and after 2 hours and 4 hours room temperature
- Secondary antibody – 1 hour at room temperature, attempted at a range
- Substrate – TMB, KPL substrate, volumes 50µl and 100µl

The final working protocol for the indirect ELISA was as follows. Cell lysates diluted to a working concentration of 1µg/µl per well in PBS. This was used as a coating buffer to dilute the samples as it was found to be more effective that the commercially-produced coating buffer. The samples were loaded in duplicate in to an ELISA plate this was then left overnight at 4°C. The following day the samples were removed from the wells and 10% v/v horse serum in PBS was used to block all nonspecific binding, this was then left for 30 minutes at room temperature (on a rocker) and then discarded. The plate was then washed 3 times with PBS for 5 minutes and PBS containing primary antibody was added to each well. Details of dilutions and antibodies used are in Table 4. On every occasion each sample was also tested using an additional ELISA for α-tubulin as a loading control to accurately determine total protein

concentration. This was left for 2 hours at room temperature, then removed and the plate washed 3 times for 5 minutes with PBS prior to a 1-hour incubation in appropriate HRP conjugated secondary antibody at 1:10000 for 1 hour. This was then removed, and the plate washed 3 times for 5 minutes in PBS prior to detection with substrate. The substrate that was used was the 2,2'-azino-bis (3-ethylbenzothiazoline-6-sulphonic acid) (ABTS) (KPL) substrate which a highly sensitive ELISA substrate. This is a 2-part kit in which solutions A and B were mixed at equal volumes immediately prior to use and 100 µl was added to each well of the plate. There were several wells of each plate lacking protein sample to check that the signal obtained was not background reactivity. The readings were taken on BioHit BP plate reader, the ABTS substrate has peaks at 630 nm which is known to be in flux. Therefore, hydrochloric acid was added to produce a stable reaction product, and this was read at 410nm. The data were grouped by each batch of cells used, the average of all wells per batch of cells was then averaged. The data for this was then collated by treatment and by experiment. The values obtained from cells which had received no treatment were presented as the untreated control and all treatments were presented as a percentage of this.

Table 4

Antibody	Concentration
Mouse α βIII tubulin (genscript)	1:2000
Mouse α Tyrosine hydroxylase (sigma)	1:5000
Mouse α 4-hydroxynonenol (abcam)	1:500
anti-extracellular signal-regulated kinase-1	1:250
Mouse α anti-neuronal nitric oxide synthase (Santa Cruz)	1:1000
Mouse α anti-inducible nitric oxide synthase (Santa Cruz)	1:2000
Mouse α anti-GluN2A (Santa Cruz)	1:500
Rabbit α APP (Genscript)	1:2000
Rabbit α pTau (ser262) (Genscript)	1:1000
Goat α anti-presenilin 1 (abcam)	1:2000
Mouse α α-tubulin (sigma)	1:1000

2.2.19 DNA extraction

Cells were grown on 35mm dishes and at the end of treatment time the cells were lysed in TE buffer (10mM Tris base and 0.5M EDTA) containing 20% w/v SDS. Proteinase K solution was then added to the sample to cleave peptide bonds adjacent to the carboxylic group of aliphatic and aromatic amino acids allowing digestion of the proteins in the sample. The cell lysates were incubated in this overnight at room temperature. The next day, 5M NaCl was added at a 1:1 v/v ratio to salt out the DNA. The supernatant was removed to a fresh tube and centrifuged

at 13000rpm to pellet the DNA. The supernatant was removed and 1:1 v/v ethanol was added to wash the pellet, this was centrifuged for 10 minutes at 13,000 RPM and the supernatant was discarded. The resultant pellet was washed 3 times in 70% v/v ethanol to remove any residual salt and then centrifuged for 10 minutes at 13,000 RPM. The supernatant was again discarded, and the pellet allowed to air-dry for 30 minutes. The pellet was then resuspended in TE buffer and this was aliquoted and stored at -80°C.

2.2.20 DNA methylation detection

To investigate the epigenetic changes with age in culture a global DNA methylation kit (MDQ1 Part 2- 96RXN) was used to measure DNA methylation. DNA samples were diluted in the manufacturer's DNA binding solution and added to an ELISA plate to allow for binding. The plate was incubated at 37°C for 1 hour to maximise DNA binding. Several wells had just DNA binding solution alone to serve as a blank. After the DNA was bound, the manufacturer supplied blocking solution was added and the plate was returned to 37°C for a further 30 minutes. This was removed, and the plate washed 3 times for 5 minutes in PBS. The capture antibody for detection of methylated DNA was added at 1:1000 diluted in the supplied wash solution at 50µl per well, this was incubated at room temperature for 1 hour. This was then washed 3 times for 5 minutes and the detection antibody was added at 1:1000 diluted in wash solution. This was then washed again as above and 100µl of detection solution was added to each well and left for 1-10 minutes, once a sufficient change from blue to a yellow colour had developed, 50µl of stop solution was then added to each well and this was read at 410nm on BioHit BP plate reader. The blank was subtracted from each of the values and the absorbance was represented as compared to 2 week samples.

2.2.21 Statistics

All data was obtained from at least 3 different cultures established on 3 separate occasions. Where possible in cell viability assays and any other assay conducted in a 96 well plate the

blank data was subtracted from the absorbance values in each case. All data was collated and any data points which were more than 3 standard deviations away from the mean were excluded as statistical outliers. For plate reader-derived data, any data points that had an absorbance above 1 were also eliminated as this is beyond the limit of linear detection of the instrument and therefore cannot be considered an accurate reading. Normal distribution was determined by plotting the residuals of ANOVA and subjecting the data to Korsakov Smirnoff test of normality as there were no more than 30 data points in any experiment. If the data was not normal, then the data was transformed using SQRT and log10 transformation as recommended for relative data. The data was then analysed with a one-way ANOVA with Tukey post hoc test. Alternatively, in cases where there was only 2 data points being compared a student's t-test was used. When data was not normal, and this was not achieved through transformations, the data was analysed using non-parametric methods. In all cases a *P* value of less than 0.05 was considered significant.

CHAPTER 3: ESTABLISHING A NOVEL METHOD FOR THE LONG-TERM CULTURE OF SH-SY5Y NEURONAL CELLS EXHIBITING BIOMARKERS OF AGEING

3.1 Introduction

One of the most commonly used *in vitro* models for neurodegeneration research is the neuroblastoma cell line SH-SY5Y (205). These cells are frequently used undifferentiated as they generate a high volume of data rapidly, with a doubling time of 48 hours (206). However, it is often appropriate when using this cell line to differentiate the cells to a more representative neuronal model (205). Although there are advantages to using undifferentiated SH-SY5Y cells, they do not possess the ability to fire action potentials, nor do the cells express an extensive array of neuronal markers or possess long neuronal processes. Differentiation of neuroblastoma cells can be achieved with several different differentiation agents such as retinoic acid (207), phorbol esters (208) or staurosporine (209). Different agents can be used depending on the resultant preferred phenotype, either cholinergic or dopaminergic. The dopaminergic phenotype makes this system ideal for PD research. For AD research, these cells and can be transfected with APP leading to endogenous overexpression of amyloid beta (210). In these experiments, SH-SY5Y cells were differentiated with retinoic acid, followed by the addition of a mitotic inhibitor, 5-fluorodeoxyuridine (5-FDU), which is discussed in more detail in section 2.2.3.

The use of undifferentiated cell lines for neuroscientific research pose several issues: prior to differentiation these cell lines often lack several receptors, either in expression or functionality, that would be required for the basic properties of a neuron such as the expression of the NMDA receptor (211). Whilst primary cultures were once the method of choice in this area, there is increasingly a call to minimise the use of animals in research (212). Furthermore, it can be difficult to obtain sufficient tissue from primary cultures for robust biochemical analysis. SH-SY5Y cells were derived from a bone marrow biopsy of a 4 year old girl and are present in two forms: the S-phase, which are free floating and are not subject to differentiation, and the N-

phase, which are adherent cells, and which can be readily differentiated with a number of compounds as outlined above and discussed in detail below (206,213)

Whilst many protocols exist for differentiation of SH-SY5Y cells to a neuronal phenotype, undifferentiated fibroblast-like cells can remain within the culture (see image 3.1). Furthermore, S-phase cells can continue to divide and be present undifferentiated in the cultures after differentiation protocols, making the analysis of compounds which are known to act on neurons problematic (206). Successful differentiation to a neuronal culture requires large amounts of maintenance, or alternatively a complex and expensive perfusion pump system, or the addition of neurotrophic factors (205,214,215). Thus, there are a number of different differentiation agents which have been reported to give rise to neuronal differentiated SH-SY5Y cultures characterised by the expression of neuron-specific markers such as NeuN (216) and βIII Tubulin (216). Phorbol esters such as 12-0-tetradecanoyl-phorbol-13-acetate (TPA) at 80nM (217), are commonly used for research for neurons of the adrenergic phenotype (218). Such esters are now more often used in conjunction with retinoic acid (RA), and the concentration most commonly used is 10μM (218–220), but the use of RA concentrations as high as 75-100μM has been reported (207). Differentiating with RA for 5 days, followed by 5 days of 50ng/ml brain-derived neurotropic factor (BDNF) gives rise to an SH-SY5Y culture with longer neuronal processes and cellular connections when compared to RA alone (221). Other growth factors such as nerve growth factor (NGF) (222) are less commonly used in SH-SY5Y cells as they do not promote as extensive neurite outgrowth as RA (223). However, exogenous growth factors upregulate pathways pertaining to cell survival in addition to neuronal differentiation, which may restrict the use of these cells for viability screening (224–226). A fully differentiated cell culture may be obtained with RA alone followed by the application of mitotic inhibitors 10mM 5-Fluorodeoxyuridine (FdUr), 10mM uridine (Ur) and 1mM cytosine arabinoside (araC) (216). Using a perfusion pump system, the cells thrived for

three weeks in culture and showed more phenotypic markers of a neuronal culture including the presence of synapses, as compared to differentiation induced using a cocktail of growth factors such as NGF and BDNF (214).

The aim was to develop a method that would not only differentiate SH-SY5Y to a neuronal phenotype capable of forming a functional neuronal network, but also which could be used to provide a simple *in vitro* model of cellular ageing. One of the most widely investigated theories of ageing centres on the accumulation of oxidative damage with age which has deleterious effects on cellular function (227,228).

To build on the previous work done by Constantinescu et al. (216) cells were differentiated with RA before, then added a mitotic inhibitor to the culture, 5FDU, to eliminate any cells that remained in the cell cycle following differentiation. The culture medium was optimised for long term growth, analysing the differential effects of using a chemically-defined serum free supplement (SR-2), comparing it to serum-containing and non-supplemented media. These studies revealed a novel and effective way to achieve high purity neuronal cultures, which after 4 weeks in culture expressed biomarkers of ageing.

3.2. Results

3.2.1 Optimisation of SH-SY5Y cell differentiation and maintenance

The initial phase of this study aimed to determine which culture medium promoted the most robust survival of RA-differentiated SH-SY5Y cells over time in culture. Initial experiments had determined that 5 days of 10μM RA treatment is best for SH-SY5Y neuronal differentiation. The next stage was to optimise the culture medium. Therefore, cells were grown without serum supplementation, in DMEM supplemented with 1% v/v FCS or in DMEM supplemented with 2% v/v SR-2. 1% v/v FCS was chosen as this is the serum concentration used during RA differentiation (229) and 2% v/v SR-2 was selected in accordance with the manufacturer's recommendations.

Phase contrast photomicrographs reveal that a robust neuronal phenotype is triggered by this differentiation protocol. Undifferentiated cells (Figure 3.1a) show a flattened morphology with few or short processes. Following 5 days of treatment with 10μM retinoic acid (Figure 3.1a) in most cells the soma is rounded, and neurites have been extended from the cells. Following a further week's treatment with 18μM 5-FDU very few undifferentiated cells remain, and an extensive neurite network covers much of the culture dish, as neurite length was not a priority in this study this was not quantified here (Figure 3.1a). There are marked differences in the viability of these cells with each of the culture media (Figure 3.1). Very few cells remain in the serum free cultures 4 weeks after RA-differentiation (Figure 3.1c) compared to those in which the DMEM had been supplemented with either 1% v/v FCS or 2% v/v SR-2 (Figure 3.1c). Collating the data from 5 experiments, it was noted that very few, or in some cases, no cells survived with serum free medium on all occasions, with most or even all cells dying in 1% v/v FCS medium on 2 of 5 occasions. In contrast, less extensive cell death was visually apparent in the 2% v/v SR-2 supplemented cultures.

Figure 3.1 Phase contrast images of cell differentiation parameters

a

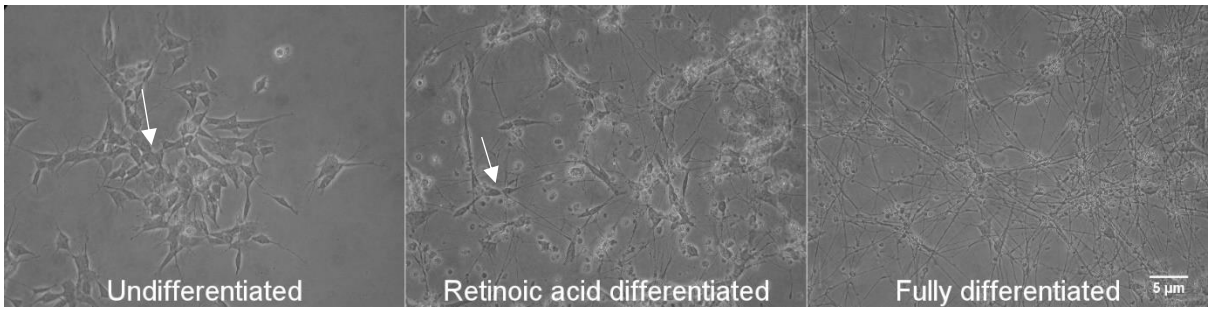

b

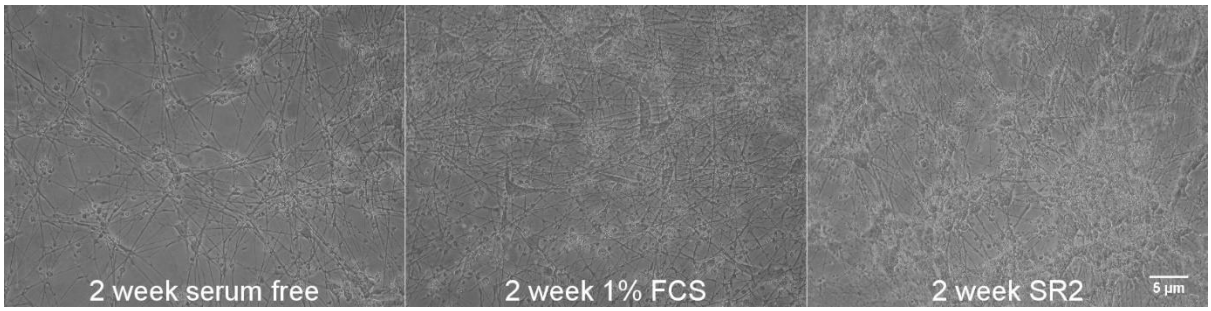

c

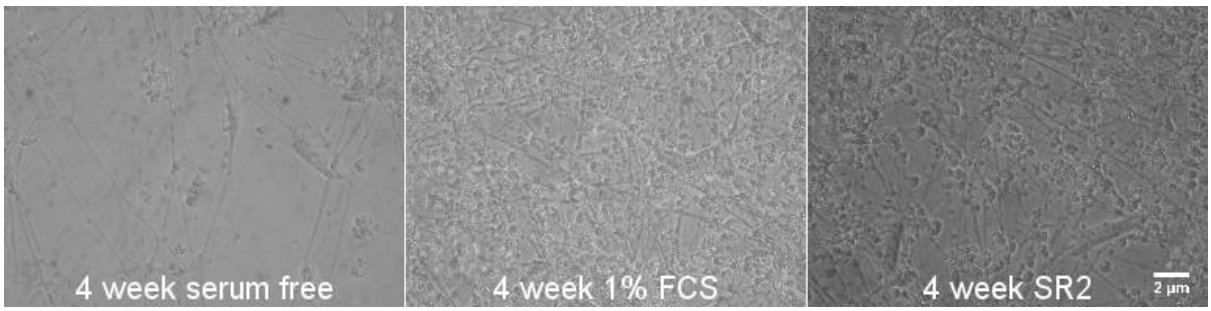

Figure 3.1 depicts phase contrast micrographs of the phases of cell development over time within our culture system, phase contrast images taken on a Nikon camera at X40 magnification in 3.1a and 3.1c. Figure 3.1a depicts the development of the cells from undifferentiated with an arrow depicting undifferentiated epithelial like cell, then treated with 10µM retinoic acid with an arrow depicting a cell which has become rounded and has undergone the differentiation process. Once treated for a week with mitotic inhibitor, the cells are shown again. Once the cells were differentiated with retinoic acid for 5 days they were transferred to media containing no serum (serum-free, 1 % serum (1% FCS) and a serum replacement (Serum replacement 2). The cells in the serum-free condition diminished over time whereas the serum replacement thrived at 4 weeks. Figure 3.1c shows the cells at 4 weeks in serum free, 1% and serum replacement 2 with few cells remaining in the serum free condition, cells in 1% FCS and SR2 are still thriving. FCS = foetal calf serum, SR2 = serum replacement 2

3.2.2 Differentiated SH-SY5Y cells are viable in culture for 4 weeks

To further determine whether differentiated SH-SY5Y cells could survive in long term culture without neurotrophins, and in the absence of a peristaltic pump, cultures of RA-differentiated cells were followed for up to 4 weeks after differentiation. These experiments aimed to quantify when, or if, the cells were dying and how the number of cells in the culture varied with time after RA differentiation. Only cells maintained in 2% SR-2 were followed for the remainder of experiments as they demonstrated highest levels of cell survival as documented from the phase contrast data. Therefore, in addition to the phase contrast micrographs (Figure 3.1), cultures maintained with 2% v/v SR-2 were assessed using lactate dehydrogenase (LDH) assay to determine membrane integrity as this is an indicator of cell death (230) and, DAPI imaging to determine nuclear number per field of view as an estimate of cell number (Figure 3.2a,b)**.** The LDH data shows that the absorbance values fall from 0.223 ± 0.018 two weeks after RA differentiation to 0.176 ± 0.016 4 weeks after retinoic acid differentiation (P=0.003, n=6; Figure 3.2a). This indicates that there was less cell death occurring at 4 weeks rather than at 2 weeks. This could be due to a loss of cells prior to 4 weeks therefore the absolute release of LDH could fall irrespective of the proportion of cells releasing this enzyme. It was therefore essential to couple this data to a measure of absolute cell number. To confirm the finding of the LDH experiments, the number of cells per field of view was established by analysing slides that had been stained with the nuclear dye DAPI for other imaging procedures (Figure 3.2). No significant reduction in cell number over time was detected (9.94 ± 2.66 cells per field of view T=2 weeks post differentiation; 6.36 ± 2.56 cells per field of view, 4 weeks post differentiation (P=0.76, n=7; Figure 3.2 b, c); Taken together this shows that there is no significant difference in the number of cells between 2 weeks and 4 week cultures. Indeed, the LDH data presents evidence of a reduction in dying neurons between 2 and 4 weeks. The likelihood of cells that remain in the cell cycle being present in the cultures will decrease with time. Thus, could be

attributed to a larger number of cells may be dying in the earlier stages of culture due to the presence of the mitotic inhibitor.

Figure 3.2 Confirmation of cell viability between 2 and 4 weeks post differentiation

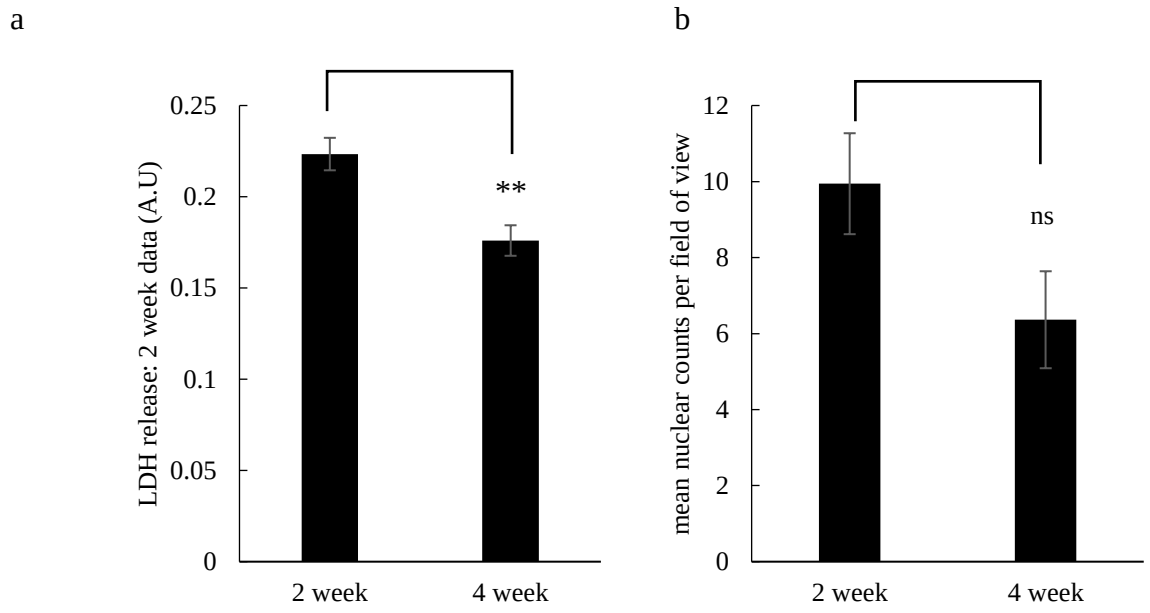

Figure 3.2 bar charts demonstrating that cells remain viable between 2 and 4 weeks in culture. Using LDH assay (a) there was a significant reduction in LDH release between 2 and 4 weeks (P=0.003, n=6; Figure 3.2a) although no significant differences in cell number were detected using DAPI counts of cell nuclei (P=0.076, n=7; Figure 3.2b, c). LDH = lactate dehydrogenase, DAPI = 4',6-diamidino-2-phenylindole

3.2.3 SH-SY5Y cells differentiated by this novel protocol express neuronal markers

To show that these cells had indeed taken on a neuronal phenotype after exposure to RA (216,229), the cells were fixed and stained in their undifferentiated state or 2 weeks after RA-differentiation for the neuronal marker, β III tubulin. βIII tubulin is the primary component on microtubules, and this isoform is almost exclusively found in neurons (231)**.** This was further supported by looking for changes in protein expression between undifferentiated and cells 2 weeks post-differentiation by using an ELISA assay for β III tubulin and tau (Figure 3.3). The immunocytochemistry showed prominent staining in differentiated cells as compared to the

undifferentiated population (Figure 3.3a) and this staining appears to localise to extended neuronal process. In confirmation of this, the ELISA showed a 39.03 ± 18.6% increase in β III tubulin in cells 2 weeks post-differentiation compared to undifferentiated cells (P=0.002, n=5; Figure 3.3b). An ELISA for tau was also performed as an additional neuronal marker and here a 91.2 ± 43.3% increase in expression is observed in 2 week differentiated cells compared to the undifferentiated population (P=0.012, n=5; Figure 3.3c). This shows that the protocol developed here results in cells which have characteristic markers of a neuronal phenotype.

Figure 3.3 Monitoring of changes in neuronal marker expression: Tau and β III tubulin

a

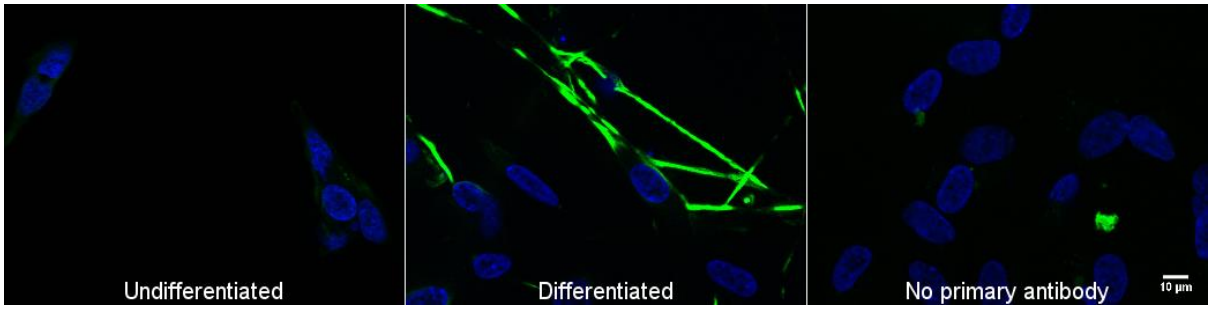

Blue = DAPI, Green = BIII tubulin

b

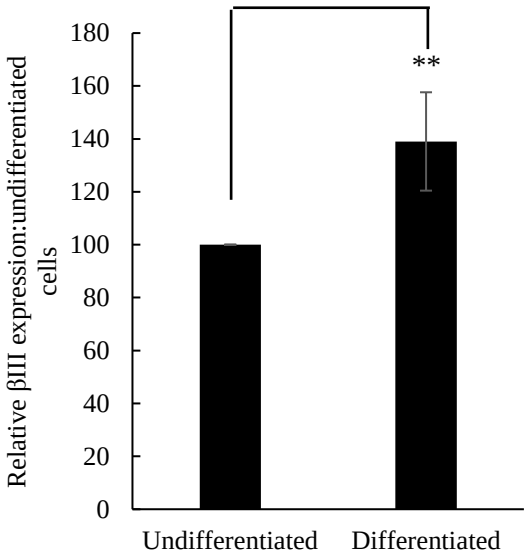

c

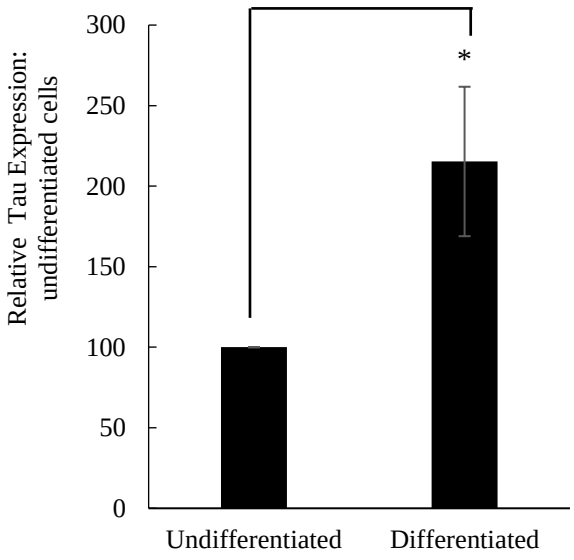

Figure 3.3 demonstrates that there is an increase in the expression of neuron-specific βIII tubulin post-differentiation as determined by an increase in βIII tubulin immunostaining (a) and this was supported by a βIII ELISA, showing an increase to 139.0 ± 18.6% relative to undifferentiated cells in 2-week post-differentiation cells (P=0.002, n=5; Figure 3.3b). An ELISA for tau was also used to support the presence of other neuronal markers which showed an increase in tau expression to 191.2 ± 43.3% in 2 week differentiated cells relative to undifferentiated cells, (P=0.012, n=5; Figure 3.3c).

3.2.4 Differentiation with retinoic acid followed by mitotic inhibitions using 5-FDU produces SH-SY5Y cells of a dopaminergic phenotype

To determine whether these cells were differentiating to a dopaminergic phenotype as reported in the literature (232), the expression of tyrosine hydroxylase, the rate limiting enzyme in dopamine biosynthesis (233), was determined using immunocytochemistry on fixed cells and ELISA on protein extracts. Immunocytochemical staining demonstrated prominent immunoreactivity for TH in 2 week post-differentiation cells, with an absence of this dopaminergic biomarker in undifferentiated cells (Figure 3.4a). In support of this, there was 54+ 25.8% increase in the expression of tyrosine hydroxylase (TH) (P=0.035, n=4; Figure 3.4b) between undifferentiated cultures and 2-week post-differentiation neurons as determined using ELISA assay (Figure 3.4b).

Figure 3.4 Once differentiated, SH-SY5Y cells express markers of dopaminergic neurons

a

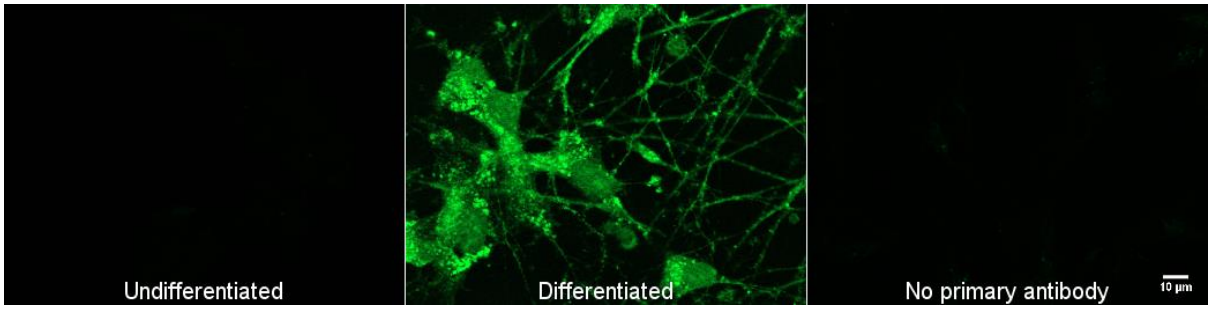

b

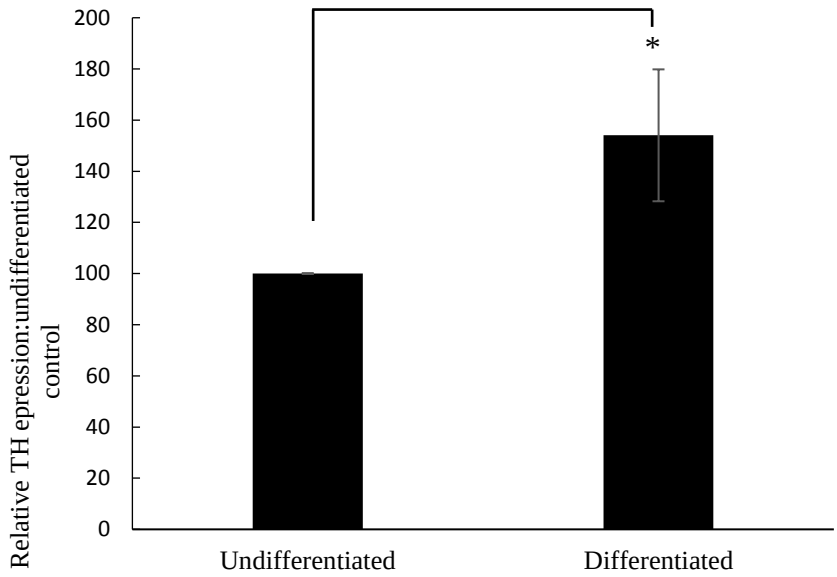

Figure 3.4 Using immunocytochemistry and ELISA, the expression of TH, a marker of dopamine biosynthesis was examined. There was an increase in TH expression observed in the ICC (Figure 3A) and this was backed up by an ELISA assay demonstrating a significant increase in TH expression between undifferentiated and differentiated cells by 154.0 ± 25.8% (P=0.035, n=4; Figure 3.4b). TH = tyrosine hydroxylase, ICC = immunocytochemistry, ELISA = Enzyme linked immunosorbent assay.

3.2.5 SH-SY5Y cells differentiated using this novel protocol form synapses and exhibit electrophysiological activity

One of the defining features of a neuronal population is the ability to form synaptic connections and a functional neuronal network (234). Therefore, it was important to establish the presence of synapses in the differentiated cultures and furthermore, it was important to determine that

any synapses present were functional. The data shown in figure 3.5a and 3.5b were from experiments conducted in collaboration with Dr GB Miles, University of St Andrews. These figures detail representative electrophysiological patch clamp recordings from the cells at 2 weeks post-differentiation. The inward sodium current was measured which gave a potential of -60mV, this is typical of normal neurons (235), furthermore the cells were capable of forming spontaneous action potentials as can be seen in figure 3.5a-b. Immunocytochemical staining for the synaptic marker, synapsin, was used to determine whether synapses were present. The images here show widespread synaptic staining using this marker which was not observed in the absence of primary antibody (Figure3.5c). Together these data show that by 2 weeks post differentiation these cells are forming functional synaptic connections with one another.

Figure 3.5 Using this differentiation protocol, these cells display several key neuronal features

a

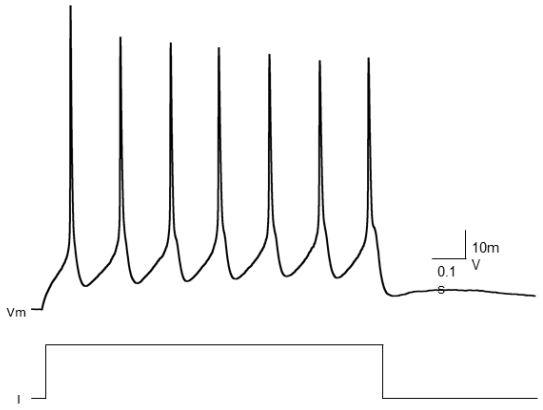

b

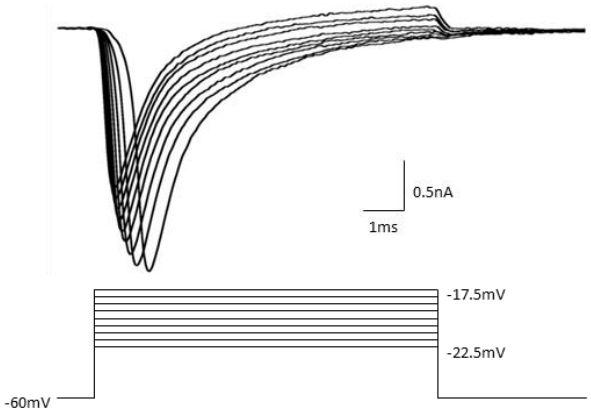

c

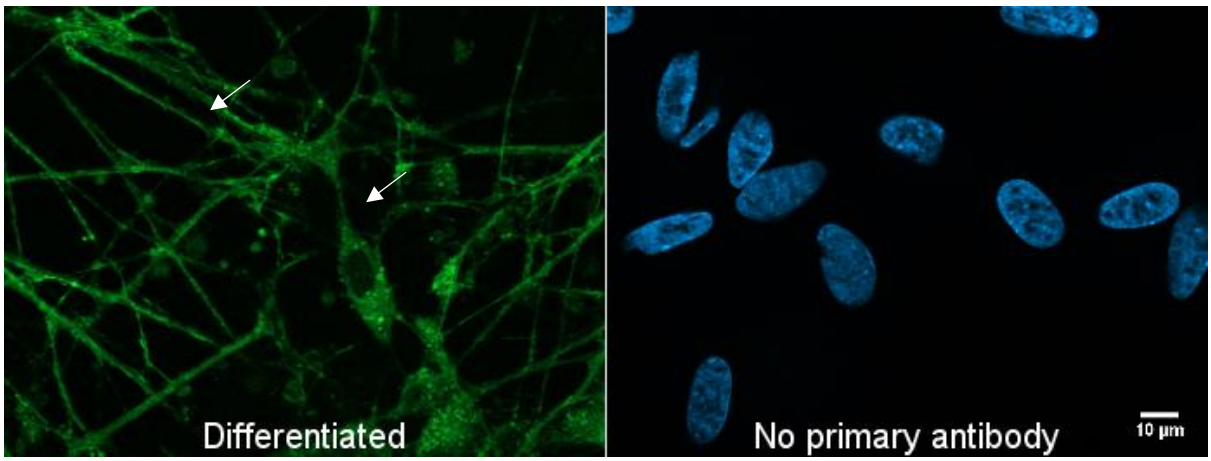

Blue = DAPI, Green = Synapsin

Figure 3.5 demonstrates that from as early as 2weeks post removal of retinoic acid, these cells exhibit synapses and a sodium current of -60mV which is in keeping with a typical neuron (a). Furthermore, spontaneous action potentials were generated from these cells, further supporting neuronal physiology (b). Robust immunoreactivity for synapsin is also apparent on these cells (c).

3.2.6 Cells prepared using this protocol show accumulations of oxidative damage to lipids with time in culture

A key feature of neuronal cell ageing is the accumulation of oxidative damage to DNA, RNA proteins and lipids (236). Although there is no definitive limits in place for cell damage which would define a cell as aged, the progressive accumulation of oxidative damage with time is proposed as a valid *in vitro* model as it replicates the *in vivo* build-up of oxidatively damaged cellular components (237). To determine whether any alterations in oxidative damage to lipids occurs with time in culture, immunocytochemistry (ICC) was used to detect 4-hydroxynonenol (HNE) (Figure 3.6). Formation of HNE results from oxidation of phospholipids containing ω-6 polyunsaturated fatty acyl chains and therefore HNE presence is a widely used as a marker of oxidatively damaged lipids (238). The intensity of the cellular staining from ICC showed an increase in positive staining between 2 and 4 weeks (Figure 3.6a). The staining appeared to localise to the cell membranes and was also apparent along neuronal processes. Although immunoreactivity was observed 2 weeks post retinoic acid differentiation there was a substantial increase in the staining intensity by 4 weeks post differentiation. This data was supported by an HNE ELISA wherein there was a 49.9 ± 23.1% increase in HNE levels (P=0.003, n=5; Figure 3.6b) between 2 and 4 weeks post retinoic acid differentiation. Together these data show that with time in culture, SH-SY5Y cells differentiated and maintained by this novel protocol show accumulating HNE levels which is a well-established biomarker of lipid peroxidation.

Figure 3.6 Cells accumulate lipid peroxidation after 4 weeks in culture

a

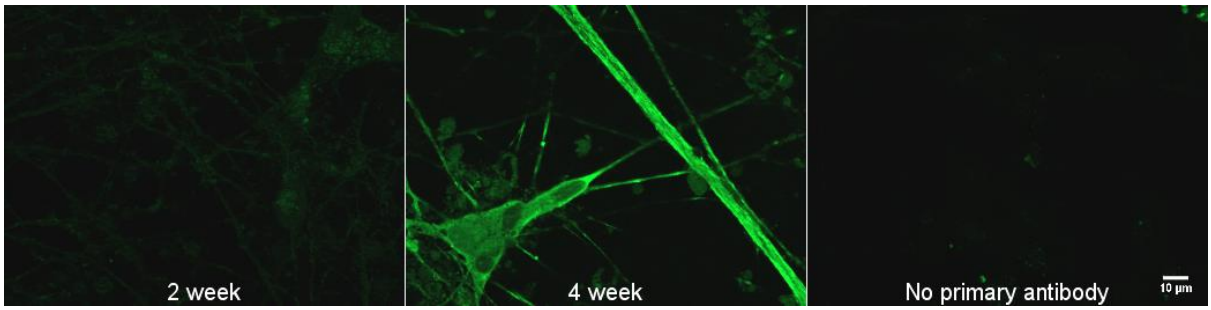

b

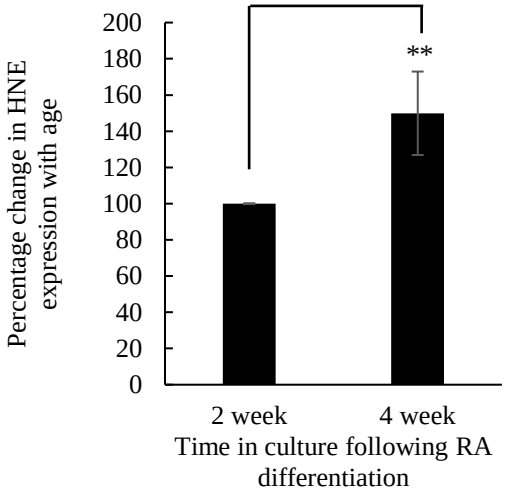

c

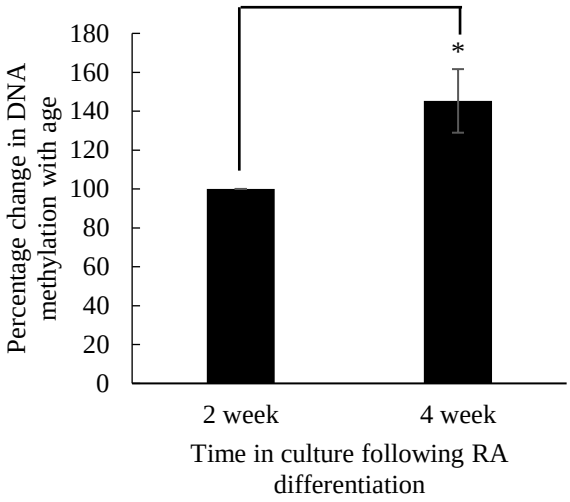

Figure 3.6 shows that in cultures stained 2 and 4 weeks, after retinoic acid differentiation an increase in positive HNE staining was observed. This was supported by an ELISA showing an increase in HNE expression between the 2 time points by 49.9 ± 23.1% (P=0.003, n=5; Figure 3.6b). Furthermore, in cells cultured for 2 and 4 weeks there was a 45.3% ±16.3% increase in DNA methylation between the 2 time points (P=0.05 n=3; Figure 3.6c). HNE = 4-hydroxy-2-nonenal, ELISA = enzyme-linked immunosorbent assay.

3.2.7 In this culture system, SH-SY5Y cells exhibit an increase in ROS generation over time and reduction of mitochondrial activity

It is well established that an accumulation of oxidative damage and an increase in ROS generation is observed in neuronal ageing (239). To determine whether there was a modulation of ROS generation between 2 and at 4 week post differentiation in this culture system, the cells were imaged using the live cell dye H_2- DCFDA. This dye binds ROS in live cells and

fluoresces green upon binding. Therefore, fluorescence intensity will reveal the relative amount of ROS in each condition. There was a very clear difference in the levels of ROS detected in 2 weeks and 4 week post-differentiation cultures (Figure 3.7a) with a marked increase in intensity by 4 weeks. Quantification of signal intensity through image analysis shows that there is a highly significant increase in the generation of ROS with time in culture from 164055 ± 42348 a.u. per cells at 2 weeks to 862539 ± 299320 a.u. per cell at 4 weeks post differentiation (P=0.000, n=8; Figure 3.8b).

As mitochondria are the major site of ROS generation (240), an MTT assay was used as a measure of mitochondrial activity 2 and 4 weeks post differentiation. This reaction measures a reduction of MTT believed to be due the activity (at least in part) of succinate-dehydrogenase (240). There is a reduction in mitochondrial activity which is not due to cell loss (see figure 3.2). Thus, the level of MTT reduction 4 weeks post differentiation was only 37.7 ± 4.1% (P=0.000, n=3; Figure 3.8c) of that observed 2 weeks post differentiation. This implies that mitochondrial function is declining over time and as such may explain the increased level of ROS produced.

Figure 3.7 Impact of time in culture on markers of oxidative stress

a

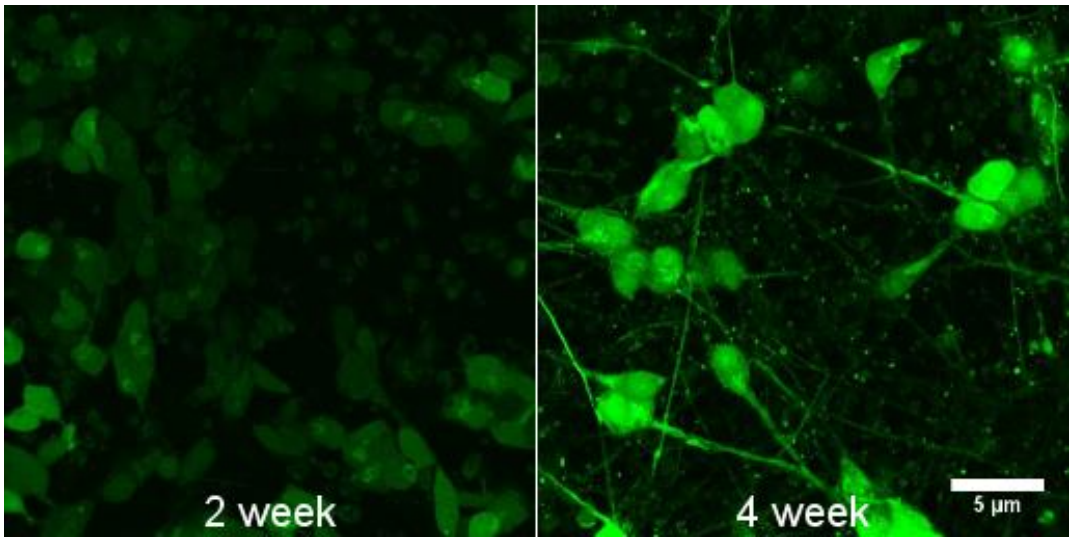

b

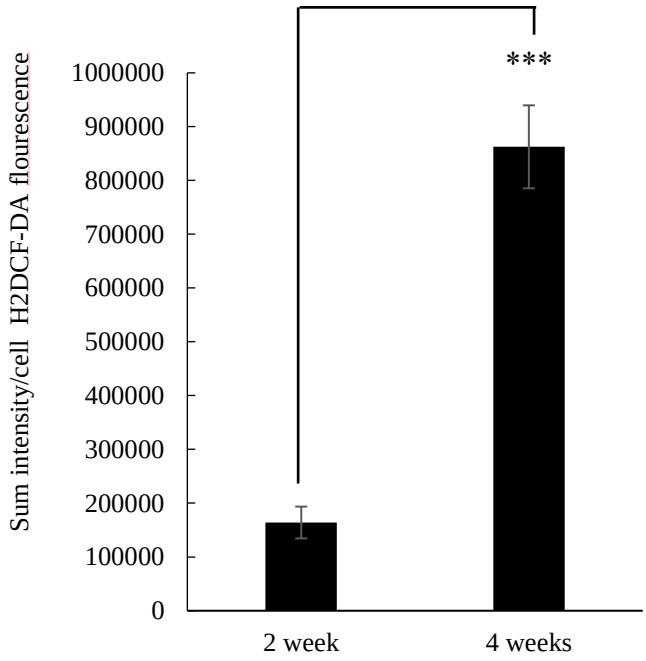

c

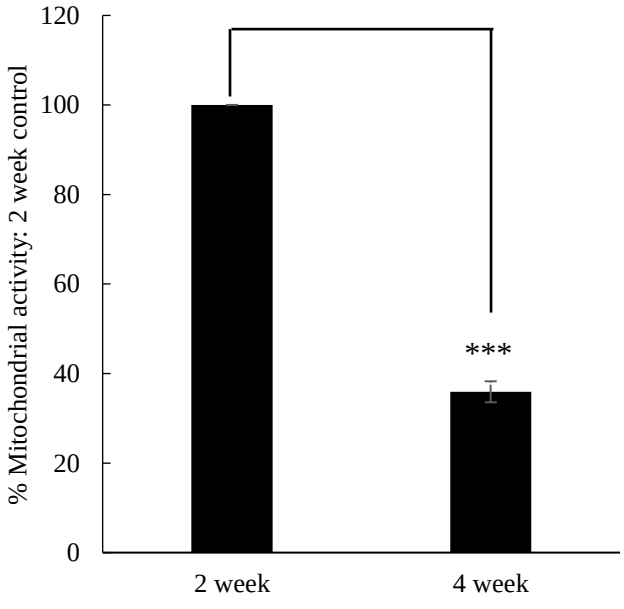

Figure 3.7a shows cells at 2 and at 4 weeks which had been imaged using the live cell dye, DCF-DA; this is represented in graphical form in panel c as arbitrary units (au). Panel c shows an increase in ROS with age (P=0.000, n=8; Figure 3.7a). Oxidative stress is a known marker shows a significant reduction in mitochondrial activity (P=0.000, n=3; Figure 3.7c). DCF-DA = 2',7' –dichlorofluorescin diacetate, ROS = reactive oxygen species

3.3 Discussion

The neuroblastoma cell line SH-SY5Y is a commonly used cell line in neurodegenerative research, as it expresses a neuronal phenotype and endogenously expresses the genes APP, tau and PS1, which are linked to familial Alzheimer's disease (241,242). Furthermore, these cells can be differentiated to express an adrenergic, cholinergic or dopaminergic phenotype by using differentiating agents such as growth factors, phorbol esters and staurosporine (219,243). RA induced differentiation is by far the most well categorised protocol for differentiation and gives rise to a dopaminergic phenotype (167). Frequently RA is used in conjunction with growth factors to promote upregulation of gene expression of neuronal markers and promotes neurite outgrowth (221). By using RA as a differentiating agent and a simple protocol post-differentiation, we have established that the human neuroblastoma cell line SH-SY5Y expresses key neuronal markers and is physiologically similar to neurons. Furthermore, it was possible to use this protocol to model cell ageing in culture (as defined by the accumulation of oxidative biomarkers) within 4 weeks.

Other systems for using this cell line for long term culture have included using growth factors such as NGF and BDNF (221) and complex systems for maintaining the cell line (159). Although maintenance of growth factors in culture would be highly advantageous, the expense of setting up such a system would be significant. In lieu of growth factor supplementation, the perfusion pump system offers a unique alternative that would be an initially costly venture and furthermore, for communal work areas this may not be suitable. With regular and consistent medium changes, and careful handling, this study has demonstrated that it is possible to maintain these cells for at least 4 weeks on glass coverslips and within nunc coated dishes (both 24 and 96 well).

These results show that the most effective medium for maintaining SH-SY5Y cells in culture for 4 weeks is using chemically-defined medium. A commercially produced serum replacement

formulation, SR2, was assessed which has the advantage of giving rise to more consistency. SH-SY5Y cells have the potential to be maintained for longer than the 4 weeks, and this was investigated here: on two occasions cells were maintained for 6 weeks. However, the cells were lost in the fixation step, therefore further steps would have to be taken to ensure the coverslip was coated- in these experiments coating with poly lysine was sufficient. Subsequent coating with laminin, fibronectin or matrigel may enhance cell adhesion. In prostate cancer cells, fibronectin, poly-L-lysine and poly-L-ornithine enhanced cell adhesion, however, laminin and collagen type IV did not promote cell adhesion and promoted cell aggregation (244). Therefore, a robust evaluation of cell adhesion matrices would be warranted if it was necessary to maintain the cultures for more than 4 weeks.

Using this protocol, it was shown that these cells express the neuronal markers β III tubulin, tau and tyrosine hydroxylase post-differentiation thus showing that these are dopaminergic neurons in culture. Furthermore, what has never been shown in these differentiated cultures until now is the presence of functional synapses. Herein is demonstrated positive immunoreactivity for the presynaptic marker, synapsin I, and this is supported with electrophysiological recordings showing that these cells are capable of firing spontaneous action potentials and that they have a sodium current typical of neurons. This could have been further examined using FM4-64 to determine actively firing neurons by cell staining as the dye is taken up by synaptic vesicles during neurotransmitter release and reuptake, furthermore a post-synaptic marker could have been examined. This protocol for neuronal differentiation is valuable as it gives rise to markers which are associated with neuronal ageing but does not result in excess cell death making study of cellular damage possible without specialist equipment.

Current theories of ageing suggest that as neurons age, they accumulate damage through generation of oxidative stress and therefore accumulate oxidative damage to DNA, RNA, lipids

and proteins (236). Studying ageing presents many challenges and predominantly, models are time consuming include longitudinal human studies, rodent and avian models (245). Using the method developed in this study, it will be possible to study the underlying mechanisms of cellular ageing and to examine potential pharmacological means of deterring the deleterious effects of ageing over a short time (i.e. 4 weeks) using human derived cells *in vitro*. In this study, these cells begin to show signs of oxidative damage to lipids as well as an increase in the generation of ROS. These are signs that are characteristic of ageing. This phenotype may be indicative of an impairment of the cellular capacity to deal with the increase in the generation of ROS and therefore it is possible that the antioxidant capacity of the cell may be reduced (228,246). Furthermore, this study has shown that there is reduction in mitochondrial activity without a concurrent reduction in cell number which may represent a loss of mitochondria or may suggest that the mitochondria are ageing, and that the accumulation of damage therein has reduced their functional capacity. Therefore, it would be interesting in the future to further examine the effects of ageing on the mitochondria and mitochondrial DNA.

In conclusion, this chapter established a novel method of culturing functional neuronal cells from the SH-SY5Y cell line which can rapidly represent an ageing phenotype. This will be an invaluable resource for future research on ageing.

CHAPTER 4: HOMOCYSTEINE THIOLACTONE AS A NEUROTOXIN

4.1 Introduction

HCy has been widely implicated in a plethora of cardiovascular and neurodegenerative disorders (15,107,247–250). In addition to excretion from the body, homocysteine has several other fates which are not conducive to optimal health (251). Further to HCy itself, there are many other derivatives which may be toxic in their own right. One such derivative is HCy-T, which is generated in cells by an error editing reaction by methionyl tRNA synthase enzyme (252). HCy-T is a highly reactive cyclic compound and has the capability to bind lysine residues on proteins and incorporate HCy in forming N-homocysteineylated proteins, thereby impairing structure and function (252). HCy-T can be converted back to homocysteine in a hydrolytic pathway by bleomycin hydrolase (127).

There is little data to date on the cellular effects of HCy-T. However it is frequently used to induce seizures in rodents (253–255) and has been implicated in cardiovascular disease (129,249). There are currently two proposed mechanisms of action for these seizure effects namely that HCy-T modulates the nitric oxide system, and in particular inhibits the actions of iNOS (254); or that it acts on the GABAergic system, which has also been shown with HCy (255,256). The GABAergic system is the main inhibitory system in the nervous system and has been strongly linked with seizures (257). Some of the toxic actions mediated my HCy may be ameliorated by blockade of the GABA-A receptor with the use of muscinol (258). When muscinol was added in conjunction with HCy, there was a reduction in ROS generation and a suppression of phosphorylated ERK (258). These features have also been associated with the blockade of the NMDA receptor but as these systems are interconnected, there may be some crossover or additive effects of HCy actions at the NMDA and GABA receptors, this may provide some insight into the actions of HCy-T. In addition HCy-T has been show to induce degeneration of retinal cells (259), this was attributed to an increase in homocysteinylation when concentrations of up to 200µM were introduced.

The proportion of HCy converted to HCy-T is approximately 60% (260), and there is the potential for cells to convert HCy back to methionine or to cysteine as part of the remethylation or transsulferation pathways respectively (Figure 1.1). However, the breakdown of HCy-T is much more complex, and therefore although HCy-T may be less abundant than HCy, it has the potential to remain intact for much longer (260). Furthermore, HCy-T has been linked to protein aggregation, which is a common factor in the development of almost all neurodegenerative diseases and in normal ageing (261).

HCy is an agonist at the NMDA receptor at the glutamate binding site and a partial agonist at the glycine binding site (112) and toxicity mediated by HCy can be prevented by the addition of NMDA receptor channel blockers (155,262–264). The aim of these experiments was to explore whether HCy-T was neurotoxic and whether it exerted any neurotoxic responses through activation of the NMDA receptor.

4.2 Results

4.2.1 Neither homocysteine nor homocysteine thiolactone are cytotoxic to undifferentiated SH-SY5Y cells

It has previously been reported that undifferentiated SH-SY5Y cells only express the GluN1 subunit of the NMDA receptor (256). Therefore, if HCy or HCy-T require activity of the GluN2A subunit to mediate a cytotoxic response, as reported previously for HCy (155), neither reagent should be neurotoxic to SH-SY5Y cells in their undifferentiated state. Therefore, undifferentiated SH-SY5Y cells were treated with a range of concentrations of HCy from 50-200μM (figure 4.1a and c) or 50-200μM HCy-T (figure 4.1b and d) for 120 hours. The toxicity of HCy and HCy-T was determined by MTT and LDH assays. There was no significant reduction in cell number even at the highest concentration tested, 200μM HCy with 91.5 ± 2.6% mitochondrial activity relative to untreated control as determined by MTT assay (P =0.622, n=3; Figure 4.1a). This was supported by a LDH assay which showed, at the same concentration 85.5 ± 9.0 LDH release relative to untreated control (P =0.070, n=3; Figure 4.1c). MTT assay revealed that 200μM HCy-T resulted in 93.0 ± 3.2% relative to untreated control (P =0.347, n=3; Figure 4.1b). This was supported by LDH assay with 92.7 ± 11.0% LDH release relative to untreated control (P=0.452, n=3; Figure 4.1d).

Figure 4.1 Neither homocysteine nor homocysteine thiolactone are cytotoxic to undifferentiated SH-SY5Y cells

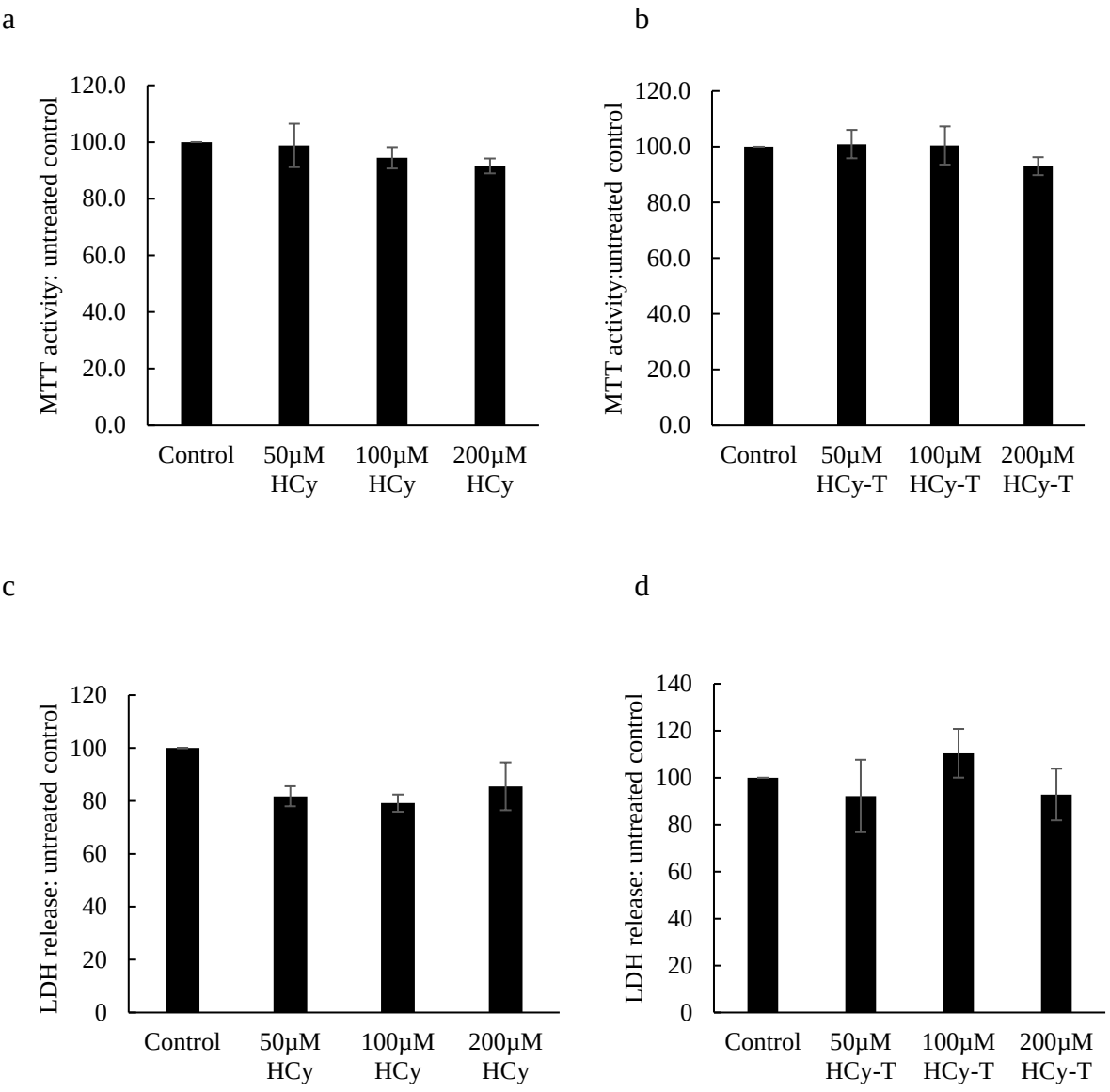

Figure 4.1 Bar charts demonstrating the dose response of undifferentiated SH-SY5Y cells to HCy and HCy-T from 50 to 200 µM, this was determined by MTT and LDH assays. There was no significant reduction in cell number even at the highest concentration tested, 200µM HCy with 91.5 ± 2.6% (*P* =0.136, n=3; Figure 4.1a), MTT relative to untreated control, this was supported by an LDH assay which showed the same concentration 85.5 ± 9.0 (*P* =0.088, n=3; Figure 4.1c). MTT assay revealed that 200µM HCy-T with 93.0 ± 3.2% (*P* =0.331, n=3; Figure 4.1b) relative to untreated control, this was supported by LDH assay with 92.7 ± 11.0% (*P*=0.053, n=3; Figure 4.1d). MTT assay = 3-(4,5-dimethylthiazol-2-yl)-2,5-diphenyltetrazolium, LDH = lactate dehydrogenase, HCy = homocysteine, HCy-T = homocysteine thiolactone.

4.2.2 Retinoic acid differentiation upregulates expression of GluN2A

One possible explanation for the lack of cytotoxic response to either HCy or HCy-T in undifferentiated SH-SY5Y cells is that these cells lack the GluN2A subunit reported to mediated their neurotoxicity (155). Furthermore, to determine whether differentiated SH-SY5Y cells are a useful model of HCy neurotoxicity and signalling it was necessary to determine whether GluN2A was expressed following retinoic acid differentiation. The literature reports both the absence (256) and presence of GluN2A post differentiation (256) and therefore re-evaluation was deemed necessary. Therefore, both undifferentiated and retinoic acid differentiated SH-SY5Y cells were used to determine the expression of GluN2A. An ELISA assay was used to determine the level of GluN2A expression in undifferentiated and differentiated SH-SY5Y cells and here a 32.4 ± 20.6% (P=0.036, n=4; Figure 4.2b) increase following differentiation was recorded.

Figure 4.2 Expression of GluN2A increases following retinoic acid differentiation after 5 days

a

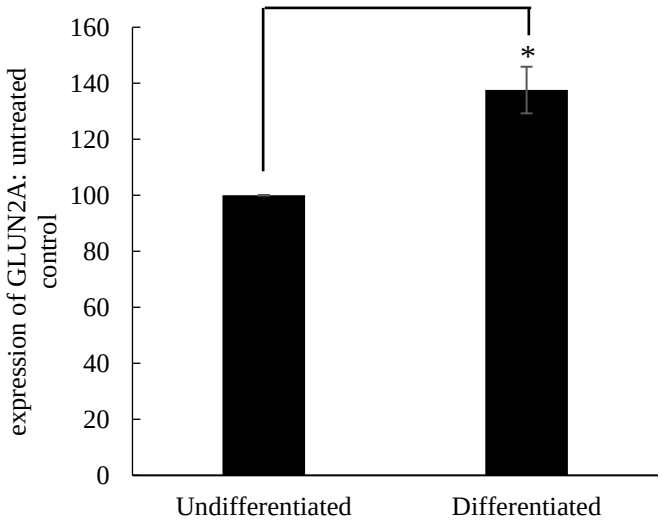

Figure 4.3: This figure shows that there is an increase in the expression in GluN2A in differentiated SH-SY5Y cells compared to undifferentiated cells. This was determined ELISA where there was a 32.4 ± 20.6% increase (P=0.036, n=4; Figure 4.2b) in GluN2A expression (STATS). ELISA = enzyme linked immunosorbent assay.

4.2.3 Both homocysteine and homocysteine thiolactone are neurotoxic to differentiated SH-SY5Y cells

Having established that retinoic acid-induced differentiation upregulates the expression of the GluN2A subunit of the NMDA receptor previously reported to be integral to HCy-mediated toxicity (155), dose responses to both HCy and HCy-T were established. Cell viability was determined using a combination of both CV assay and LDH assay to determine cell number and membrane permeability, respectively. After 120 hours treatment with HCy, a significant reduction in cell number was observed at 100 and 200µM HCy showing a reduction of 71.5 ± 4.2% (P = 0.010 n=8; Figure 4.3a) and 63.2 ± 4.4% (P = 0.001, n=8; Figure 4.3a). After 120 hours in culture, there was no significant decrease in viability at any concentration below this as determined by either CV (Figure 4.3a) or LDH with 100 and 200µM HCy showing an increase in LDH release of 124.0 ± 7.9% (P = 0.045, n=6; Figure 4.3b) and 131.0 ± 4.6% (P = 0.008, n=6; Figure 4.3b) respectively. After 120 hours exposure to 100µM HCy-T, in comparison to the untreated control, only 65.2 ± 10.4% of cells remained in the culture as determined by CV assay (P=0.007; n=8; Figure 4.3c). Accordingly, a significant increase in LDH release was detected in 100µM HCy-T treated cultures 118.1 ± 5.1% (P=0.002, n=23; Figure 4.3d). Together these data reveal that differentiated SH-SY5Y cells are vulnerable to both HCy and HCy-T and this contrasts with the findings for this cell line in its undifferentiated state.

Figure 4.3 Both homocysteine and homocysteine thiolactone are neurotoxic to differentiated SH-SY5Y cells

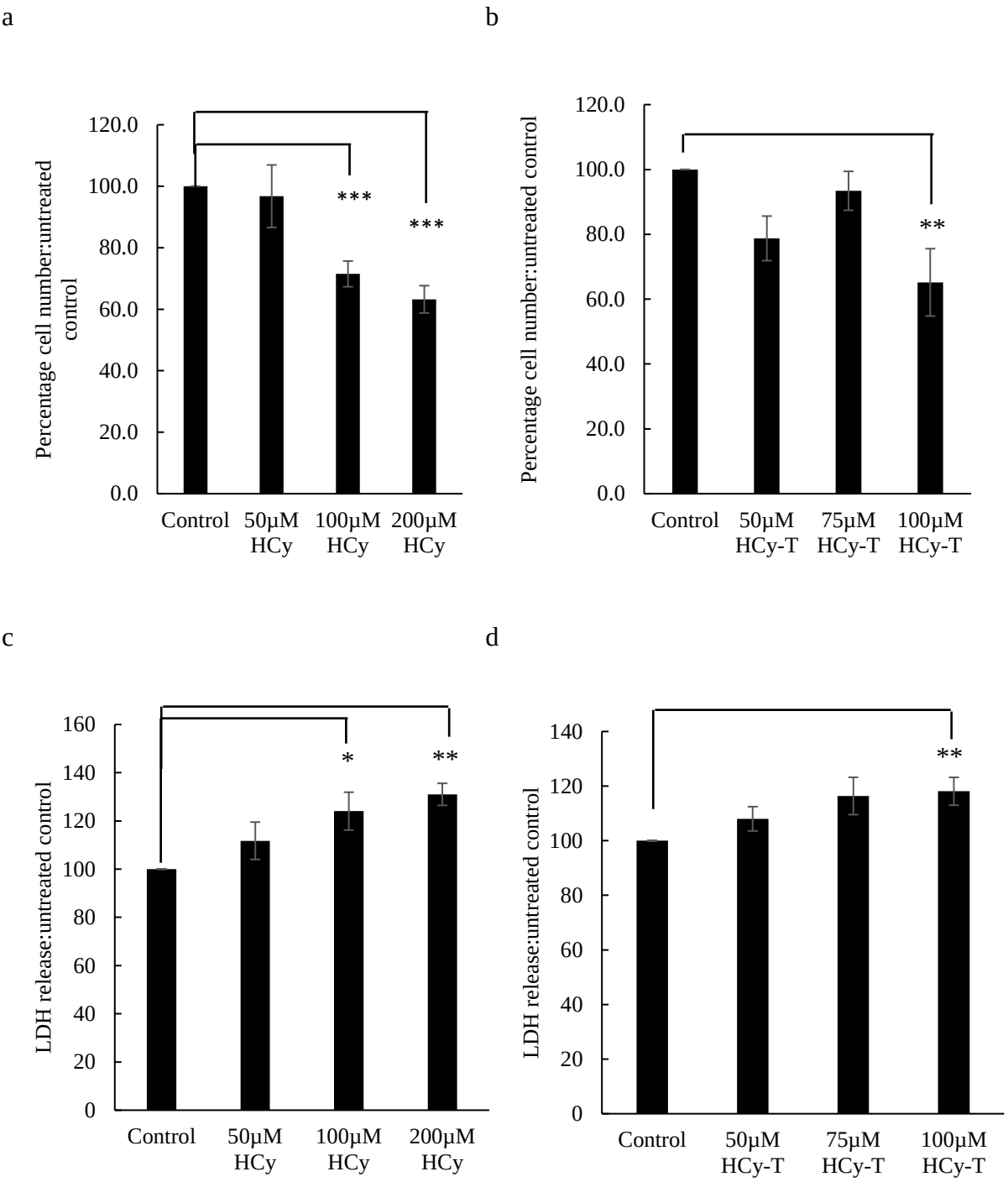

Figure 4.3: Differentiated SH-SY5Y cells treated for 5 days with HCy (a-b) or HCy-T (c-d), were assayed for viability in response to a range of concentrations of each metabolite by CV (a, c) or LDH (b, d) assay. For HCy after 120 hours a significant reduction in cell number was observed at 100 and 200µM HCy showing a reduction of 71.5 ± 4.2% (P = 0.001 n=8; Figure 4.3a) and 63.2 ± 4.4% (P = 0.0004, n=8; Figure 4.3c) HCy-T, after 120 hours in culture, there was no significant decrease in viability any concentration below this as determined by either

CV or LDH with 100 and 200μM HCy showing an increase in LDH release of 124.0 ± 7.9% (P = 0.045, n=6; Figure 4.3b) and 131.0 ± 4.6% (P = 0.008, n=6; Figure 4.3b) HCy. However, after 120 hours exposure to 100μM HCy-T, in comparison to the untreated control only 65.2 ± 10.4% of cells remained in the culture as determined by CV assay (P = 0.007; n=8; Figure 4.3c). Accordingly, a significant increase in LDH release was detected in 100mM HCy-T treated cultures 118.1 ± 5.1% (P = 0.002; n=23; Figure 4.3d). HCy = homocysteine, HCy-T = homocysteine thiolactone, LDH = lactate dehydrogenase, CV assay = crystal violet assay.

4.2.4 Homocysteine thiolactone toxicity is ameliorated by blockade of the NMDA receptor with Mk801

It is well documented that HCy is neurotoxic by acting on the glutamate binding site of the NMDA receptor and is also a partial agonist at the glycine binding site of the receptor (112). Many studies have shown that blockade of the NMDA receptor in a competitive and non-competitive manner is sufficient to ameliorate HCy-mediated cell loss (112). As HCy-T induces seizures in rodents that are linked to NMDAR over-activation, the possibility that HCy-T neurotoxicity is mediated via NMDAR was investigated (265). Therefore, retinoic acid differentiated SH-SY5Y cells were incubated with either 50 or 100μM HCy-T (Figure 4.3) alone or in combination of 0.2μM non-competitive NMDAR antagonist Mk801, although this blocker is only affective upon activation of the receptor (149). In confirmation of the previous findings there was no decrease in SH-SY5Y viability with 50μM HCy-T (Figure 4.4b). As above there was a significant decrease in cell number relative to control after 120h incubation with 100μM HCy-T 21.2 ± 3.4% (P=0.014, n=6; Figure 4.4b), but very little difference detected following co-administration of MK801 19.7 + 7% decrease in survival relative to control although the latter was no longer statistically significantly different to control (P=0.295, n=6; Figure 4.4b, d). The data derived from LDH assay clearly showed that HCy-T increases membrane permeability with a 21.7 ± 4.6% increase relative to the untreated control after 120h (P=0.000, n=14; Figure 4.4d). However, in the presence of Mk801, only a 13.1 ± 3.3% increase in LDH was detected which was not different to control (P=0.122, n=14; Figure 4.4d). Taken together these data imply that HCy-T toxicity is indeed mediated via the NMDAR.

The same experiments were conducted using HCy at a range of concentrations to 100µM HCy with co-application of 2µM Mk801 to ensure that HCy could be blocked with Mk801 as has been shown from other groups. No significant results were obtained with CV assay with 100µM reduction to 75.4 ± 13.4% (P=0.312, n=4; Figure 4.4a) this was a result to issues with the assay as an original n=11 was conducted but had to be excluded as they did not meet the criteria of 20% cell death with toxin alone. Using LDH it was not possible to support previous results and it was shown that application of 100µM HCy caused a 124.0 ± 7.9% increase in LDH (P=0.045, n=6; Figure 4.4c), there was no significant decrease when 2µM Mk801 was co-applied 124.9 ± 5.6% (P=0.057, n=6; Figure 4.4c) but the data for Mk801 administration was not significantly different to control viability.

Figure 4.4 Homocysteine thiolactone cell death may partially be ameliorated with Mk801

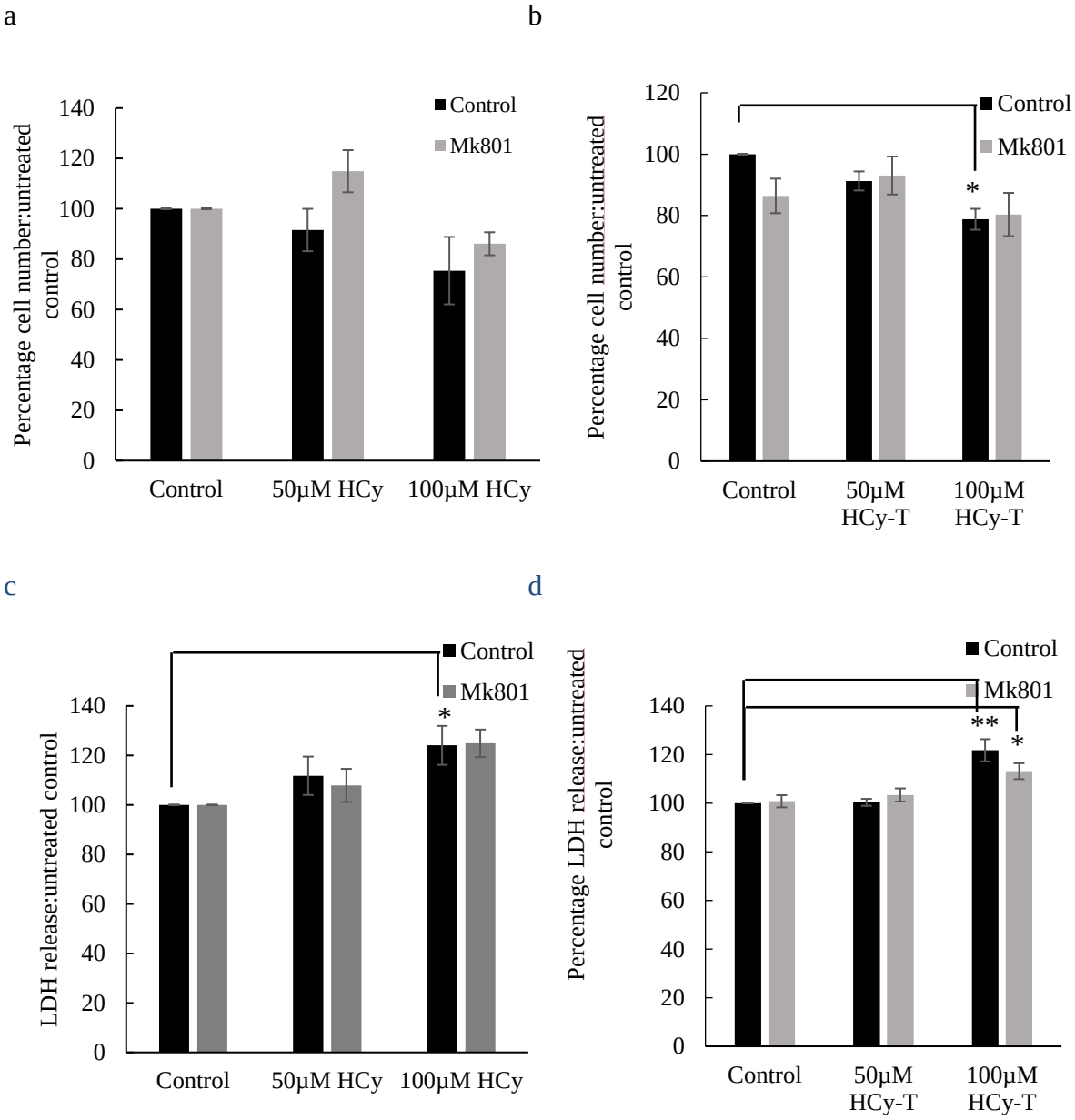

Figure 4.4 As above there was a significant decrease in cell number relative to control after 120h incubation with 100µM HCy-T 21.2 ± 3.4% (P=0.014, n=6; Figure 4.4b). Co-administration of MK801 caused a 19.7 + 7% decrease in survival relative to control (P=0.275, n=6; Figure 4.4b, d). The LDH assay showed that HCy-T increases membrane permeability with a 21.7 ± 4.6% increase relative to the untreated control after 120h (P=0.009, n=14; Figure 4.4d). However, in the presence of Mk801, a 13.1 ± 3.3% increase in LDH was detected which was different to control (P=0.033, n=14; Figure 4.4d). Using 100µM HCy with co-application of 2µM Mk801 there was no significant results with CV assay 75.4 ± 13.4% (P=0.193, n=4; Figure 4.4a) Using LDH it was shown that 100µM HCy caused a 124.0 ± 7.9% increase in LDH (P=0.04, n=6; Figure 4.4c), there was no significant increase when 2µM Mk801 was co-applied 124.9 ± 5.6% (P=0.057, n=6; Figure 4.4c). HCy = homocysteine, HCy-T = homocysteine thiolactone, LDH = lactate dehydrogenase, CV assay = crystal violet assay.

4.2.5 Homocysteine thiolactone toxicity is ameliorated by blockade of the NMDA receptor with D-L APV

Retinoic acid differentiated SH-SY5Y cells were incubated with either 50 or 100μM HCy-T (refer to figure 4.3) alone or in combination of 200μM competitive NMDAR antagonist, D-L APV (187). As above there was a significant decrease in cell number relative to control after 120h incubation with 200μM HCy (68.9 ± 7.4%, P=0.412, n=2; Figure 4.4a), but very little difference detected following co-administration of APV 69.3 + 1.7% decrease in survival relative to control although the latter was no longer statistically significantly different to control (P=0.101, n=2; Figure 4.4a). The data derived from LDH assay clearly showed that HCy increases membrane permeability with a 114.0 ± 1.0% increase relative to the untreated control after 120h (P=0.006, n=4; Figure 4.5c). However, when APV was co-administered with HCy, none of the concentrations were significantly increased compared to untreated control with 200μM showing an increase to 116.3 ± 2.6% increase in LDH (P=0.067, n=4; Figure 4.5c). In confirmation of the previous findings there was no decrease in SH-SY5Y viability with 50μM HCy-T (Figure 4.4b, d). As above there was a significant decrease in cell number relative to control after 120h incubation with 200μM HCy-T 70.4 ± 3.3%, (P=0.014, n=5; Figure 4.4b), but very little difference detected following co-administration of APV 92.8 + 11.3% decrease in survival relative to control although the latter was no longer statistically significantly different to control (P=1.000, n=5; Figure 4.4b). The data derived from LDH assay clearly showed no significant increase relative to the untreated control after 120h (P=0.298, n=8; Figure 4.5d). Together the data demonstrate that the HCy or HCy-T treated cultures did not significantly differ from those co-treated with 200μM D-L APV.

Figure 4.5 Cell death is not ameliorated with D-L APV

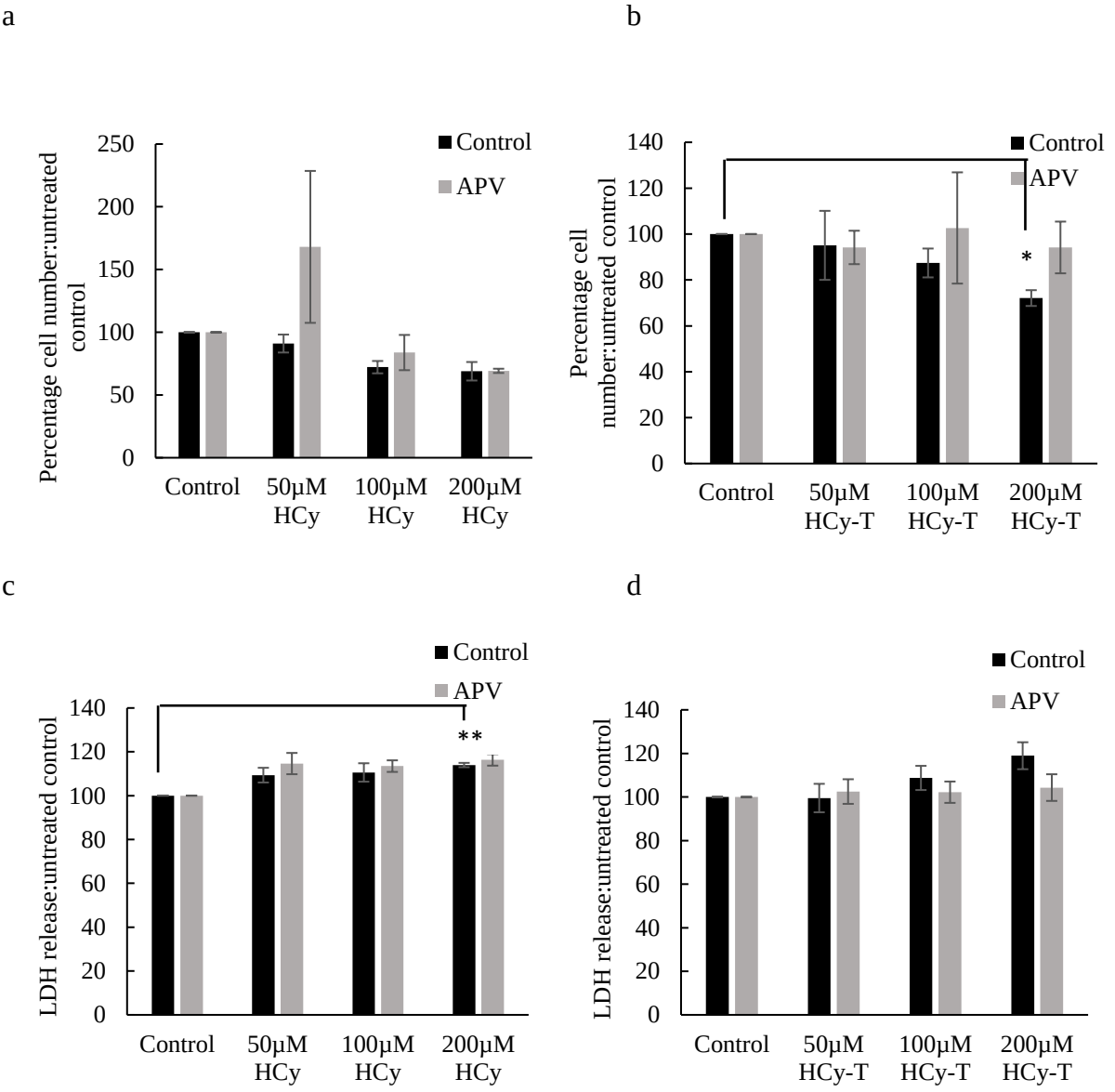

Figure 4.5 shows a significant decrease in cell number relative to control after 120h incubation with 200µM HCy 68.9 ± 7.4% (P=0.412, n=2; Figure 4.5a) but very little difference detected following co-administration of APV 69.3 + 1.7% decrease in survival relative to control; Figure 4.5a although the latter was no longer statistically significantly different to control (P=0.101, n=2; Figure 4.5a). Figure 4.5c showed that HCy increases membrane permeability with a 114.0 ± 1.0% increase relative to the untreated control after 120h (P=0.006, n=4; Figure 4.5c). However, in the presence of 200µM APV there were no significant differences in any condition, with 200µM showing an increase to 116.3 ± 2.6% increase in LDH (P=0.067, n=4; Figure 4.5c). In confirmation of the previous findings there was no decrease in SH-SY5Y viability with 50µM HCy-T Figure 4.4b, d. As above there was a significant decrease in cell number relative to control after 120h incubation with 200µM HCy-T 70.4 ± 3.3% (P=0.014, n=5; Figure 4.4b) but very little difference detected following co-administration of APV 92.8 + 11.3% decrease in survival relative to control although the latter was no longer statistically significantly different to control (P=1.000, n=5; Figure 4.4b). The data derived from LDH assay clearly showed no significant increase

relative to the untreated control after 120h (P=0.298, n=8; Figure 4.5d). HCy = homocysteine, HCy-T = homocysteine thiolactone, LDH = lactate dehydrogenase, CV assay = crystal violet assay.

4.2.6 Homocysteine thiolactone and homocysteine toxicity is not potentiated by co-administration of NMDA receptor co-agonist glycine

As HCy is a partial antagonist of the NMDAR through its actions on the glycine binding site of the receptor, it has previously been documented that co-administration of glycine with HCy potentiates its neurotoxicity as glycine out-competes HCy for access to the co-agonist site (112). Differentiated SH-SY5Y cells were cultured with a range of concentrations from 0 to 100μM HCy together with 100μM glycine (Figure 4.6a-d). There was a significant decrease in cell number relative to control after 120h incubation with 100μM HCy (72.9 ± 1.6% P=0.006, n=8; Figure 4.6a), following co-administration of glycine, 100μM showed no further reduction to 60.1 ± 7.7 (P=0.145, n=4; Figure 4.6a). The data derived from LDH assay clearly showed that 200μM HCy increases membrane permeability to 121.8 ± 3.9% relative to the untreated control after 120h (P=0.039, n=4; Figure 4.5c). When co-applied with glycine, no concentrations were significantly increased compared to untreated control with 200μM HCy with 100μM glycine showing an increase to 134.0 ± 6.1% increase in LDH was detected (P=0.140, n=4; Figure 4.5c). There was a significant decrease in cell number relative to control after 120h incubation with 100μM HCy-T 65.2 ± 10.4%, (P=0.603, n=8; Figure 4.4b), but very little difference detected following co-administration of glycine 54.8 + 13.4% decrease in survival relative to control (P=0.023, n=4; Figure 4.4b). The data derived from LDH assay clearly showed no significant increase relative to the untreated control after with concentrations up to 100μM HCy-T at 120h to 116.8 ± 7.3% (P=0.509, n=3; Figure 4.5d). However, when 100μM glycine was added in conjunction there was no significant increase in lactate dehydrogenase released at any concentration to 122.7 ± 10.2% (P=0.899, n=3; Figure 4.5d).

Taken together, glycine has not been shown to potentiate both HCy and HCy-T toxicity as determined by CV and LDH assays.

Figure 4.6 Homocysteine thiolactone and homocysteine toxicity is not potentiated by co-administration of NMDA receptor co-agonist glycine

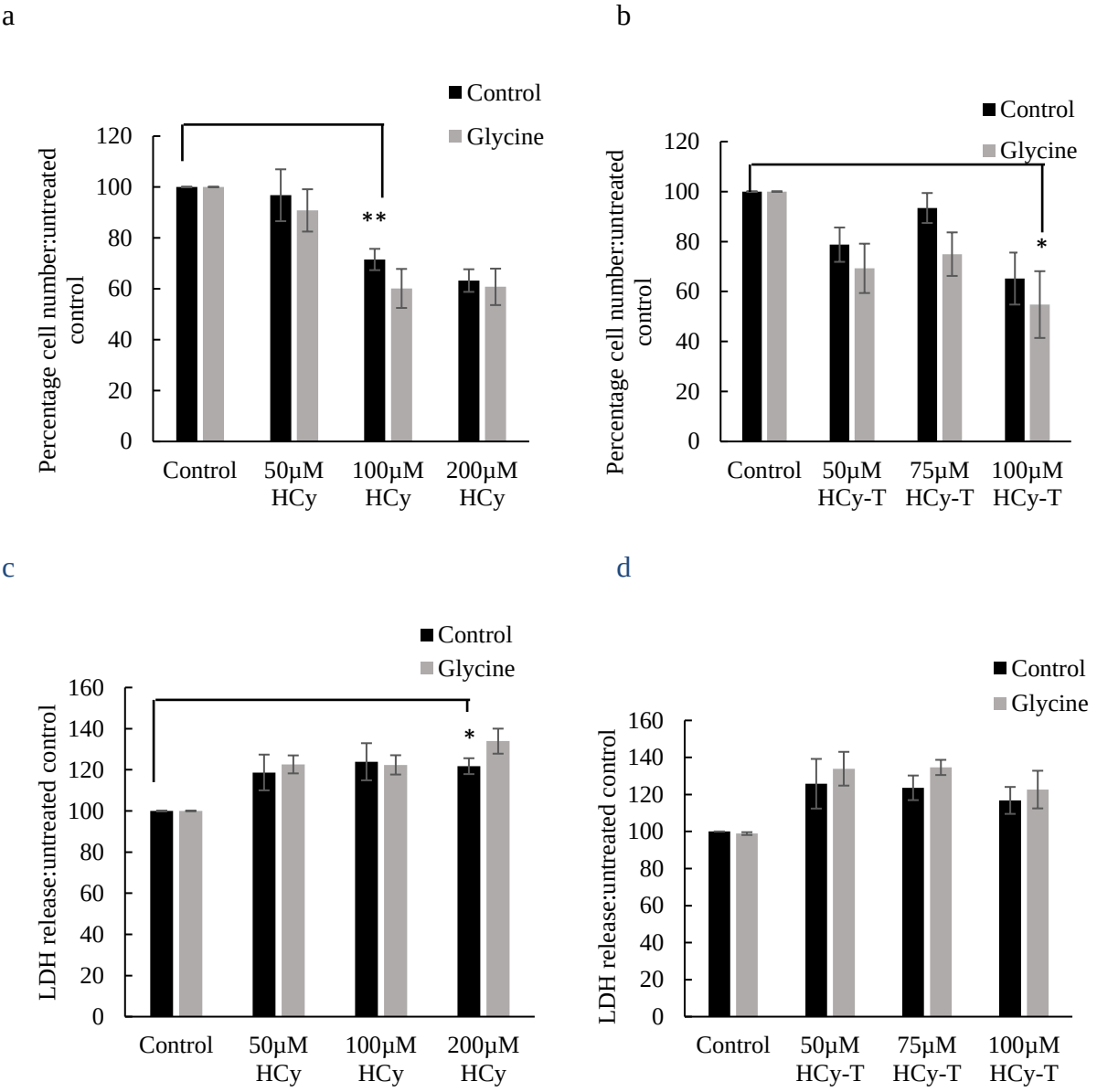

Figure 4.6 5 shows a significant decrease in cell number relative to control after 120h incubation with 100µM HCy 63.2 ± 4.4% (P=0.006, n=8; Figure 4.6a) co-application of glycine showed no significant reduction to 60.1 ± 7.7 (P=0.145, n=4; Figure 4.6a). The data derived from LDH assay clearly showed that 200µM HCy increases membrane permeability to 121.8 ± 3.9% increase relative to the untreated control after 120h (P=0.039, n=4; Figure 4.5c). However, in the presence of glycine, co-administration of no concentrations of HCy were significantly increases compared to untreated control with all concentrations tested showing an increase to 134.0

± 6.1% increase in LDH was detected which was not different to control (P=0.140, n=4; Figure 4.5c). 100μM HCy-T showed a reduction in cell number to 65.2 ± 10.4%, (P=0.603, n=8; Figure 4.4b), but very little difference detected following co-administration of glycine 54.8 + 13.4% decrease in survival relative to control (P=0.509, n=4; Figure 4.4b). The data derived from LDH assay clearly showed no significant increase relative to the untreated control after with concentrations up to 100μM HCy-T at 120h to 116.8 ± 7.3% (P=0.518, n=3; Figure 4.5d). However, when 100μM glycine was added in conjunction there was no significant increase in lactate dehydrogenase released at any concentration of HCy-T to 122.7 ± 10.2% (P=0.899, n=3; Figure 4.5d) HCy = Homocysteine, HCy-T = homocysteine thiolactone, CV=crystal violet assay, LDH = lactate dehydrogenase.

4.2.7 Homocysteine thiolactone toxicity is not potentiated by co-administration of NMDA receptor co-agonist D-serine

As it was shown that glycine potentiated HCy and HCy-T toxicity, it was important to determine if other agonists of the NMDA receptor had the same effect. Therefore, to further substantiate whether the NMDAR was central to HCy-T-mediated neurotoxicity, differentiated SH-SY5Y cells were cultured with a range of concentrations of from 0 to 200μM HCy or HCy-T together with 10μM D-serine (266) (Figure 4.7a-d). There was a significant decrease in cell number relative to control after 120h incubation with all concentrations up to 200μM HCy 63.2 ± 4.4% (P=0.001, n=8; Figure 4.7a), but no difference could be determined following co-administration of D-serine 59.8 + 15.6% (P=0.092, n=4; Figure 4.7a). The data derived from LDH assays showed a significant increase with 200μM HCy in LDH to 115.1 ± 18.5% (P=0.033, n=4; Figure 4.7c). There was again no difference with co-administration of D-serine at any of the concentrations of HCy tested, with 200μM HCy showing no significant difference (P=0.380, n=2; Figure 4.7c). There was no significant decrease in cell number relative to control after 120h incubation with 100μM HCy-T (65.2 ± 10.4%, (P=0.603, n=8; Figure 4.7b), and no difference detected following co-administration of D-serine 57.4 + 14.7% (P=0.382, n=4; Figure 4.7b). The data derived from LDH assay clearly showed no significant increase relative to the untreated control after with concentrations up to 100μM HCy-T at 120h to 107.7 ± 10.2% (P=0.819, n=4; Figure 4.5d). However, when 10μM D-serine was added in conjunction there was still no significant increase in lactate dehydrogenase released at any

concentration of HCy-T (P=0.380, n=4; Figure 4.5d). Therefore, application of D-serine does not exacerbate cell death induced by either HCy or HCy-T.

Figure 4.7 Homocysteine thiolactone and homocysteine toxicity is not potentiated by co-administration of NMDA receptor co-agonist D-serine

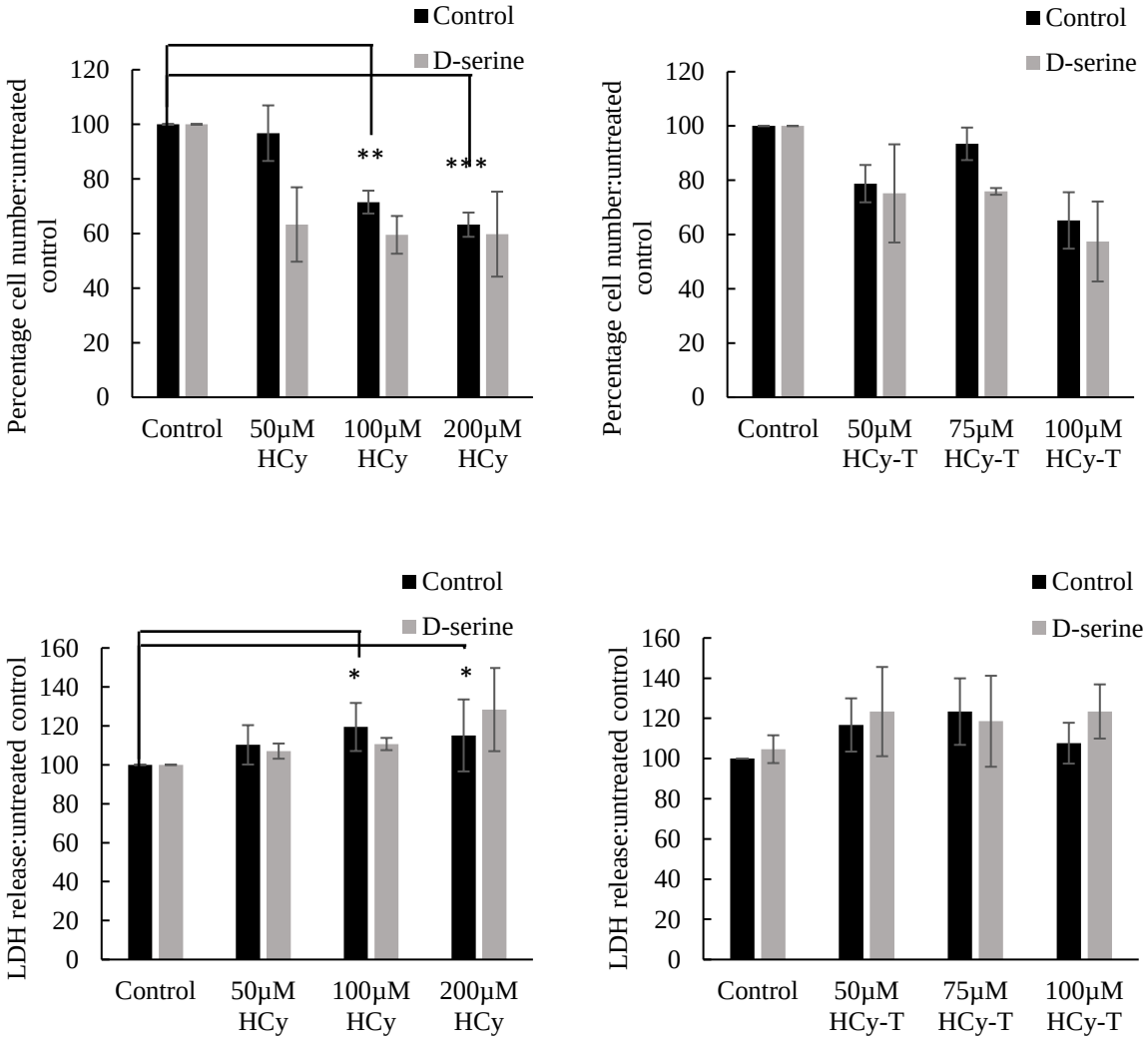

Figure 4.7 shows a significant decrease in cell number relative to control after 120h incubation with 200µM HCy 63.2 ± 4.4% (P=0.001, n=8; Figure 4.6a) co-application of co-administration of D-serine 59.8 + 15.6% (P=0.092, n=4; Figure 4.7a). The data derived from LDH assays showed a significant increase with 200µM HCy in LDH to 115.1 ± 18.5% (P=0.033, n=4; Figure 4.7c). There was still no difference with co-administration of any of the concentrations of HCy showing 128.4 ± 21.4% increase in LDH (P=0.380, n=2; Figure 4.7c). There was a significant decrease in cell number relative to control after 120h incubation with 100µM HCy-T (65.2 ± 10.4%, (P=0.603, n=8; Figure 4.7b), but very little difference detected following co-administration of D-serine 57.4 + 14.7% (P=0.382, n=4; Figure 4.7b). The data derived from LDH assay clearly showed no significant increase relative to the untreated control after with concentrations up to 100µM HCy-T at 120h to 107.7 ± 10.2% (P=0.819,

n=4; Figure 4.5d). However, when 10μM D-serine was added in conjunction there was still no significant increase in lactate dehydrogenase released at any concentration of HCy-T to 123.4 ± 13.5% (P=0.380, n=4; Figure 4.5d). HCy = homocysteine, HCy-T = homocysteine thiolactone, LDH = lactate dehydrogenase, CV assay = crystal violet assay.

4.2.8 Homocysteine thiolactone alters downstream signalling of NMDA receptor

Although HCy has been shown to act at the glutamate binding site of the NMDA receptor (112), the downstream signalling activated is ultimately different from glutamate *per se*. Under excitotoxic conditions when glutamate binds the NMDA receptor, it causes a transient phosphorylation of extracellular (ERK) within 2.5 minutes of application. When HCy is added, the phosphorylation of ERK in the first few minutes is mimicked however there is a subsequent increase in pERK 2-6 hours post application which is not seen when glutamate is added (151). To determine whether HCy-T altered the same downstream signalling as that seen with HCy, ELISA was used to determine the levels of phosphorylated ERK from protein extracted at a range of timepoints. The results showed a 138.9% ± 6.3% (P=0.001, n=13; Figure 4.8a) increase in phosphorylated ERK after 2.5 minutes. This returned to the same as control conditions between 2.5 to 5 minutes and continued to increase again at 6 hours with a significant increase of 237.1% ± 29.8% at 6 hours post treatment (P=0.005, n=13; Figure 4.8a). This is a similar pattern to that observed by other authors with HCy though not with glutamate (153).

Figure 4.8 Homocysteine thiolactone induces ERK activation both transiently and chronically

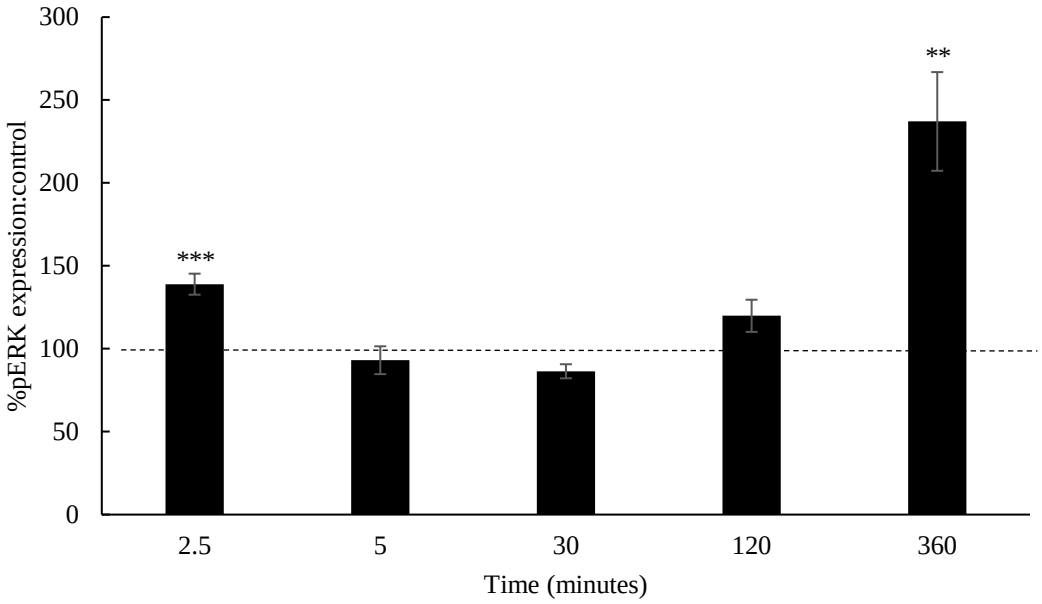

Figure 4.6 showed an ELISA depicting the timecourse of ERK activation. This showed an increase at 2.5 minutes to 138.9% ± 6.3% (P=0.001, n=13; Figure 4.8) which is indicative of a transient ERK activation, similar to that seen in HCy. This returned to the same as control conditions between 5 minutes and began to increase again at 2 hours with a significant increase of 237.1% ± 29.8% (P=0.005, n=13; Figure 4.8) at 6 hours post treatment. ERK = Extracellular Signal-regulated Kinase-1, HCy = homocysteine.

4.3 Discussion

HCy exerts neurotoxicity via binding and activation of the NMDA receptor and is a partial antagonist at the glycine binding site. Using the cell differentiation protocol as outlined in chapter 3, the results have shown that HCy is neurotoxic at the NMDA receptor as previously shown by other authors, in other cell types (121,150,267,268). Initial experiments focussed on the use of undifferentiated SH-SY5Y cells, however cell death was not observed. As in other cell types, such as HT22 cells, many neuronal features are not expressed. Initial experiments focussed on the GluN2A receptor subunit of the NMDA receptor as this has been shown to be the receptor HCy exerts actions upon, GluNR2B containing subunits are predominantly glutamate activated and therefore not examined in this experiment (155). Using ELISA, the GluN2A subunit is shown to be upregulated upon differentiation in keeping with other cell types (211). Although this is unlikely to be the only factor impairing HCy toxicity to undifferentiated cells. Compared to neurons, neuroblastoma cell lines can be difficult to induce cell death in, it is therefore unsurprising that upon differentiation, the cells become more sensitive to stress. Furthermore, differentiation prior to HCy application made this more representative of elevated HCy in the brain.

HCy-T is most commonly researched due to its ability to cause homocysteinylation and exert toxicity in the CNS via its effects within the vasculature (255). It was important to first determine at what concentration HCy and HCy-T were toxic within these cells, both HCy and HCy-T were neurotoxic at 100μM. When using higher concentrations of HCy-T, cell viability assay was not possible due to high variability. As mentioned before, D-L HCy and HCy-T were used, the dose expressed is half that stated as only the L-isoform of HCy is toxic, thus toxicity was observed at 50μM. This is the concentration at the upper range of being a risk factor for CVD and classified as mild to moderate hyperhomocysteinemia (269) To determine if HCy-T was neurotoxic via the same or distinct mechanisms as HCy, a selection of experiments

previously conducted using HCy were repeated. These included using Mk801 and APV which have shown that blockade of the receptor reduces cell death induced by HCy (142, 256, 263). This was done for HCy to show that these results are in keeping with the literature, HCy-T was tested as this has not been shown before in neurons. The addition of NMDA receptor channel blocker reduces the seizure incidence in rats who had been exposed to HCy-T (265). Furthermore, blocking NMDA receptors in vascular tissue reduces the toxic effects of HCy (271). It was therefore likely that this would be the case within neurons. Figure 4.4 and 4.5 show the effects of both HCy and HCy-T in the presence of Mk801 and the competitive antagonist APV, all conditions showed a significant increase in cell death as determined by LDH and CV with HCy and HCy-T alone. This was not the case with the addition of Mk801 with both HCy and HCy-T and APV only effective in blockade of HCy toxicity. Therefore, HCy has a more potent action upon the NMDA receptor than HCy-T in this cell type, glycine had no additive effect. However, blockade of the receptor itself does not conclusively indicate that HCy-T binds the receptor. With both HCy and HCy-T, the reduction in cell death was modest by comparison to the experiments that had been replicated, however several of these had used much higher concentrations of HCy (96).

A subsequent method used to determine that HCy neurotoxicity involves NMDA receptors is the addition of glycine. As HCy is a partial agonist at the glycine binding site of the NMDA receptor, when glycine levels are elevated, HCy becomes neurotoxic at much lower concentrations as it can no longer act as an antagonist at the glycine binding site (112). Therefore, experiments using an excess of glycine were repeated in the differentiated SH-SY5Y cells with both HCy and HCy-T. With both metabolites, there was an exacerbation of neuronal cell death however, this was more marked with HCy treated cultures. This further implicates HCy-T acting at the same sites as HCy, however this was only supported in the LDH assay at low concentration HCy-T. D-serine acts as a co-agonist at the glycine binding site of

the NMDA receptor, therefore it is possible this may have also enhanced neurotoxicity induced by HCy and HCy-T, as was achieved with the application of glycine. However, no significant differences were observed in any condition. The final area to be examined was the downstream signalling upon activation of the NMDA receptor. Upon application of HCy, there was an increase in the levels of phosphorylated ERK, this occurred in a different time frame to that observed upon glutamate binding (figure 1.2). When glutamate binds the NMDA receptor, there is a transient phosphorylation of ERK between 2 and 5 minutes which returns to baseline HCy causes the same transient increase which returns the baseline then increases again after a period of 6 hours (153). As this required almost 100 protein samples, only HCy-T was examined, the same timeframe of ERK phosphorylation was observed.

Taken together, this strongly suggests that HCy-T does have neurotoxic properties that mimic NMDA receptor, although this is not as potent as HCy itself. This could be a result of the difference in structure compared to HCy as HCy-T is cyclic. Alternatively, HCy-T may modulate NOS activity, thereby enhancing the sensitivity of the NMDA receptor to further stimulation as will be discussed in more detail in chapter 5. HCy-T is also known to increase ROS generation and oxidative stress, blockage of the NMDA receptor can reduce cell stress therefore these results may be a generic reduction in ROS by blocking the NMDA receptor and not necessarily related to any interaction between the two.

CHAPTER 5: EFFECTS OF HOMOCYSTEINE AND HOMOCYSTEINE-THIOLACTONE ON OXIDATIVE AND NITROSYLATIVE STRESS

5.1 Introduction

Mitochondrial abnormalities are present in age-related diseases; such as AD, prior to symptom onset (198). The mitochondria are the powerhouse of the cell and are responsible for energy generation in the form of ATP (272). The mitochondria are also the main contributor to the generation of reactive oxygen species (ROS), a by-product in the generation of ATP (273). ROS is responsible for causing cellular damage to DNA, RNA and proteins (274). The cells have the capacity to deal with ROS generation and the associated cellular damage, through their own antioxidant capacities. However, if there is an imbalance between the generation and removal of these toxic species, cellular damage will occur (275).The mitochondria are highly dynamic organelles and may be recruited to any area of the cell, as required for cellular processes (184). Furthermore, the mitochondria can undergo the processes of fusion and fission for the generation of new mitochondria or under conditions of stress (276). These processes are regulated by several proteins such as Mfn1 and fis1 which are regulated by several genes (277).

Under conditions where cellular stress has been induced by treating with neurotoxins, the mitochondria can undergo excessive fusion or fission. This impairs the function of the mitochondria as a network and can impair the cells ability to generate energy which ultimately leads to cell death. Furthermore, when the cells are under stress, it has been shown in cells that there is an increase in the generation of ROS and subsequent oxidative damage. The mitochondria have a gradient to allow the transition of ions through the membrane, in an excitotoxic event, which disrupts the mitochondrial membrane potential and therefore the overall function of the mitochondria (278). There has been little research to date about the effect of HCy or HCy-T on mitochondrial kinetics.

In addition to mitochondrial dysfunction, NO is a gaseous modulator within the CNS and the vasculature (163), and is generated by nitric oxide synthases (NOS); enzymes categorised by

anatomical location and named for the properties that they possess. These are as follows: endothelial NOS (eNOS), inducible NOS (iNOS) and neuronal NOS (nNOS) (164). There is some research suggesting that there may be an entity known as mitochondrial NOS, but this is disputed, and some authors believe that this may in fact be a variation of another NOS isoform (270, 272). This debate results from the action the NO has within the mitochondria to disrupt mitochondrial respiration, it has been found in some preparations that the mitochondria may be capable of generating NO. If this is the case that would require NOS to be present within the mitochondria however, none of the NOS isoforms contain a sequence to cross into the mitochondria, suggesting an entity to be known as mitochondrial NOS. However, this has not been found using western blot analysis or sequencing. eNOS is predominantly found within the vasculature, and is responsible for the induction of vasodilation (161), it is not widely expressed within the CNS in comparison to nNOS and iNOS and was therefore not examined by this study. iNOS is activated in a calcium dependent manner and predominantly occurs within the nervous system (170). The final generator of NO: nNOS, is calcium independent (268), and the effect of elevated HCy on iNOS and nNOS were examined as part of the current study.

NO has several actions in the brain, one of which is to modulate NMDA receptor activity. NOS enzymes can be activated in response NMDA activation, thus resulting in an increase in NO generation (280). HCy is also reported to alter NO signalling and NO can cause an increase in the generation of ROS from the mitochondria and therefore indirectly increase oxidative stress and oxidative damage (281). This may in part be mediated by activation of the NMDA receptor, which can both affect NOS signalling and mitochondrial wellbeing by modulating the influx of calcium post activation (279). The effect that HCy has on NO generation has been extensively studied with respect to CVD (282–284).

Scavenging NO from cells which had been treated with HCy has proven effective in preventing neuronal cell death (285), thereby indicating a possible role of HCy in NO generation. Furthermore, HCy-T is known to generate high levels of peroxynitrite through PON1 activation (135), therefore it was important to determine if scavenging peroxynitrite would ameliorate the deleterious effects of HCy-T. This study aims to assess whether HCy-T also modulates NO signalling, and if it causes the same effects as reported with HCy within differentiated SH-SY5Y cells, and furthermore, whether HCy influences NOS expression. The categorisation of the mitochondrial network dynamics is based on a paper by Wappler and colleagues, and defines the mitochondria as highly interconnected, rounded, normal or poorly labelled and therefore this was adopted for categorisation within these experiments (198).

As both nitrosylative and oxidative stress have been implicated in HCy-induced cellular damage it was important to determine if, in SH-SY5Y cells, HCy and HCy-T caused an increase in NO and ROS generation. The potential role of RNS and ROS in HCy and HCy-T-mediated cell death was explored by pharmacological modulation of NO and ROS levels. As changes to expression of NOS isoforms could underpin the previously reported NO-mediated cell death in response to HCy, the levels of nNOS and iNOS were analysed in HCy and HCy-T-treated neurons. Finally, as mitochondrial dynamics are robustly altered under conditions of cellular stress, the effects of HCy and HCy-T on mitochondrial networks was examined. Together these experiments aimed to determine whether HCy and HCy-T mediate changes in the generation of NO or ROS and whether their known deleterious effects involved changes in the mitochondrial network.

5.2 Results

5.2.1 Neither metabolite (homocysteine or homocysteine thiolactone) modulates the expression of neuronal NOS or inducible NOS

It has previously been reported that HCy-T toxicity is increased by inhibition of iNOS (286), and that NO plays a crucial role in HCy-mediated neuronal death. Therefore, to determine if either metabolite altered iNOS or nNOS expression ELISA was used, it was determined that there was no significant effect of the application of 100μM HCy-T on nNOS expression, 83.6 ± 41.1% relative to untreated control (P=0.470, n=3; Figure 5.1a), and there was also no effect of HCy-T on iNOS 123.3 ± 47.6% expression relative to untreated control (P=0.650, n=3; Figure 5.1b). Additionally, there was no significant effect of the application of 100μM HCy on nNOS expression, 82.2 ± 41.1% relative to untreated control (P=0.470, n=3; Figure 5.1a) or on iNOS 97.7 ± 47.6% relative to untreated control (P=0.650, n=3; Figure 5.1b). Thus, the reported NO-mediated effects of HCy and HCy-T are not underpinned by changes in the expression of either nNOS or iNOS protein.

Figure 5.1 Effects of homocysteine or homocysteine thiolactone on expression of neuronal NOS and inducible NOS

a

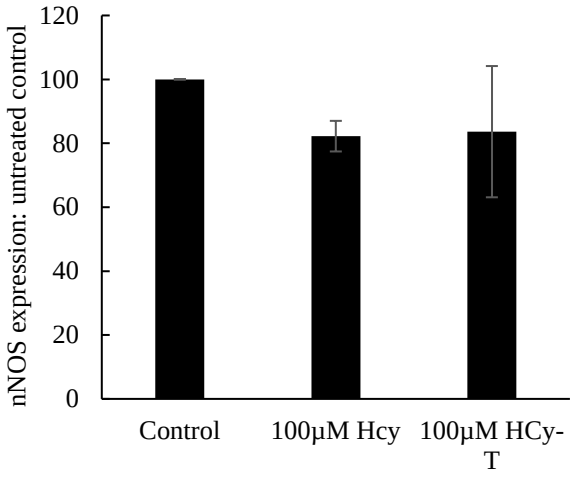

b

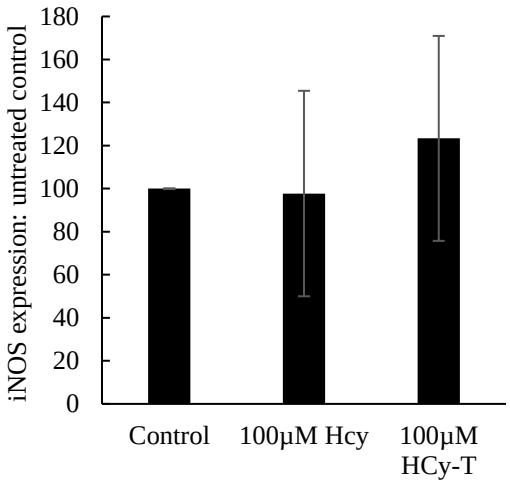

Figure 5.1a shows the effects of the application of 100µM HCy and HCy-T on the expression of nNOS1 enzyme found within neuronal tissue. eNOS was not examined as this is not a predominant form in neuronal tissue. This shows there was no significant effect with the application of HCy 82.2 ± % (n=3 *P*=0.) or HCy-T on nNOS expression, 83.6 ± 41.1% (*P*=0.470, n=3; Figure 5.1a). Figure 5.1b shows there was no effect of HCy on iNOS 97.7 ± % (*P*=0., n=3; Figure 5.1b) There was also no effect of HCy-T on iNOS 123.3 ± 47.6%, (*P*=0.650, n=3; Figure 5.1b). HCy= homocysteine, HCy-T = homocysteine thiolactone, NOS = nitric oxide synthase, nNOS = neuronal nitric oxide synthase, iNOS = inducible nitric oxide synthase.

5.2.2 Homocysteine and homocysteine thiolactone do not increase nitric oxide generation in SH-SY5Y cells

To determine if HCy or HCy-T altered the generation of NO either acutely (after 3 hours incubation) or chronically (after 48 hours incubation), a cell-permeable dye used to detect NO generation, 4,5-Diaminofluorescein diacetate (DAF2-DA; 1µM), and the relative fluorescence intensity per cell was measured. An intermediate (24 hour) time point was also investigated. Thus, cells were treated with two concentrations of HCy or HCy-T, 100 and 200µM, for 3, 24 and 48 hours. DAF-2DA was added to the cells for 15 minutes at the end of the treatment time to determine if the treatments had altered the rate of NO generation. There was no significant

change in NO levels following 3 hours of HCy treatment (178.1 ± 59.7% for 100µM relative to untreated control (P=0.484, n=5; Figure 5.2a-b) and 179.8 ± 53.3% (P=0.469, n=5; Figure 5.2a, b) for 200µM. Similarly, there was no significant change observed at 24 hours, with 100µM giving 94.0 ± 22.5% (P=0.964, n=5; Figure 5.2a, b) and 200µM showing 146.2 ± 35.7, P=0.617, n=5; Figure5.2a, b). Similar data was obtained after 48 hours incubation, with 100µM giving 126.5 ± 30.0% (P=0.918, n=5; Figure 5.2a, b), and 200µM showing 182.8 ± 61.3% (P=0.371, n=5; Figure 5.2a, b). HCy-T also did not modulate NO generation with 116.2 ± 12.5% of control levels observed after 3 hours application of 100µM HCy-T (P=0.889, n=6; Figure 5.2a-b) and 179.8 ± 53.3% of control levels observed after 3 hours application of 200µM (P=0.295, n=6; Figure 5.3a-b). Again, no significant difference was observed after 24 hours with 100µM giving 147.2 ± 27.3% of control levels (P=0.429, n=6 Figure 5.2a-b), and 200µM showing 152.0 ± 38.1% of control levels (P=0.429, n=5; Figure 5.2a-b). Finally, at 48 hours no significant difference was detected at 100 µM (P=0.755, n=5; Figure 5.2a-b) or 200 µM (P=0.565, n=5; Figure 5.2a -b). The data from these experiments was highly variable therefore these experiments was repeated several times. Thus, despite a robust analysis of approximately 5 coverslips per condition on each occasion and 5-6 biological repeats, there was no statistically significant difference in the levels of NO generation in these cells in response to 100 or 200µM of either HCy or HCy-T.

Figure 5.2 Effects of homocysteine on nitric oxide generation

a

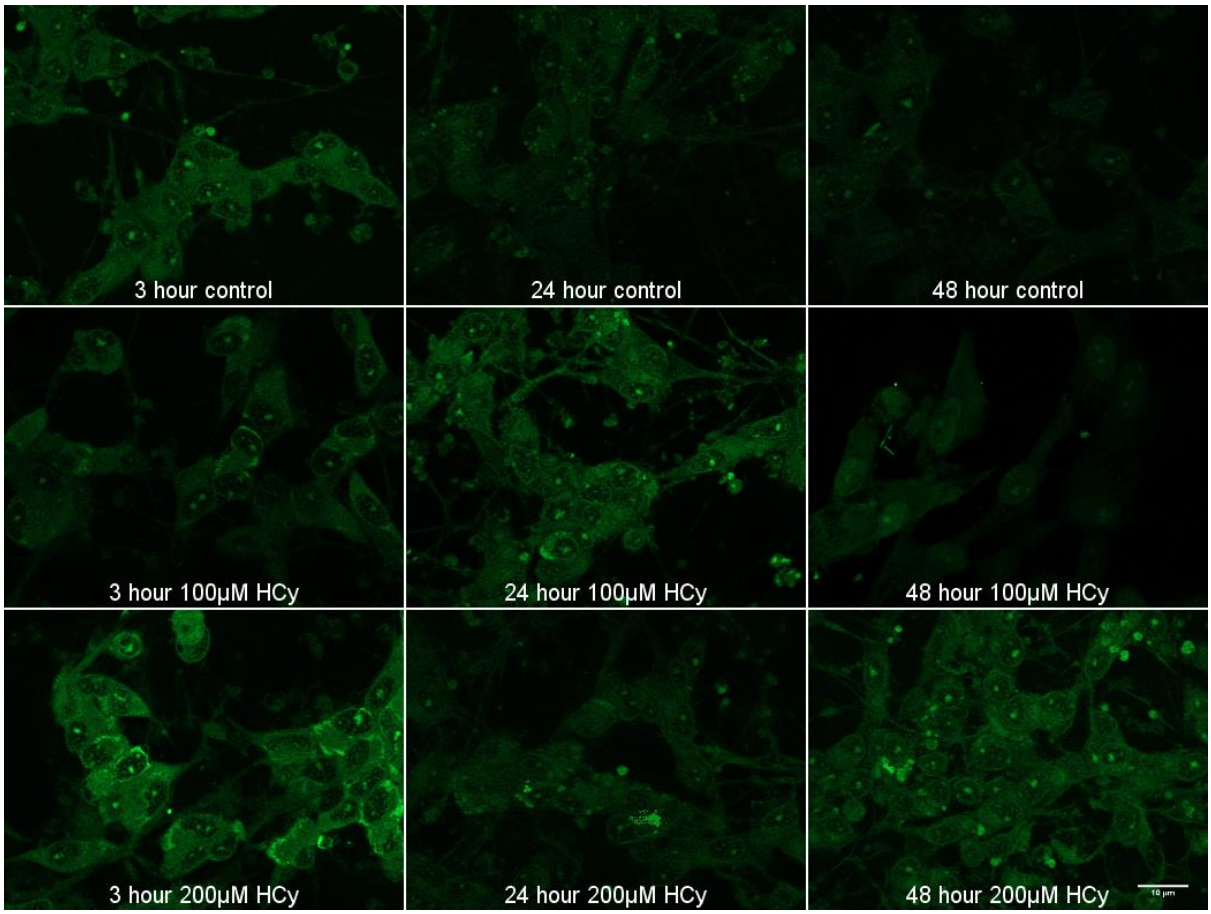

b

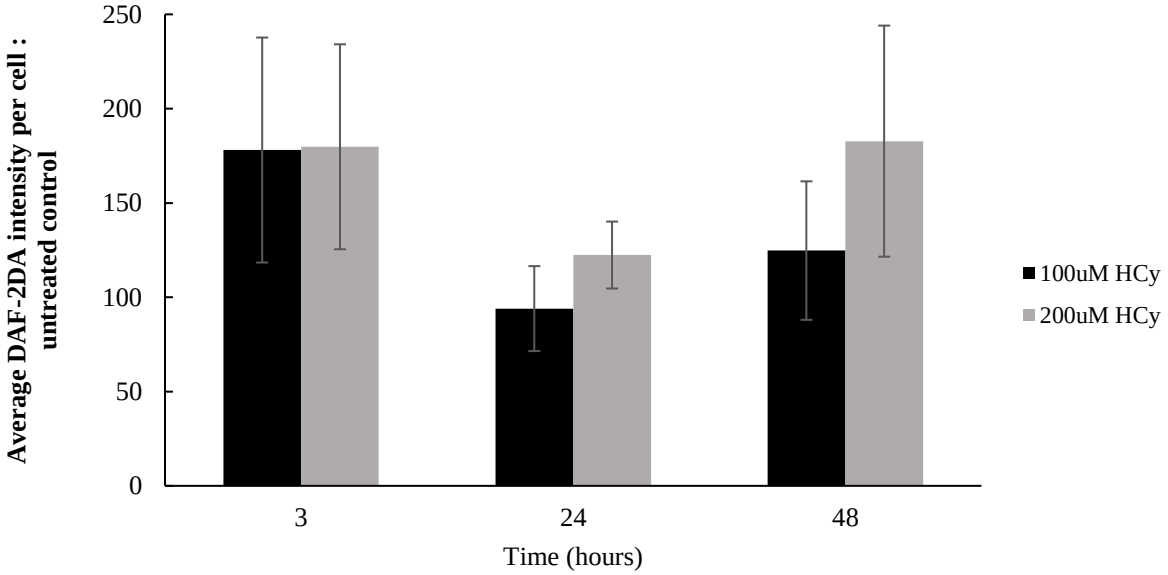

Figure 5.2a shows the effect on increase concentration of HCy of 0, 100 and 200µM respectively at 3 hours and at 24 hours and 48 hours. The generation of NO as determined by the dye, DAF2-DA, these are the images obtained. When quantified as average fluorescence per cell this was plotted as figure 5.2b this showed no change, 178.1 ± 59.7% for 100µM (P=0.484, n=5; Figure 5.2b) and 179.8 ± 53.3% (P=0.469, n=5; Figure 5.2b) for 200µM at 3 hours post application. No change was observed at 24 hours with 100µM giving 94.0 ± 22.5% (P=0.964, n=5; Figure 5.2b) at 24 hours. 200µM at 48 hours giving an increase of 182.8 ± 61.3% (P=0.371, n=5; Figure 5.2b). However, despite an almost 2-fold increase no significant results were obtained (n=5). HCy = homocysteine, NO = nitric oxide, DAF2-DA = 4,5-Diaminofluorescein diacetate.

Figure 5.3 Effects of homocysteine thiolactone on nitric oxide generation

a

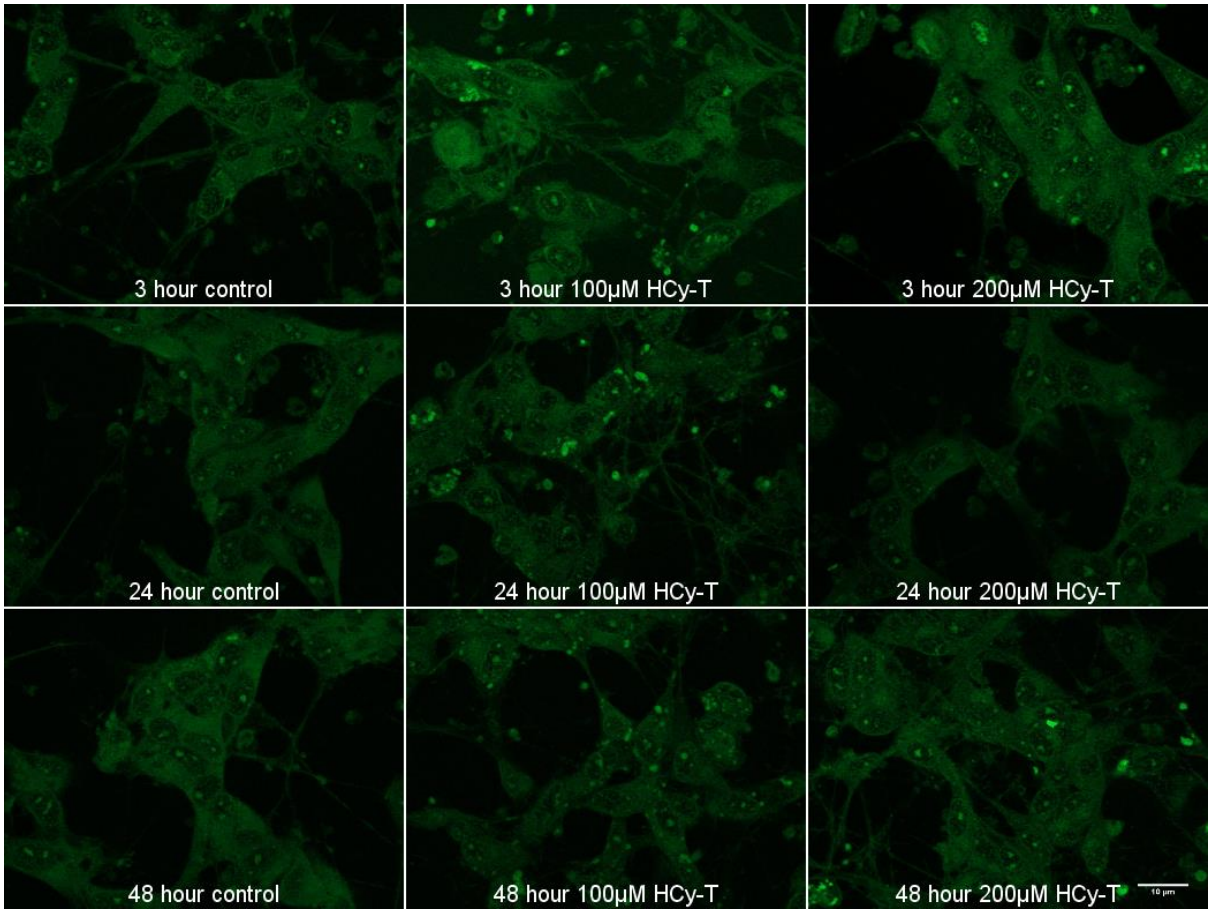

b

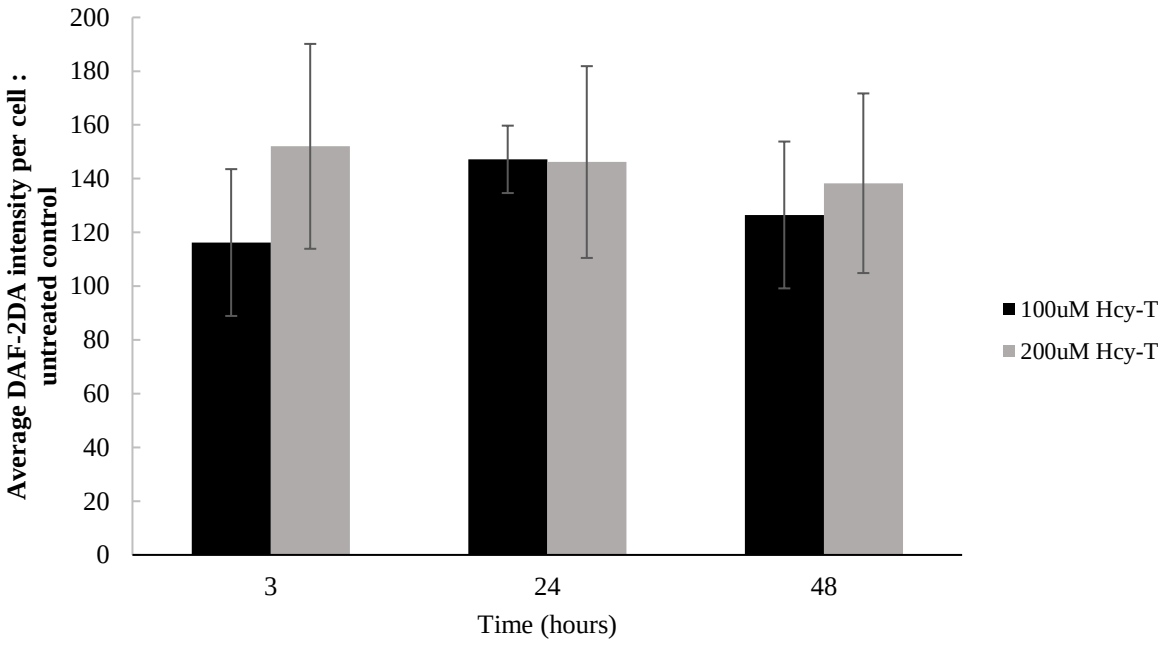

Figure 5.3a shows images obtained from a time course and dose response for the generation of NO as determined by the dye, DAF2-DA. When plotted as average fluorescence per cell, this showed no change of 116.2 ± 12.5% for 100µM HCy-T (P=0.889, n=6; Figure 5.3b) and 179.8 ± 53.3% for 200µM (P=0.295, n=6; Figure 5.3b) at 3 hours post application. This showed an increase at 24 hours with 100µM giving 147.2 ± 27.3% (P=0.429, n=5; Figure 5.3b), matched with 200µM. This increase was maintained with both concentrations; at 48 hours no significant result was obtained at 100 µM (P=0.755, n=5; Figure 5.3b) and 200 µM (P=0.565, n=5; Figure 5.3b). HCy-T = homocysteine thiolactone, NO = nitric oxide, DAF2-DA = 4,5-Diaminofluorescein diacetate.

5.2.4 Scavenging nitric oxide and peroxynitrite does not ameliorate cell death caused by homocysteine and homocysteine thiolactone in SH-SY5Y cells

It has previously been reported that NO mediates the neurotoxic effects of HCy (285), although the role of NO in HCy-T-mediated neurotoxicity remains to be determined. The data presented above elucidates that neither HCy nor HCy-T upregulate NO generation (Figures 5.2-5.3). Furthermore, neither of these two compounds modulate the expression of the NO generating enzymes iNOS and nNOS (Figure 5.1). Nonetheless the possibility that HCy and/or HCy-T modulate viability by interacting with NO at the level present within these cells remains. Although there is no increase in NO generation, there is NO present within these cells that may be being harnessed to mediate cell death. Therefore, the effects of pharmacological modulators

of NO and its metabolite peroxynitrite on HCy and HCy-T-mediated neurotoxicity was determined.

SH-SY5Y cells were treated with known toxic doses of 100μM HCy or HCy-T (Chapter 3, Figure 3.2), with the addition of 100μM of the nitric oxide scavenger 2-4-carboxyphenyl-4,4,5,5-tetramethylimidazoline-1-oxyl-3-oxide (CPTIO) (285) or 10μM of the peroxynitrite scavenger manganese (III) tetrakis (4-benzoic acid) porphyrin chloride (MnTbap) (285). The CV assay was used to determine cell viability by measuring the number of adherent cells after 5 days treatment with HCy or HCy-T in the presence of peroxynitrite and NO scavengers respectively. The addition of CPTIO or MnTbap alone had a large effect on cell number within these cultures in some experiments, although this was very variable (Figure 5.4b).

In the NO scavenging experiments, 100μM HCy alone resulted in a reduction in cell number to 53.7 ± 3.6% of control survival (P=0.062 n=6; Figure 5.4a) and when NO was scavenged with CPTIO in HCy-treated cultures this resulted in a reduction in cell number of 34.7 ± 1.3% (P=0.017, n=6; Figure5.4a). When peroxynitrite was scavenged in the absence of HCy there was again a variable effect on cell number. In these experiments, 100μM HCy alone resulted in a reduction in cell number to 65.5 ± 13.7% of control survival (P=0.688, n=6; Figure 5.4b). Co-application of MnTbap resulted in 85.5 ± 38.3% viability (P=0.883, n=6; Figure 5.4b). For HCy-T, cell number fell to 60.4 ± 6.2% (P=0.821, n=6; Figure 5.4a), and 53.3 ± 25% (P=0.748, n=6; Figure 5.4a) respectively. This increased to 97.9 ± 43.3% with NO scavenger (P=1.000, n=6; Figure5.4a) and with peroxynitrite scavenger this resulted in 68.8 ± 20.3% (P=0.999, n=6; Figure 5.4b). This could not be supported by LDH assays as there was a problem with the components of the assay and the samples had to be discarded. Furthermore, due to the variation in scavenger alone with both drugs, no conclusive result could be obtained. Together the data obtained does not support a role for NO signalling mediating the downstream effects of HCy or HCy-T in SH-SY5Y cells. However, there does appear to be a variable effect

of scavenging endogenous NO or $ONOO^{\cdot}$ in untreated SH-SY5Y that may be confounding the data.

Figure 5.4 Effects of scavenging nitric oxide or peroxynitrite on either homocysteine or homocysteine thiolactone treatment

a

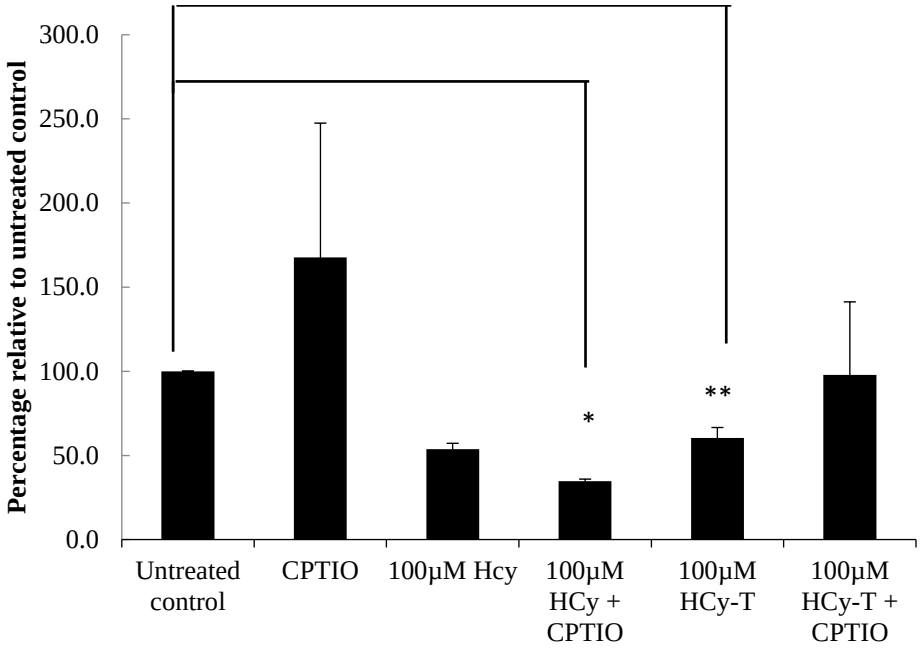

b

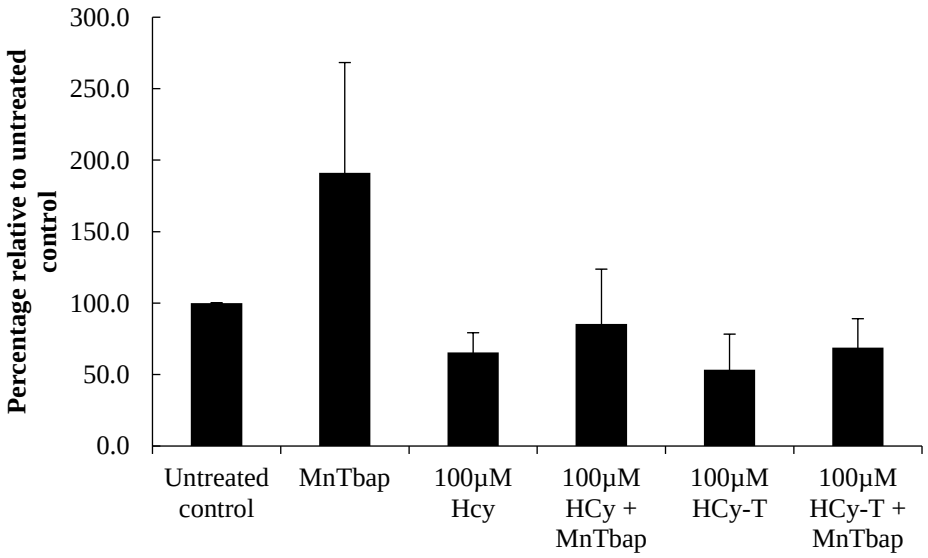

Figure 5.4 HCy alone resulted in a reduction in cell number as determined by CV assay of 53.7 ± 3.6% and 65.5 ± 13.7%, (*P*=0.688, n=6; Figure 5.4b), and when NO was scavenged with CPTIO this resulted in a reduction in cell number of 34.7 ± 1.3% (*P*=0671, n=6; Figure5.4a) and with MnTbap reduction this was 85.5 ± 38.3% viability (*P*=0.883, n=6; Figure 5.4b). For HCy-T, cell number fell to 60.4 ± 6.2% (*P*=0.821, n=6; Figure 5.4a), and 53.3 ± 25% (*P*=0.748, n=6; Figure 5.4a). This was ameliorated to 97.9 ± 43.3% with NO scavenger (*P*=1.000, n=6; Figure5.4a) and with peroxynitrite scavenger this resulted in 68.8 ± 20.3% (*P*=0.999, n=6; Figure 5.4b). HCy =

homocysteine CV = crystal violet, NO = nitric oxide, CPTIO = 2-4-carboxyphenyl-4,4,5,5-tetramethylimidazoline-1-oxyl-3-oxide, MnTbap = manganese (III) tetrakis (4-benzoic acid) porphyrin chloride, HCy-T = homocysteine thiolactone, LDH = lactate dehydrogenase.

5.2.5 Homocysteine thiolactone increases reactive oxygen species generation

Despite the negative data obtained for NO generation, the potential for other ROS rather than NO to mediate the deleterious effects of HCy and/or HCy-T remains. Therefore, the generation of total reactive oxygen species was determined after 48 hours incubation with 100μM of either metabolite using the dye H_2-DCFDA. This is a cell-permeable live cell dye which fluoresces green upon binding to ROS. Because both HCy and HCy-T are likely to interact with the cell via the NMDAR, the NMDAR blocker Mk801 (2μM) was also analysed in these experiments, both alone and in combination with HCy or HCy-T (100μM). Due to the complexities of live-cell imaging, a single concentration of HCy or HCy-T was analysed and 100μM was selected as it exhibits neurotoxicity (Chapter 3, figure 3.2) yet is within the potential physiological range. In these experiments there was a striking effect of Mk801-mediated blockade of the NMDAR. This treatment increased the level of ROS detected from 2356216 ± 490382a.u. in untreated control to 5141105 ± 1244191a.u. in Mk801-treated cells (P=0.001, n=3; Figure 5.5 a-c). This is in keeping with previous studies showing increased ROS generation following Mk801 administration in the rat retrosplenial/posterior cingulate cortex *in vivo* (287). Intriguingly, 100μM HCy did not modulate ROS levels in these cells; 3637922a.u. ± 797758 compared to 2356216 ± 490382a.u. in untreated control (P=0.320, n=3; Figure 5.5b), but it did negate the increase in ROS mediated by Mk801. Thus, cells co-treated with HCy and Mk801 exhibited 3334510 ± 498468a.u. average intensity which, in contrast to the findings for Mk801 alone. The result for the HCy and Mk801 co-treated cultures was not statistically significantly different to untreated control (P=0.992, n=3; Figure 5.5b).

In contrast, HCy-T which showed a significant increase in fluorescence to 4790103± 849961 a.u. compared to the untreated control reading of 2356216 ± 490382a.u. (P=0.003, n=3; Figure

5.5 a, c). This was unchanged in the presence of Mk801 where fluorescence intensity was 4536405 ± 1337647a.u. (P=0.023, n=3; Figure 5.5a, c). These data highlight some very important differences between HCy and HCy-T in these cells. Whilst HCy does not increase ROS generation after 48 hours in culture HCy-T does. There is a striking increase in ROS generation when Mk801 is added to SH-SY5Y cultures that is ameliorated by the presence of HCy but not HCy-T. This finding makes a crucial step towards our understanding of how these metabolites mediate their neurotoxicity and how we can best counteract it.

Figure 5.5 Effects of homocysteine, homocysteine thiolactone and Mk801 on reactive oxygen species generation in SH-SY5Y cells

a

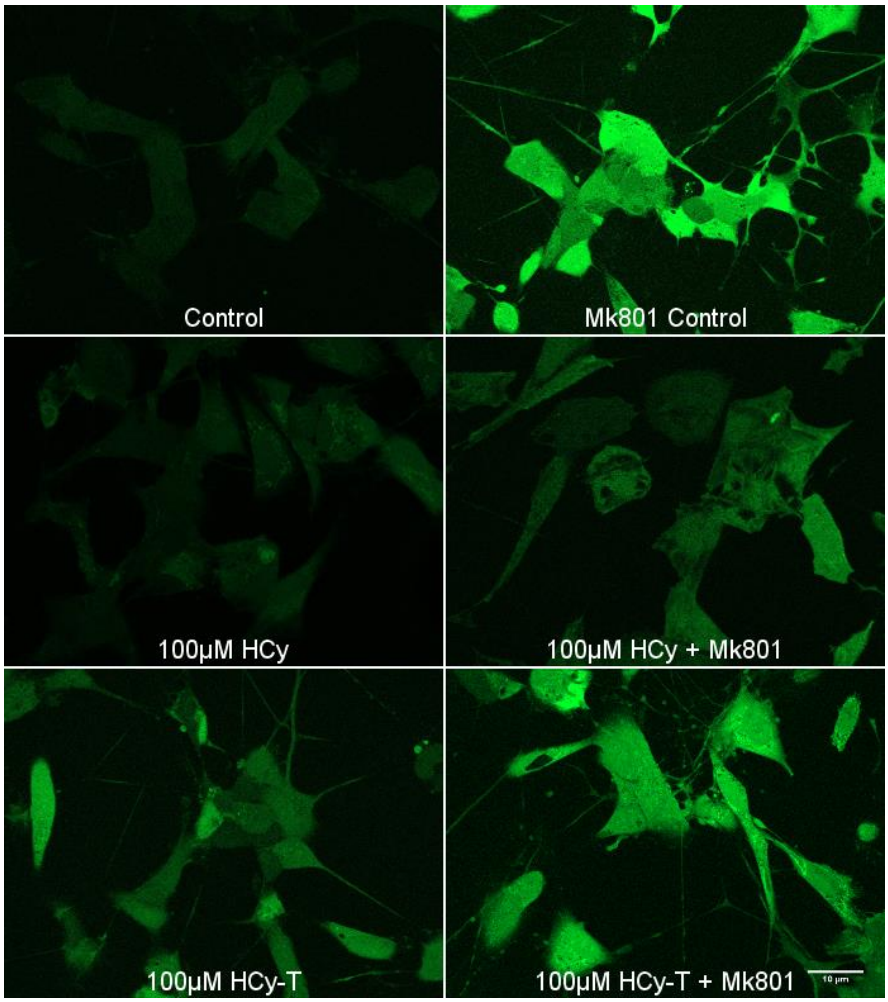

b

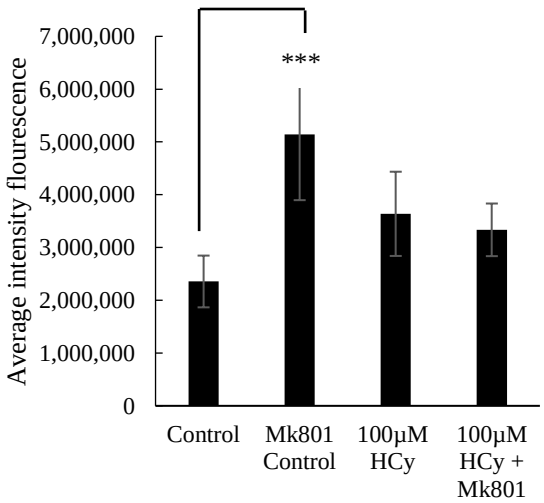

c

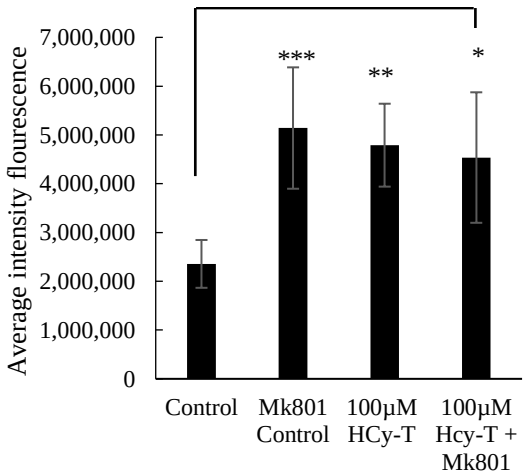

Figure 5.5a shows the increase in average fluorescence intensity emitted per cell upon the addition of the dye,

DCFDA, which gives an approximation of ROS generation by the cells with each treatment. When quantified as average fluorescence per cell this was plotted as figure 5.5b for HCy and Figure5.5c for HCy-T. This showed an increase from 2356216 ± 490382 in untreated control to 5141105 ± 1244191 in Mk801 alone (P=0.001, n=3; Figure 5.5b). No significant result was observed with HCy alone with an increase to 3637922 ± 797758 (P=0.320, n=3; Figure 5.5b). The same was not observed for Figure5.5c HCy-T which showed an increase in fluorescence to 4790103 ± 849961 (P=0.003, n=3; Figure 5.5c) this was unchanged in the presence of Mk801 where fluorescence intensity was increased to 4536405 ± 1337647 (P=0.023, n=3; Figure 5.5c). DCFDA = 2',7' – dichlorofluorescin diacetate, ROS = reactive oxygen species, HCy = homocysteine, HCy-T = homocysteine thiolactone.

5.2.6 Differential effects of homocysteine and homocysteine thiolactone in mitochondrial network morphology

The data presented in section 5.2.5 reveal a key difference between HCy and HCy-T with respect to ROS generation. As mitochondria are the major source of intracellular ROS, a fuller understanding of the effects of HCy and HCy-T on the mitochondrial network may elucidate some of the mechanisms underpinning this exciting finding. Therefore, to determine if HCy or HCy-T alter mitochondrial network dynamics preceding the observed increase in ROS generation, cells were stained after 24 hours with MitoTracker dye to specifically image mitochondria. This live cell dye was applied at 100nM as describe in chapter 2 at the end of the culture period, then the cells were fixed, fields of view were imaged with cell number counted, and the mitochondria characterised. As can be seen in the images obtained, HCy increased the number of cells with predominantly rounded mitochondria (as analysed by the criteria of Wappler (198)) at 24 hours showing predominantly rounded mitochondria compared to untreated control. In contrast, 24 hours treatment with 100μM HCy-T resulted in a marked increase in cells with predominantly highly interconnected mitochondria (Figure 5.6a, c).

To determine whether this change in mitochondrial network morphology was enhanced with longer term exposure to HCy or HCy-T (both at 100μM), analysis was repeated at 120 hours, which was the end point of the viability experiment reported in chapter 3 Figure 3.3. After 120 hours exposure to 100μM HCy showed no significant change in any morphology category,

compared to untreated controls (n=3; Figure 5.6b, d). There was a significant reduction in the number of normal mitochondria when treated with HCy-T from 76.7 ± 8.6% to 24.8 ± 2.9% (*P*=0.033, n= 3; Figure 5.6d). The enhanced number of cells with predominantly highly interconnected mitochondria was maintained in 100µM HCy-T-treated cultures with 47.9% ± 6.7% showing this morphology compared to 3.7 ± 1.2% of untreated control cells (*P*=0.039, n=3; Figure 5.6d).

Figure 5.6 Effects of homocysteine and homocysteine thiolactone on mitochondrial morphology

a

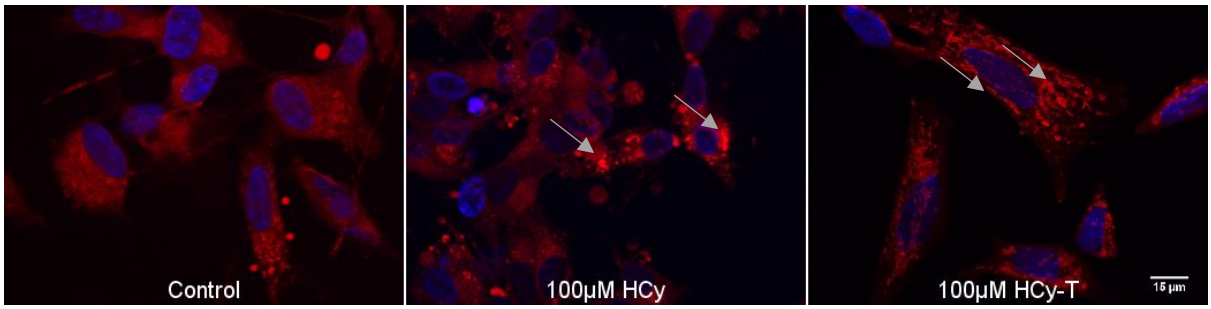

b

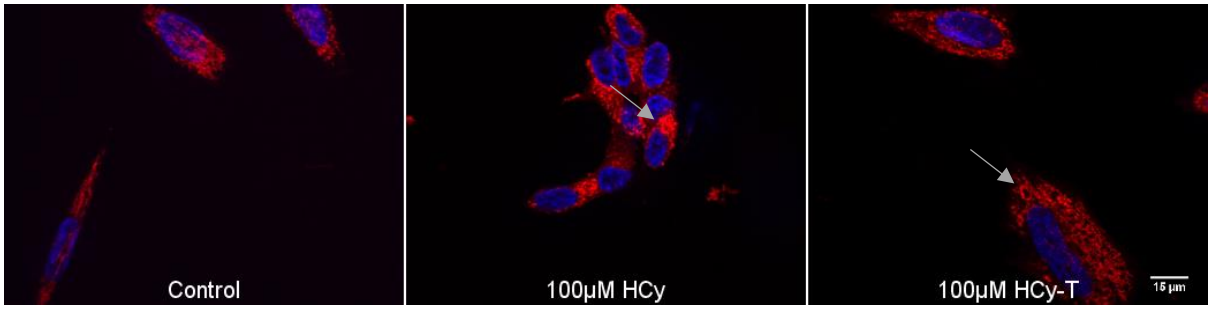

c

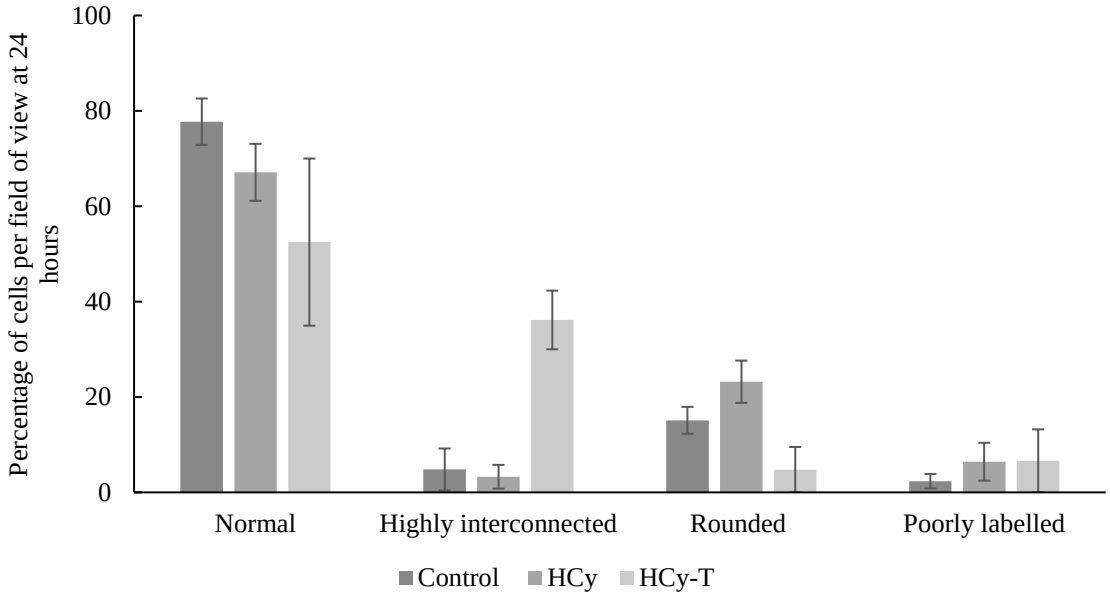

d

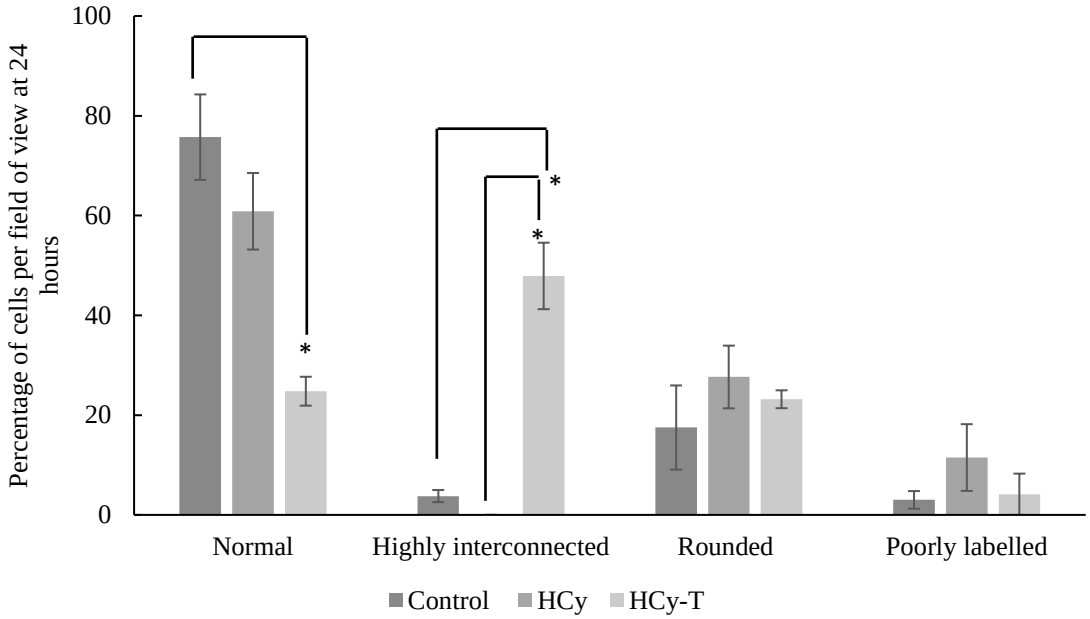

Figure 5.6a-b shows HCy increased the number of cells with predominantly rounded mitochondria at 24 hours with 15.1 ± 5.6% of cells in control culture showing predominantly rounded mitochondria. In contrast, 24 hours treated with 100µM HCy-T resulted in an increase in cells with predominantly highly interconnected mitochondria (Figure 5.6a) However there was no significant changes in any group as compared to untreated control. After 120 hours exposure to 100µM HCy showed no significant change in any morphology category, compared to untreated controls (n=3; Figure 5.6b, d). There was a significant reduction in the number of normal mitochondria when treated with HCy-T from 76.7 ± 8.6% to 24.8 ± 2.9% (*P*=0.033, n= 3; Figure 5.6d). The enhanced number of cells with predominantly highly interconnected mitochondria was maintained in 100µM HCy-T-treated cultures with 47.9% ± 6.7% showing this morphology compared to 3.7 ± 1.2% of untreated control cells (*P*=0.039, n=3; Figure 5.6d). HCy = homocysteine, HCy-T = homocysteine thiolactone.

5.2.7 There was a reduction in the mitochondrial membrane potential with acute application of homocysteine or homocysteine thiolactone but not chronic application

Given the striking effects on the morphology of the mitochondrial network, it was important to determine whether HCy or HCy-T were affecting mitochondrial membrane potential as a measure of mitochondrial wellbeing. This was determined using the JC-1 dye to stain the mitochondria. This dye penetrates the cell and it accumulates in healthy mitochondria where

(due to high mitochondrial membrane potential) the dye aggregates yielding a red to orange coloured emission. In contrast when mitochondrial membrane potential is reduced, JC-1 is predominantly a monomer that yields green fluorescence. The acute effects of HCy and HCy-T (100μM) were examined by imaging cells 45 minutes after co-administration of JC-1 and either HCy or HCy-T. The rationale for this is that membrane depolarization events tend to be rapid and therefore it was hypothesised that this may precede the changes in mitochondrial network morphology. 10 images were obtained per experiment and counted, and the cells were characterised as either all green, mainly mixed or all red. As can be seen there is a reduction in the presence of red stained mitochondria, therefore a reduction in mitochondrial membrane potential, after this acute treatment. 100μM HCy showed a reduction to 80.1 ± 2.6% of predominantly red cells compared to untreated control (P=0.018, n=3; Figure 5.6c), and 100μM HCy-T showed a reduction to 73.7 ± 3.6% (P=0.000, n=3; Figure 5.6c). Thus, both metabolites significantly decrease mitochondrial membrane potential rapidly after administration.

Decreased mitochondrial membrane potential has previously been associated with enhanced ROS generation (288). This experiment was repeated after 48 hours of treatment with HCy or HCy-T (100μM), the time point at which differential effects of these metabolites on ROS generation was detected (Figure 5.5). The image analysis data revealed no significant differences in mitochondrial membrane potential after 48 hours (Figure 5.6 b-d) implying that the effects of the metabolites on this parameter are acute rather than sustained.

Figure 5.7 Effects of homocysteine and homocysteine thiolactone on mitochondrial membrane potential

a

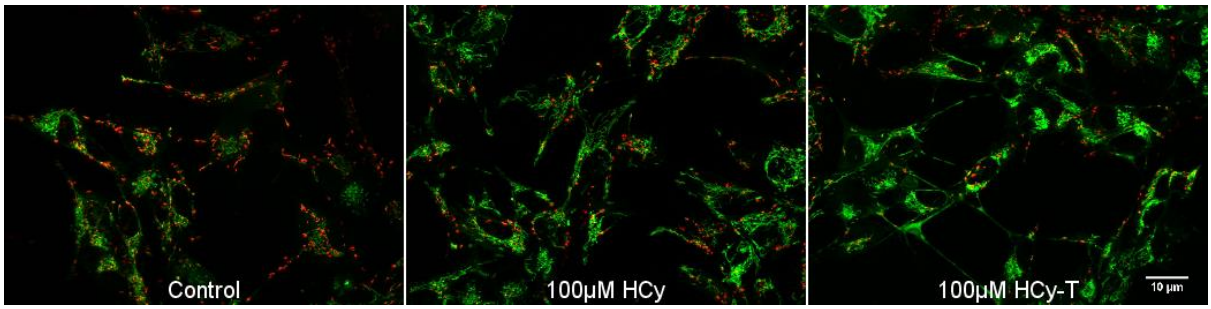

b

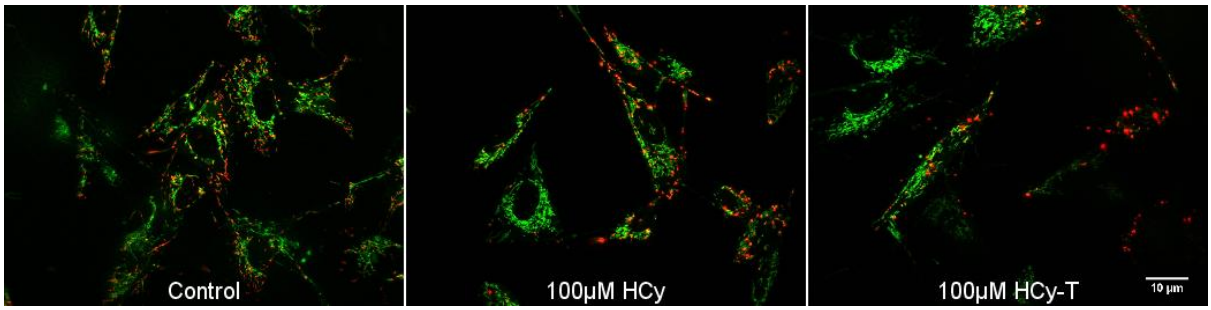

c

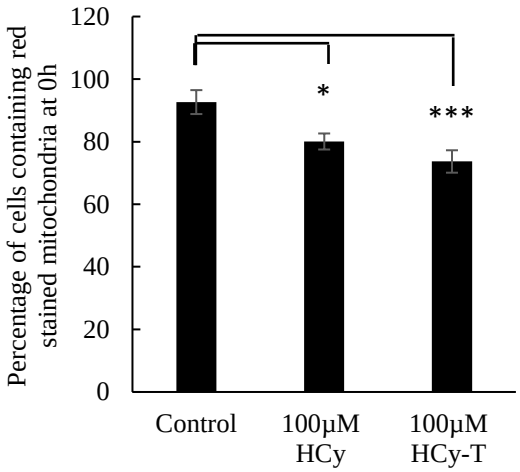

d

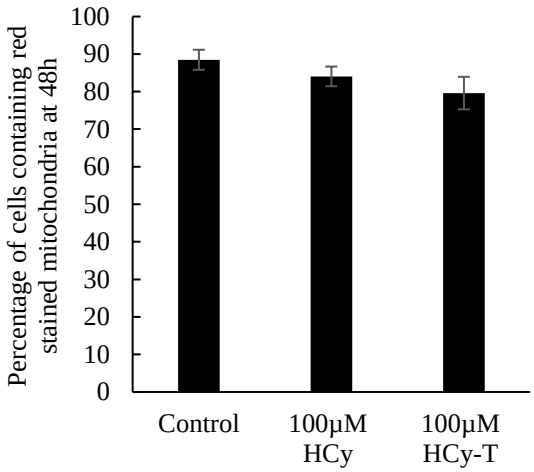

Figure 5.7a-b shows representative images of cells which has been treated with 100µM HCy and HCy and immediately stained with the live cell dye, JC-1. The total number of cells in the field of view were counted and presented as a proportion of mixed red and green cells vs completely green, in each condition, the percentage of red containing cells within the field of view was plotted. This indicates a change in mitochondrial membrane potential. This was plotted as figure 5.7b for immediate staining (0 hours) and Figure5.6c for 48 hour treatment then stained. This showed a reduction in cells containing red stained mitochondria with 100µM HCy at 80.1% ±

2.6% (*P*=0.018, n= 5; Figure 5.7d). 100μM HCy-T with a reduction to 73.7 ± 3.6% (*P*=0.000, n=5; Figure 5.7c). There were no significant results at 48 hours. JC-1 = 2',7' (5,5′,6,6′-tetrachloro-1,1′,3,3′-tetraethylbenzimidazolocarbo-cyanine iodide), HCy = homocysteine, HCy-T = homocysteine thiolactone.

5.2.8 Effects of mitochondrial reactive oxygen species scavenging with MitoTempo on cell viability in response to homocysteine or homocysteine thiolactone

As stated above, one of the major sites of ROS generation is the mitochondrion. The data presented in this chapter has demonstrated an acute effect of either HCy or HCy-T (100μM) in reducing mitochondrial membrane potential. Thereafter these metabolites have differential effects on mitochondrial network morphology with HCy inducing an increase in rounded mitochondria and HCy-T inducing a highly interconnected network. Moreover, HCy-T increases the generation of ROS in these cells but not in a time frame that aligns with the changes observed in mitochondrial membrane potential. Therefore, it is essential to establish whether mitochondrial ROS generation is contributing to HCy and/or HCy-T neurotoxicity. In these experiments cells were treated with 100μM HCy or HCy-T and 5nM of MitoTempo (288) for 120 hours, a mitochondrial specific antioxidant which scavenges mitochondrial superoxide (281). If cell death was predominantly a direct result of mitochondrial oxidative damage, then it is likely an amelioration of cell death induced by these toxins would be observed in the presence of MitoTempo. Cell viability was analysed by a combination of CV and LDH assay. The presence of MitoTempo alone had no effect on cell viability (*P*=0.727, n=4; Figure 5.8a). 100μM HCy did not significantly reduce viability in these experiments although there was a reduction in cell number detected with crystal violet to 80.6 ± 13.5% (*P*=0.341, n=4; Figure 5.8a) and no difference was noted with the addition of MitoTempo (72.1 ± 14.9% viability relative to untreated control, *P*= 0.072, n=4; Figure 5.8a). Similarly, the reduction in viability with HCy-T was detected by CV was not significant in these experiments 74.2 ± 18.6% (*P*= 0.111, n=4; Figure 5.8a). However, when co-applied with MitoTempo this was increased to

100.6 ± 3.5% (P= 1.000, n=4; Figure 5.8a) making the cultures indistinguishable from the untreated control. A similar trend was observed LDH assay however again, no significant results were obtained. Thus, there was a trend towards amelioration of HCy-T but not HCy-mediated cell loss with MitoTempo, as this is a mitochondrial specific antioxidant this suggests that HCy-T is likely affecting the mitochondria more than HCy. However, the lack of a significant toxicity in this experiment means that this cannot be definitively concluded.

Figure 5.8 Effects of MitoTempo on SH-SY5Y viability in response to homocysteine or homocysteine thiolactone

a

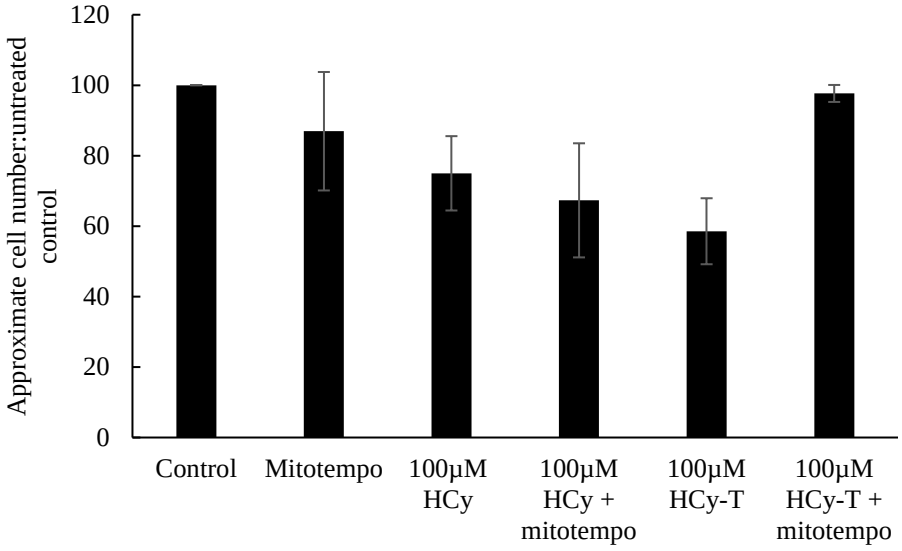

b

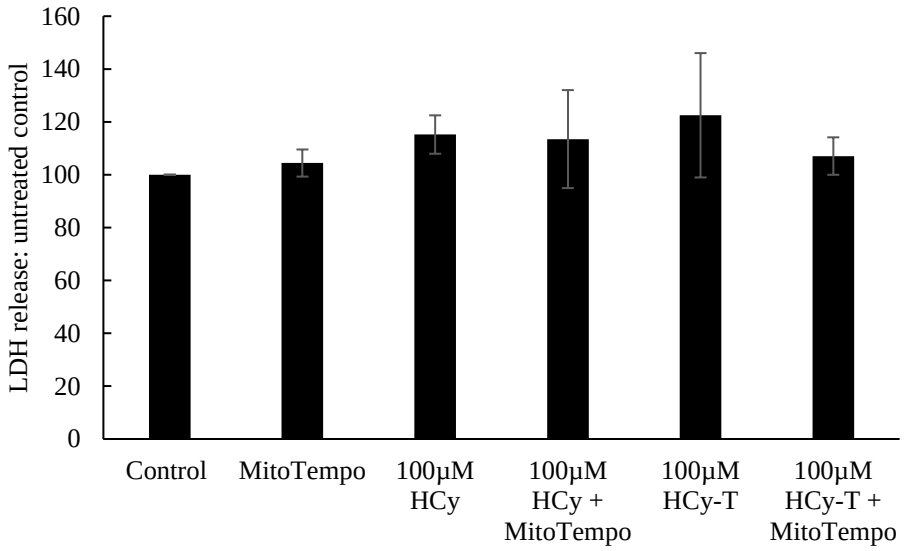

Figure 5.8 shows No change in any group with too much variation in MitoTempo alone to continue experiments. The results from Figure5.7a and Figure5.7b showed that the presence of MitoTempo alone had no effect on cell viability, 100.0 ±0.0 % to 86.9 ± 16.8% (P=0.727, n=4; Figure 5.8a). When treated with 100µM HCy, the approximate cell number dropped to 80.6 ± 13.5% (P=0.341, n=4; Figure 5.8a) this was exacerbated with the addition of MitoTempo 72.1 ± 14.9%. (P= 0.072, n=4; Figure 5.8a). The same control for both untreated and MitoTempo alone were used and Figure5.7b shows that in response to HCy-T alone showed a reduction in cell

number to 74.2 ± 18.6% (*P*= 0.111, n=4; Figure 5.8b) when co-applied with MitoTempo this was increased to 100.6 ± 3.5% (*P*= 1.000, n=4; Figure 5.8b). This was supported by LDH assay however again, no significant results were obtained. ROS = reactive oxygen species, HCy = homocysteine, HCy-T = homocysteine thiolactone, LDH = lactate dehydrogenase.

5.2.9 Glutathione prevented homocysteine thiolactone induced cell death but not homocysteine

As HCy-T significantly enhanced the generation of ROS it seemed likely oxidative stress may play a role in cell death induced by these metabolites. The data from experiments negating solely mitochondrial ROS were inconclusive. However, one other way to determine whether oxidative stress played a role was to scavenge ROS using a cellular antioxidant rather than a mitochondrial-specific one, and using CV and LDH assays, determine if cell death is ameliorated. The following experiment looked at the effects of incubation of the cells with the same treatment as above, but with 250μM glutathione (290) added as an antioxidant. This is a more generic antioxidant and has been shown to protect cellular components from oxidative damage. The CV assay conducted after 120 hours of treatment (Figure 5.9a) showed that there was no difference in the number of adherent cells with HCy compared to HCy with glutathione 62.4 ± 13.8% cells in cultures treated with HCy compared to 61.8 ± 42.3% cells treated with HCy and glutathione (*P*=1.000, n=4; Figure 5.9a). For HCy-T there was a marked decrease in cell number to 68.5 ± 5.4% of untreated control cultures. There was an increase to 98.8 ± 28.3% in cultures co-treated with glutathione although this did not approach significance (*P*=0.256, n=4; Figure 5.9a). Looking specifically at membrane rupture, there was a significant increase with HCy (100μM) to 127.3 ± 13.9% of control levels (Figure 5.9b) which was ameliorated by co-administration of 250μM glutathione to 94.2 ± 8.8% (*P*=0.001, n=5; Figure 5.9b). Similarly, with HCy-T a significant increase compared to untreated control culture 118.4 ± 16.9% (*P*=0.040, n=5; Figure 5.9b) which was reduced in the presence of glutathione to be

statistically indistinguishable to control. Thus, a general cellular antioxidant appears to ameliorate cell death induced by HCy and HCy-T.

Figure 5.9 Effects of glutathione on neurotoxicity via homocysteine and homocysteine thiolactone

a

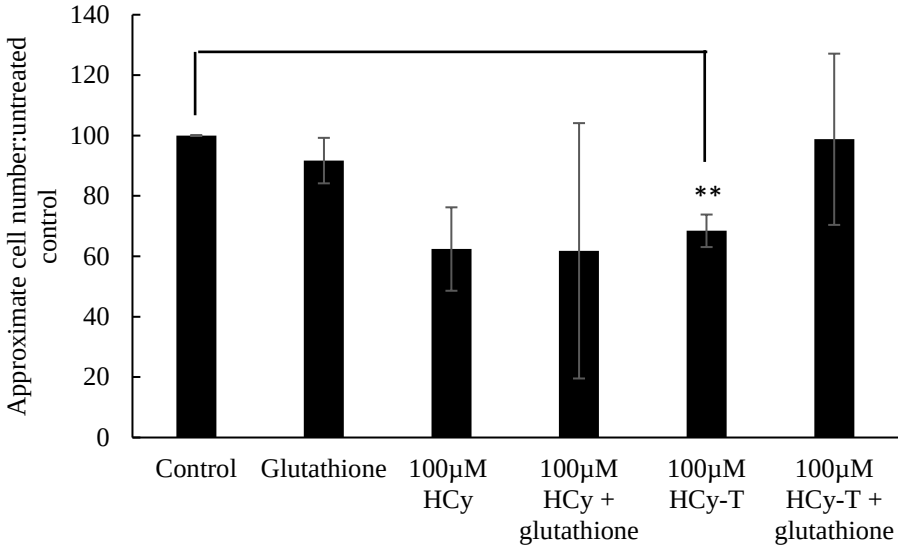

b

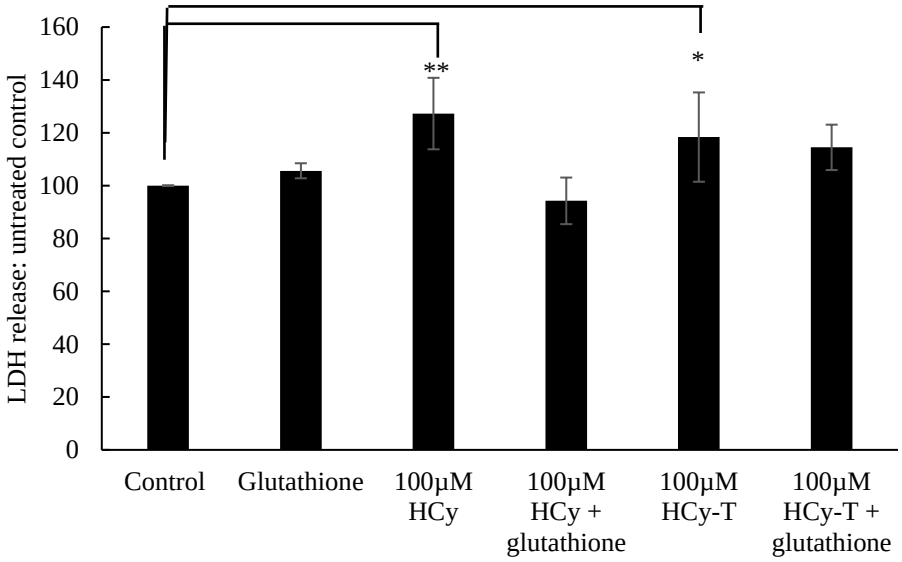

Figure 5.9 shows that there may not be any significant change in approximate cell number as determined by the CV assay with HCy and only 100 µM HCy-T (P=0.008, n=5; Figure 5.9a), this was not supported by the LDH assay which showed HCy toxicity could be ameliorated by the addition of glutathione 127.3 ± 13.9% to 94.2 ± 8.8 (P=0.001, n=5; Figure 5.9b). HCy-T showed an increase in LDH release as determined by the LDH assay. This showed an increase from 118.4 ± 16.9% (P=0.040, n=5; Figure 5.9b). In the presence of glutathione as well

this was 114.5 ± 8.6%. CV = crystal violet, HCy = homocysteine, HCy-T = homocysteine thiolactone, LDH = lactate dehydrogenase.

5.3 Discussion

It has previously been shown in other cell types that HCy causes an increase in the generation of NO and ONOO. To determine if HCy-T would have the same effect, and whether these changes were mediated by alterations in NOS enzyme expression or activity, it was important to determine if either metabolite change of the expression of the predominant NOS isoforms found in the brain. However, no significant effects of HCy or HCy-T were observed on iNOS or nNOS. This implies that HCy does not modulate neuronal NOS expression levels, at least with respect to nNOS and iNOS which were evaluated here. It has previously been shown that HCy upregulates the expression of iNOS in vascular endothelial cells (291). In contrast in macrophages, HCy increases the activity of C5MTase and thus the level of iNOS gene DNA methylation, resulting in a decrease of iNOS expression (292), thus the effects of HCy on iNOS expression vary with cell type. Although iNOS is expressed in neurons and in differentiated SH-SY5Y cells as demonstrated here (Figure 5.1), it is predominantly expressed in glial cells (292). Whilst this was beyond the scope of this project, future studies should focus on whether HCy modulates iNOS expression in the support cell populations of the CNS which may elucidate further crucial clues to its CNS actions. HCy is not known to dynamically modulate nNOS expression and no evidence for this was found in this study. Homocysteine thiolactone has not been shown to modulate NOS expression *per se*. However, other components of the NO generation pathway, such as the enzyme dimethylargininase are susceptible to downregulation through homocysteinylation of the enzyme (292). As HCy, and even more potently HCy-T, have been implicated in protein modification in this way, this suggests that investigation into post-translational homocysteinylation of components of the NO system warrants future investigation to fully understand the role of HCY and/ or HCy-T in its regulation.

Previous studies have demonstrated an increase in NO generation in response to HCy (293). Therefore, the NO live cell dye DAF-DA was used and pharmacological methods of NO and ONOO- modulation to elucidate the role of NO in SH-SY5Y neuronal cells. Neither of these methods yielded significant results. However, in primary sensory neurons there is also no increase in NO observed following HCy administration (285), therefore my data is in accordance with this finding. There are a number of potential reasons why NO and ONOO scavenging did not ameliorate HCy or HCy-T-mediated toxicity including the relatively low levels of HCy and HCy-T used in these studies in comparison to that used by other authors (285). As my studies aimed to keep levels of these neurotoxins as close as possible to that observed in patients with hyperhomocysteinemia, these differences may be of high importance. Thus, the effective concentration of physiologically active HCy or HCy-T in my studies was 50μM as compared to 125μM in the primary sensory neurons mentioned above. Levels of 125μM are only observed in homocysteinuria and the downstream signalling triggered by HCy/ HCy-T in such patients may be very different from individuals with non-symptomatic elevated HCy. It is the latter group that have a prospective risk of AD and that are central to this study. Therefore, one could hypothesise that NO and ONOO may be important in the cell death which is part of the cognitive impairment observed in individuals with homocysteinuria, but that the role of these RNS in converting moderately elevated HCy in individuals at risk of neurodegeneration to neurotoxicity remains unproven.

Studies on the effects of HCy on mitochondria within neuronal cells have been very sparse to date and due to the ease of use of the SH-SY5Y system, it has been possible to examine this in depth. It was initially important to determine if these metabolites effected the generation of ROS within these cultures. Therefore, cells were treated with a known toxic dose of HCy and HCy-T (100 μM; effective concentration 50 μM as D-L isoform was used) and used the live cell dye, DCF-DA, after a period of several days. A significant increase in ROS generation was

observed after 48 hours exposure HCy-T but not HCy. This immediately demonstrated a marked difference between HCy and HCy-T in their effects on oxidative stress. An interesting aside finding from these experiments was the effect of blocking the NMDA receptors using Mk801 on ROS generation, which markedly enhanced the generation of ROS in SH-SY5Y neurons. The intension of this set of experiments was to determine if the activation of the NMDA receptor was the initiating factor in the generation of ROS and therefore any observed effects on the mitochondria. There have been previous reports of ROS upregulation following Mk801 administration (24) and the current studies results are in keeping with this. However, it is also interesting to note that HCy, but not HCy-T significantly reduced Mk801-mediated ROS generation to control levels (Figure 5.5b-c). One plausible explanation for this is that because HCy is well established to interact with the NMDAR (112), it is interfering with the binding, and antagonism of the receptor, mediated by Mk801 alone. In contrast, HCy-T is not. This could imply that HCy-T does not mediate its ROS-generating effects by NMDAR. Thus, the presence of NMDAR antagonist does not therefore interfere with its ability to upregulate ROS generation. What is interesting is that whether it is Mk801 or HCy-T that is inducing oxidative stress, the levels produced are similar, perhaps because the levels may have reached the maximum detection limit of the system, thus no additive effects are observed. Alternatively, both Mk801 and HCy-T may interact with the same binding site on the NMDAR to induce the same response.

Oxidative stress and oxidative damage are often attributed to the mitochondria, the powerhouse of the cell and the main contributor to increases in ROS. Wappler and colleagues had shown that following oxygen-glucose deprivation, the dynamics of the mitochondrial network was disrupted to deal with stress and the mitochondria undergo fusion and fission to deal with the stress. Images were defined as normal, well defined mitochondria; rounded which was postulated to be excessive fusion; highly interconnected which they defined as a lack of fission

where the mitochondria appear to form strings; and the final characterisation was poorly labelled, this is where there do not appear to be mitochondria present. After 0 or 48 hours HCy application resulted in predominantly rounded mitochondria, a result which was more prominent at 48 hours. HCy-T application, in contrast, induced more highly interconnected mitochondrial networks. Again, this highlights a key difference between the two metabolites in how they affect the mitochondria.

As alterations to the mitochondrial network have been closely linked to mitochondrial dysfunction, the mitochondrial membrane potential was measured following application of HCy and HCy-T, both acutely and after 48 hours incubation. There was an acute effect on the mitochondrial membrane potential at where both metabolites resulted in a reduction in the mitochondrial membrane potential, but this was not maintained at 48 hours. It is well established that dysfunctional mitochondria are removed from the cell by mitochondrial autophagy (294). Therefore, my findings raise the possibility that both HCy and HCy-T initially induce mitochondrial dysfunction and that these mitochondrial are removed from the mitochondrial pool by mitophagy as part of a defence mechanism by the cell (294). This would result in a 'survivor' population of mitochondria at the 48 hour time point that show greater resilience to HCy and HCy-T. To test this hypothesis a number of experiments would be needed including time course analysis of mtDNA by qPCR load to determine mitochondrial number within the cells (198) or citrate synthase activity assay for mitochondrial mass (295). This could be coupled to electron microscopy analysis of mitochondria to identify mitophagy (295). This finding is also intriguing as the increase in ROS mediated by HCy-T was observed markedly at 48 hours. As mitochondrial membrane potential decreases are associated with ROS generation (288) we would hypothesise that if the main source of HCy-T-triggered ROS was mitochondrial the decrease in mitochondrial membrane potential would still be apparent after 48 hours in these cultures. Further to this, pharmacological methods were used to determine if

mitochondria-specific antioxidant, MitoTempo could ameliorate the cell death induced by HCy or HCy-T. Intriguingly this reagent did not significantly protect against HCy mediated cell death although there was a non-significant increase in survival in HCy-T/ MitoTempo co-treated cultures. For the general antioxidant glutathione, LDH assay revealed that both HCy and HCy induced cell death could be ameliorated, however, this could not be supported by CV assay. It has been shown that cytosolic sources can also generate ROS in addition to the mitochondria (296). Therefore, the potential for mitochondrial-independent sources in these cells warrants future analysis.

Taken together it can be concluded that using physiological levels of HCy or HCy-T (effective concentration 50μM), NO and ONOO signalling are not required to mediate a neurotoxic response. Thus, in contrast to experiments conducted that are more pertinent to homocysteinuria (296), nitrosylative stress is not central to HCy-mediated toxicity in SH-SY5Y cells at concentrations seen in hyperhomocysteinemia. A role for ROS is strongly alluded to for HCy-T as there is a marked increase in ROS generation and this can be ameliorated with glutathione and potentially MitoTEMPO. For HCy, the data is less clear, but the neuroprotective actions of glutathione imply a role for ROS. A fuller time course may reveal an increase in ROS mediated by HCy that was not revealed in these experiments. These data present, for the first time, a clear indication that there are marked differences in the cellular effects of HCy and HCy-T in regulating mitochondrial network and ROS generation.

CHAPTER 6: CHRONIC EFFECTS OF HOMOCYSTEINE, HOMOCYSTEINE-THIOLACTONE AND HOMOCYSTEIC ACID USING A LONG TERM CULTURE SYSTEM

6.1 Introduction

Longitudinal experiments have shown that elevated levels of HCy increase the risk of the development of many diseases, such as CVD (297) and neurodegenerative diseases (84,248,298). Long term folate deprivation in rodent models has given rise to MCI (299) and impaired LTP (86). However, the contribution of HCy to these impairments is still very much elusive. In cell culture examining HCy, supraphysiological concentrations of 1M and above, are applied for acute periods up to 6 days (155,157,300). However, in addition to the acute mechanisms of cell damage induced by HCy outlined in chapters 4 and 5, it was important to determine if cell damage was induced by HCy, HCy-T and homocysteic acid at physiological levels with chronic application. This was important to determine as high acute doses of these metabolites are not necessarily representative of what would be observed in most of the population with moderately elevated HCy. Additionally, the mechanisms underpinning cellular toxicity induced by HCy at acute high doses may not be the same as chronic, moderate concentrations.

In addition to HCy and HCy-T, homocysteic acid (HCA) was investigated in this chapter. HCy can auto-oxidize to produce HCA (301). HCA induces intraneuronal accumulation of neurotoxic Aβ1-42 *in vitro* (301). In addition, studies of both AD patients and 3xTg-AD model mice (expressing three dementia-related transgenes, namely APPSWE, PS1M146V, and tauP301L) corroborate these observations. High HCA concentrations are detected in both AD patients and 3xTG-AD mice compared to age-matched controls (301). Together these findings suggest that HCA may play an important role in AD.

As elevated HCy has been implicated in the development of neurodegenerative diseases (84,248,298) and HCy lowering strategies in elderly people has proved effective at reducing MCI (90), it was therefore important to determine what damage is elicited by moderate, representative doses of HCy and metabolites in a cell culture system. In ageing and

neurodegenerative diseases, several damaging effects and features are apparent, which may also be examined within a culture system, these include an increase in oxidative stress and oxidative damage (228). Additionally, most neurodegenerative diseases display some form of protein aggregation, in AD this is predominantly amyloid plaques (302) and in PD this is synuclein (303).

Therefore, this chapter aimed to expand on the chapter 3, developing a culture system to study ageing, and examine what effect a neurotoxin may have on the ageing cells. As shown in earlier chapters, this culture system illustrates that these fully differentiated cells show signs of cell loss, oxidative damage and increase in oxidative stress markers such as HNE, all key features of neuronal cell ageing as described in section 3.2.7. Therefore, HCy and metabolites were applied at concentrations of 50 and 100μM, these were chosen as 100μM has previously shown some toxicity within 5 days however 50μM has not (section 4.2.3). As 100μM was not enough to cause more than 20% cell death over a period of 5 days, it was presumed that this concentration would be appropriate for this study.

This chapter aims to elucidate whether chronic administration of physiological levels of HCy, HCy-T and HCA (50μM) would be damaging to ageing SH-SY5Y cells *in vitro* and by also working with a concentration of these metabolites known to induce rapid neurotoxicity (100μM), a comparison of toxic and sub-toxic concentrations can be made. Specifically, the extent to which HCy and metabolites affected oxidative stress and damage in the culture system outlined in chapter 3 will be determined. For instance, there is an enhancement of ROS generation with age using this culture (section 3.2.9), this chapter aims to determine if HCy and metabolites hasten the expression and accumulation of ageing markers. Furthermore, the increase in oxidative stress and oxidative damage in this culture over a period of 4 weeks made it possible to determine to what extent HCy exacerbated cell damage at lower concentrations than those used in chapter 4 and 5. Finally, the expression of biomarkers linked to AD

(specifically APP, PS1 and p-tau) were investigated using this system. It should be noted that as D-L HCy, HCy-T or HCA was used, that 50µM HCy is the equivalent upper dose considered to be a risk factor for CVD (304).

6.2 Results

6.2.1 A reduction in cell viability was observed after 2 and 4 weeks with homocysteine, homocysteic acid and homocysteine thiolactone

As very few publications in the literature have reported HCy-mediated apoptosis at physiologically relevant concentrations, one of the most important aspects of this chapter was to determine what effect sub-toxic doses of these metabolites had on cell viability in a model of cellular ageing. Therefore, cells were treated with each of the metabolites and cell viability determined with phase contrast micrographs and LDH assays at 4 weeks. There was an exacerbation of cell death at 2 and 4 weeks in the presence of HCy with an increase in LDH release (142.2 ± 26.9% P=0.030, n=5; Figure 6.1c) but not HCy-T (153.2 ± 59.1% P=0.164, n=5; Figure 6.1c) or HCA 155.5 ± 97.9% (P=0.573, n=5; Figure 6.1c) as determined by the LDH assay. However, when examined the phase contrast micrographs, HCy and HCy-T have the most pronounced reduction in cell number as these had images taken which were not exposed to a staining procedure. This could not be determined by CV as in previous chapters, as the cells became detached during the staining process. However, taken together the phase contrast images show markedly reduced cell number with HCy, HCy-T and HCA. LDH assay detects only the enzyme released in the previous 12 hours of culture, therefore the time points tested here only represent short snap shots of the dynamics of the extended culture period. Nonetheless, significant cell death was observed after treating with 100μM HCy at 4 weeks showing that cell death is ongoing in these cultures. The timing of death in HCy-T and HCA is not established using these 2 time points.

Figure 6.1: Viability of SH-SY5Y cells in response to 50 and 100µM homocysteine following 2 or 4 weeks administration

a

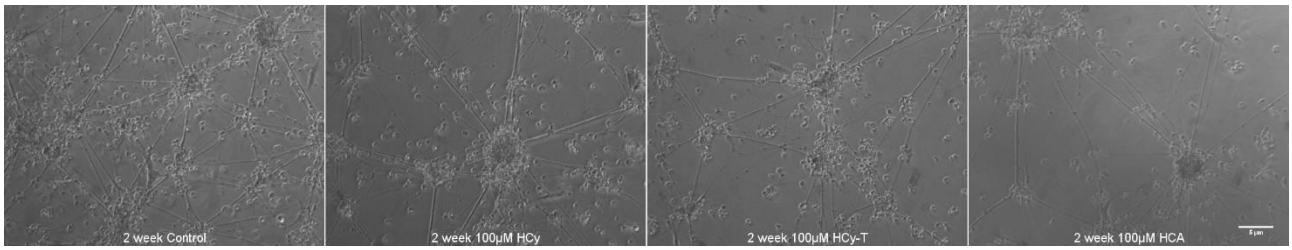

b

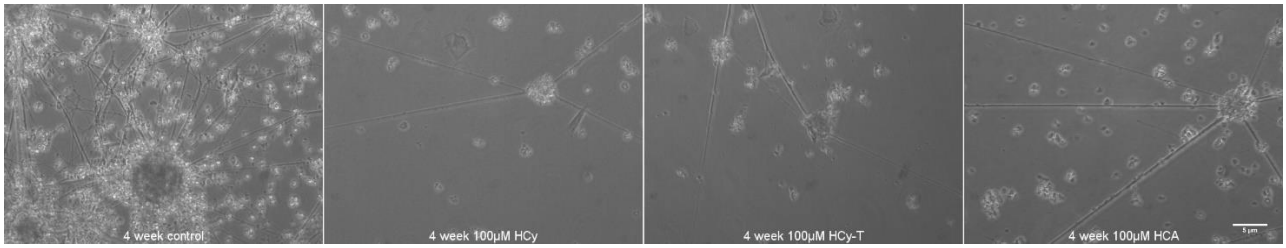

c

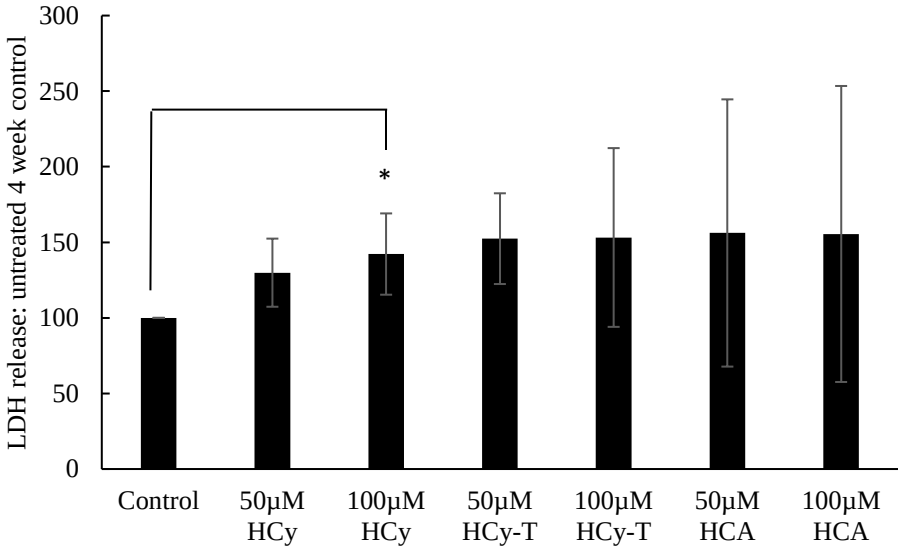

Figure 6.1 shows phase contrast micrographs of cells treated 100µM HCy, HCy-T and HCA. The images show a reduction in cell number with 2 weeks application (Figure 6.1a), very few cells at 4 weeks were remaining (Figure 6.1b). Figure 6.1c shows the LDH release after 4 weeks treatment with 50 and 100µM HCy this showed a dose dependant increase in LDH release to 142.2 ± 26.9% (P=0.030, n=5; Figure 6.1c). 50 and 100µM HCy-T showed no significant increase in LDH release to 153.2 ± 59.1% (P=0.164, n=5; Figure 6.1c) the same was observed with

HCA, no significant increase in LDH release to 155.5 ± 97.9% (P=0.573, n=5; Figure 6.1c). HCy = homocysteine, HCy-T = homocysteine thiolactone, HCA = homocysteic acid, LDH = lactate dehydrogenase

6.2.2 After 4 weeks, cells treated with 100μM homocysteic acid had increased reactive oxygen species generation

Oxidative stress is a feature of ageing and neurodegenerative diseases and is apparent prior to onset of symptoms. It was therefore important to determine if this was observed after 2 and 4 weeks in culture. Thus, cells were treated for 2 weeks with either HCy, HCy-T or HCA (50 or 100μM) and then stained with the dye DCF-DA, which fluoresces green in the presence of ROS. To determine if there was an increase in the generation of ROS as compared to untreated control cells, this was analysed using the average fluorescence per cell in 5 images per slide, each slide was generated from cells of different cultures. None of the treatments resulted in an increase in ROS generation at 2 weeks and, at the 4 week time point, only 100μM HCA resulted in a significant increase in ROS generation from 3688003 ± 713922.1a.u. in untreated control cells to 18417321 ± 4724582 in 100μM HCA-treated cultures, (P=0.001, n=20 Figure 6.4b). These data demonstrated an interesting dynamic of ROS generation with levels similar to those in control untreated cultures after 2 weeks incubation and a highly significant increase in HCA-treated cultures after 4 weeks demonstrating differential time dependant effects of these metabolites on ROS generation. This could be in part due to the acidity of HCA as compared to HCy and HCy-T.

Figure 6.2 shows reactive oxygen species generation as determined by DCF-DA at 2 and 4 weeks

a

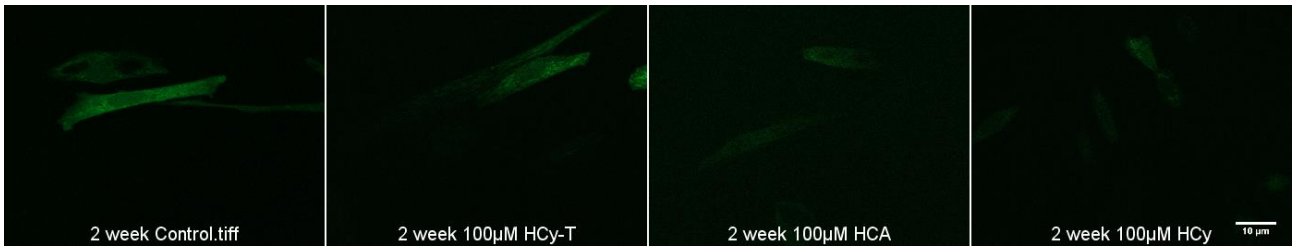

b

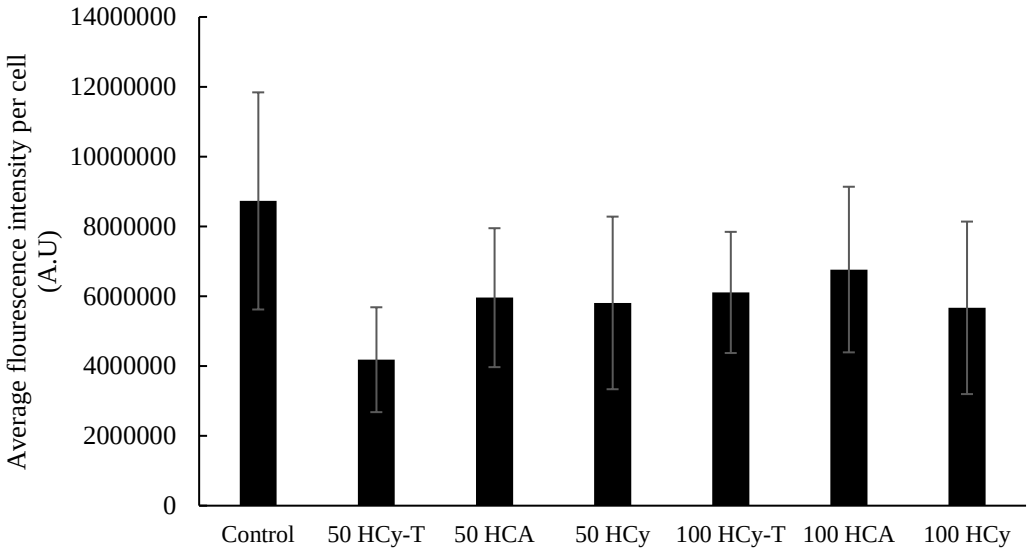

c

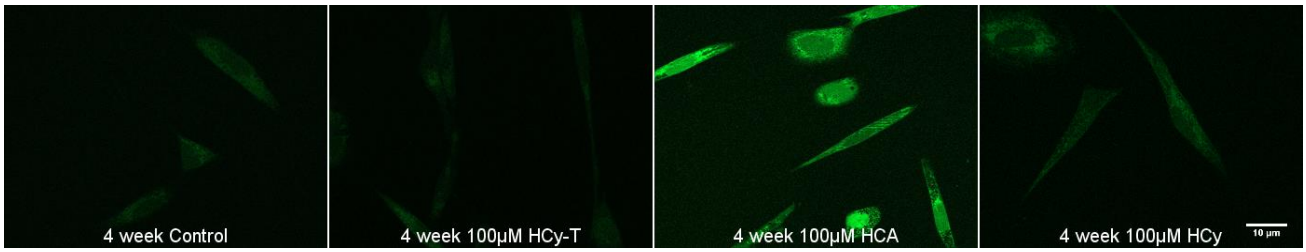

d

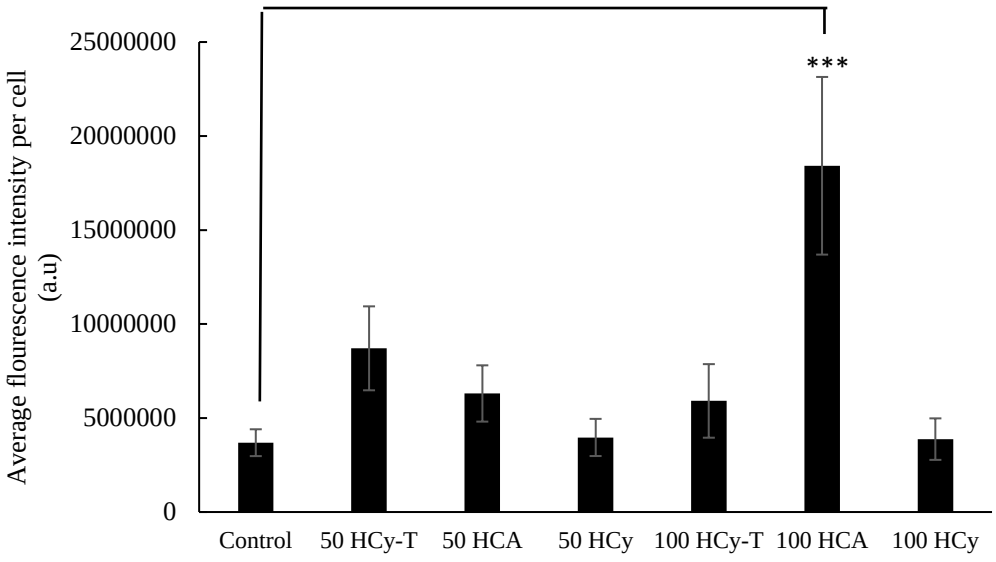

Figure 6.2a-b shows the changes in ROS generation in response to 50 and 100µM HCy, HCy-T and HCA at 2 weeks. No treatment was any different to the untreated control. Figure 6.2c-d shows the change in ROS generation at 4 weeks, the only treatment that was increased as compared to the untreated control was 100µM HCA. This showed an increase from 3688003 ± 713922.1 to 18417321 ± 4724582 (P=0.001 n=20; Figure 6.2b). HCy = homocysteine, ROS = reactive oxygen species, HCy-T = homocysteine thiolactone, HCA = homocysteic acid.

6.2.3 Homocysteine, homocysteine thiolactone or homocysteic acid do not modulate the expression of the AD-linked biomarker, APP

To determine if the expression of biomarkers associated with age-linked neurodegeneration were modulated within this system, the expression of APP by ELISA was determined. This was achieved by growing cells for 2 weeks with the addition of 50 and 100µM HCy, HCy-T or HCA and the protein extracted thereafter for analysis. The aim was also to determine this at 4 weeks however not enough protein could be obtained. There was no significant change observed for any metabolite at any concentration, such that 100µM HCy (Figure 6.3a) HCy caused an increase in APP expression relative to untreated controls of 117.7 ± 6.7%, (P=0.428, n=6; Figure 6.3b) for 100µM HCy-T this was 130.9 ± 22.4% (P=0.530, n=6; Figure 6.3c) and

for HCA 150.1 ± 33.1% (*P*=0.204, n=6; Figure 6.3c). Thus, chronic administration of HCy, HCy-T or HCA to SH-SY5Y cells does not modulate APP expression.

Figure 6.3 There is no difference in expression of APP expression at 2 weeks in the presence of 100µM homocysteine, homocysteine thiolactone or homocysteic acid

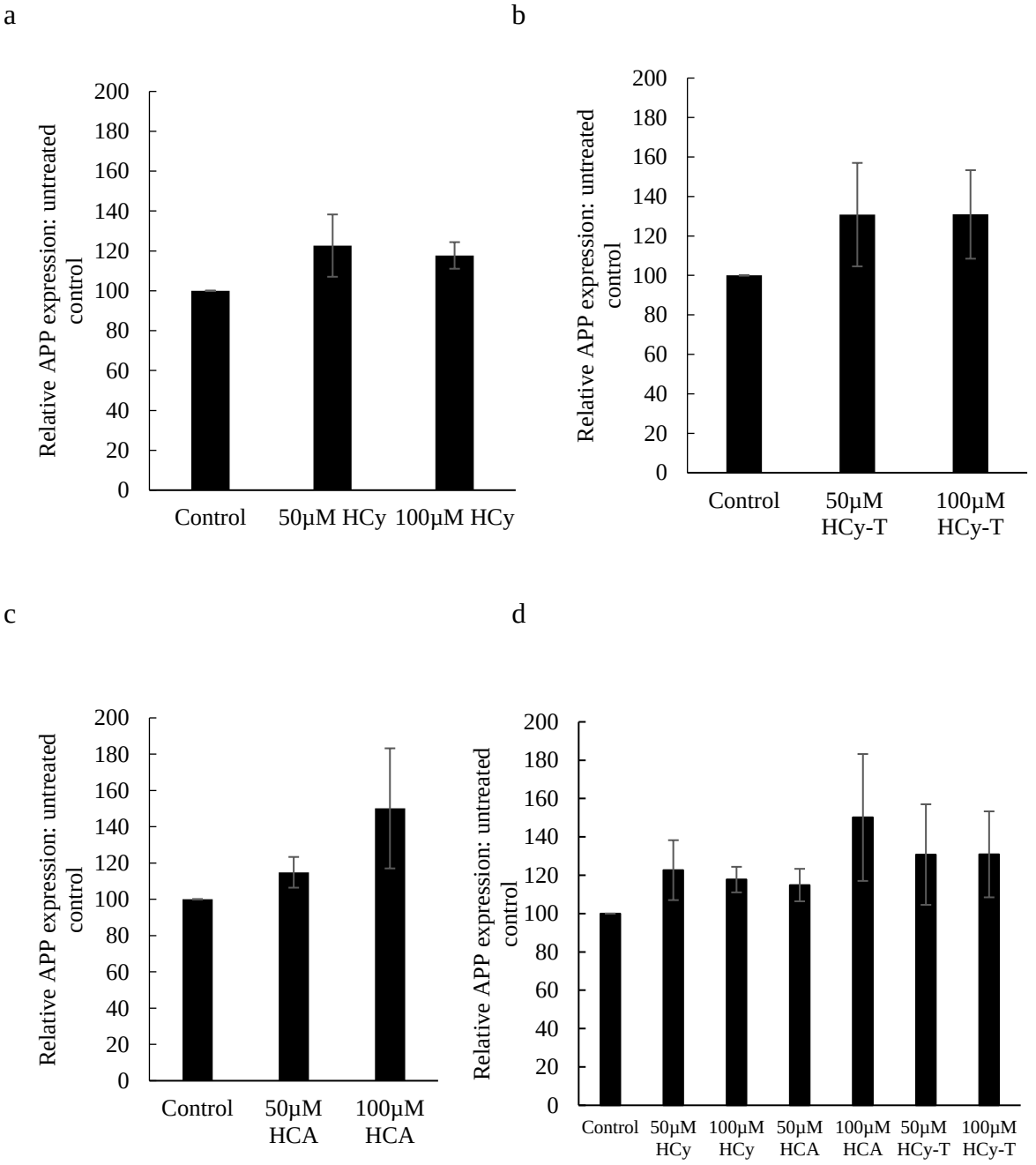

Figure 6.3 shows that there was no change in the expression of APP with 100µM HCy APP 117.7 ± 6.7%, (*P*=0.428, n=6; Figure 6.3a). Additionally, there was no change with 100µM HCy-T 130.9 ± 22.4% (*P*=0.530,

n=6; Figure 6.3b) or HCA, 150.1 ± 33.1%, (*P*=0.204, n=6; Figure 6.3c). HCy = homocysteine, HCy-T = homocysteine thiolactone, HCA – homocysteic acid, APP = amyloid precursor protein

6.2.4 Chronic administration of homocysteine, homocysteine thiolactone or homocysteic acid does not modulate the expression of p-tau

Using the same protein extracts as in 6.2.3 above, the levels of p-tau (phosphor-threonine 181) were determined by ELISA because pTau 181 is widely accepted as an AD biomarker and is known to be elevated in mild to moderate AD (305). There was no significant change observed for any metabolite at any concentration, thus for 100µM HCy (Figure 6.4a) p-tau levels were 122.0 ± 9.1%, (*P*= 0.232, n=6; Figure 6.4b) relative to untreated control cultures, for 100µM HCy-T p-tau expression was 140.5 ± 21.2% (*P*=0.281, n=6; Figure 6.4b) and for HCA 156.7 ± 32.2% (*P*=0.120, n=6; Figure 6.4c). Thus, chronic administration of HCy, HCy-T or HCA to SH-SY5Y cells does not modulate p-tau expression.

Figure 6.4 There is no difference in expression of p-tau after 2 weeks in the presence of 100µM homocysteine, homocysteine thiolactone or homocysteic acid

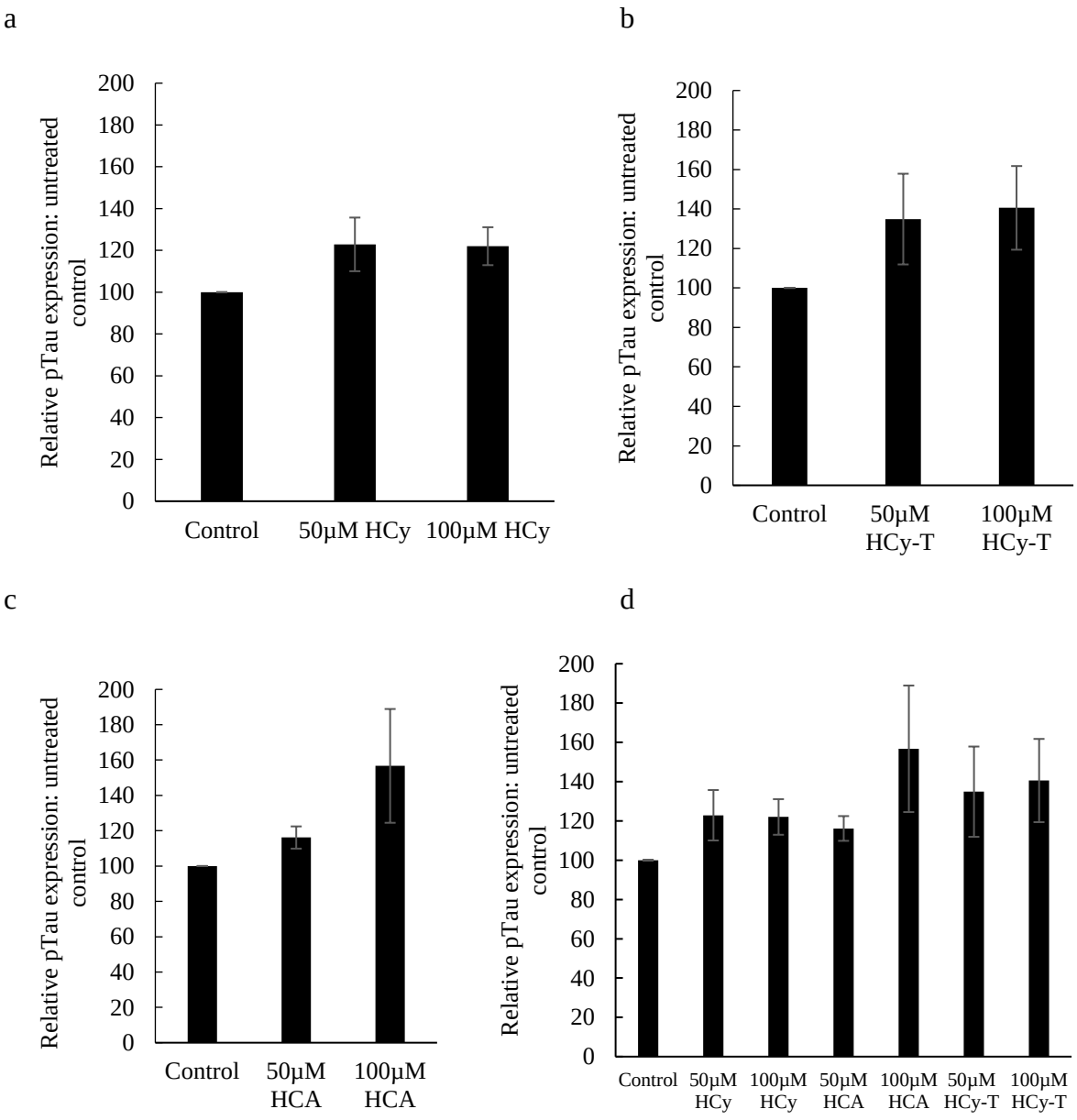

Figure 6.4 shows no change in p-tau with any metabolite examined. P-tau expression with 100µM HCy was 122.0 ± 9.1% (P= 0.232, n=6; Figure 6.4a) with HCy-T this was 140.5 ± 21.2% (P=0.281, n=6; Figure 6.4b) and HCA showed 156.7 ± 32.2% (P=0.120, n=6; Figure 6.4c). HCy = homocysteine, HCy-T = homocysteine thiolactone, HCA – homocysteic acid, pTau = phosphoTau

6.2.5 There is no difference in expression of PS1 expression at 2 weeks in the presence of 100μM homocysteine, homocysteine thiolactone or homocysteic acid

The final biomarker selected was PS1, this was selected as it is one of the main enzymes associated with cleaving APP to form the toxic form Amyloid β 1-42, and again this was examined by ELISA. This was achieved by growing cells for 2 weeks with the addition of 50 and 100μM HCy and the protein extracted for analysis. ELISA was done using an antibody against PS1 and α-Tubulin as a loading control. There was no significant change observed any metabolite at any concentration, thus for 100μM HCy PS1 levels were 128.8 ± 9.8% of the untreated control (P=0.144, n=6; Figure 6.5a) for 100μM HCy-T 144.9 ± 27.2%. (P=0.341, n=6; Figure 6.5b) and for HCA 163.7 ± 42.1% (P=0.202, n=6; Figure 6.5c). Thus, chronic administration of HCy, HCy-T or HCA to SH-SY5Y cells does not modulate PS1 expression.

Figure 6.5 There is no difference in expression of Presenilin 1 after 2 weeks in the presence of 100µM homocysteine, homocysteine thiolactone or homocysteic acid

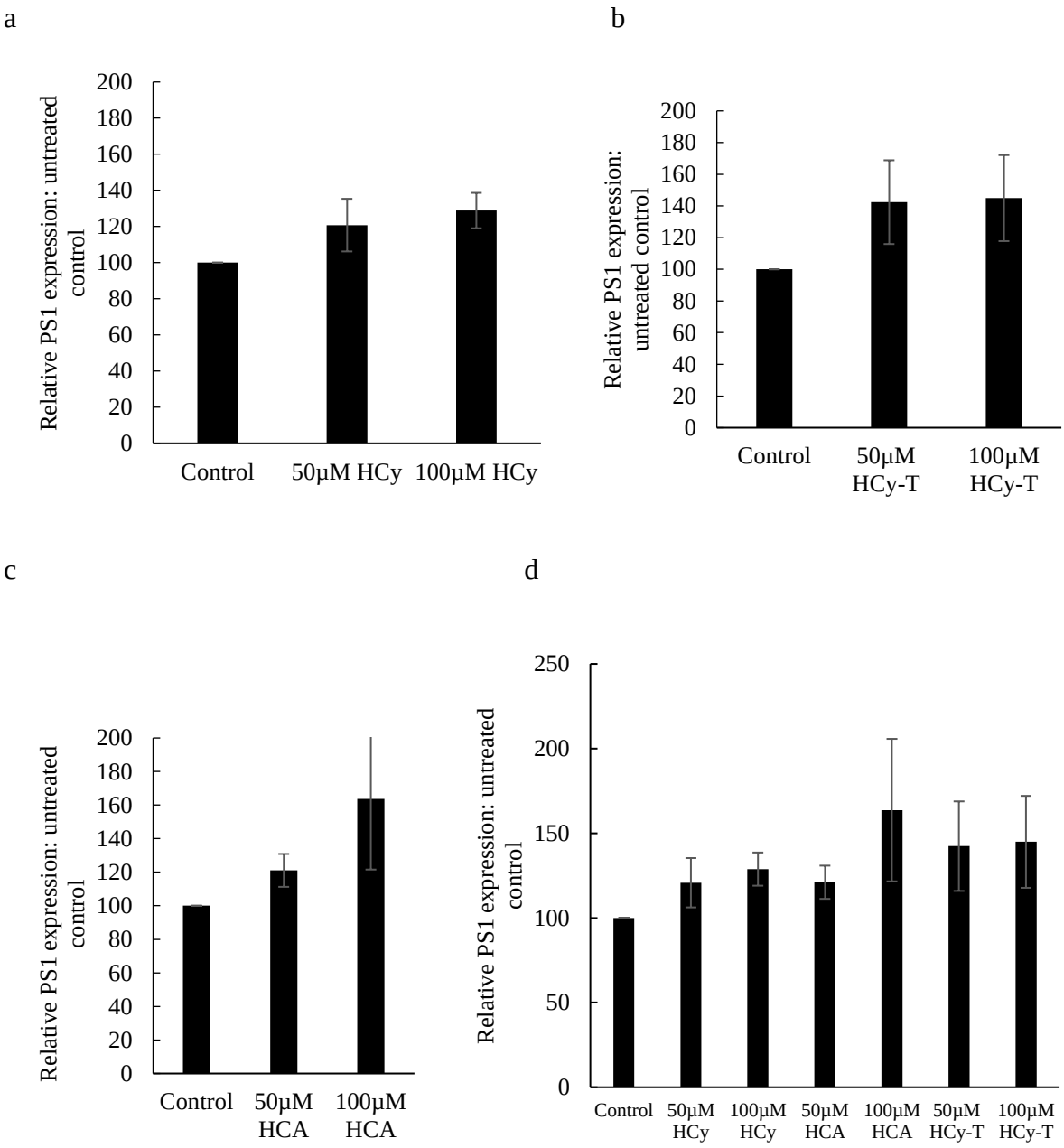

Figure 6.5 shows no change in PS1 with either concentration of HCy Figure 6.5a, HCy-T Figure6.7b and HCA Figure6.7c. There was a tendency towards increase in PS1 expression with 100µM HCy 128.8 ± 9.8% (P=0.144, n=6; Figure 6.5a) with HCy-T 144.9 ± 27.2%. (P=0.341, n=6; Figure 6.5b) and HCA 163.7 ± 42.1% (P=0.202, n=6; Figure 6.5c). HCy = homocysteine, HCy-T = homocysteine thiolactone, HCA = homocysteic acid, PS1 = presenilin 1

6.3 Discussion

These experiments have shown that HCy, HCA and HCy-T are all potentially neurotoxic at lower concentrations than is used in most other cell culture toxicity experiments (306,307), over a prolonged period of time in culture. It should be noted that this was apparent using D-L HCy, HCA and HCy-T, as in all other experiments discussed previously, only the L-isoform of HCy is toxic and can be converted to HCy-T. However, both D and L isoforms of HCy-T and HCA have similar properties.

There is a clear discrepancy between the phase contrast photomicrographs which show marked cell death with HCy- T and HCA which was not observed by LDH assay. As these experiments were done over a prolonged period of time and the half-life of LDH in culture media is 12 hours, it is possible that the LDH may have been removed from the culture media through repeated media changes and could have been detected at earlier time points. These data suggest that for future experiments, serial measurements of LDH should be made and that a lower concentration of these metabolites might been worth evaluating. Other methods of evaluating cell number such as determining the number of cells per view in higher power phase contrast images, or determining nuclear number using DAPI staining could also be considered. Another aspect to be considered was the large variation of the data obtained from these experiments, therefore with increased repetitions, statistical significance for other metabolites may have been attained. Particularly when looking at HCA, some plates had so few cells remaining at 4 weeks, the variation was very large and therefore a lower concentration may have been required. However, whilst the technical demands of working with these cultures has impeded the use of techniques such as crystal violet assay (which rely upon sustained cell attachment throughout repeated wash steps in the assay), there is remarkable loss of neurons with relatively low levels of HCy, HCy-T and HCA in cells that model the accumulation of an aged phenotype in culture (as observed in the photomicrographs). This suggests an enhanced sensitivity to the

neurotoxic effects of HCy, HCy-T and HCA and should be further investigated in future with more repeat measures, a greater range of empirical techniques and a greater range of metabolite concentrations as outlined above.

When looking at signs of damage within this culture, keeping cells viable was less successful than in chapter 3 due to treated cells not adhering to the coverslips for the duration of the staining procedure. Repeat staining for oxidative damage to DNA and lipids by OhdG and HNE staining respectively was attempted, however this was unsuccessful for all metabolite treatments. This may reflect the greater fragility of the metabolite-treated cells compared to the untreated ageing cells in chapter 3. It is possible that execution of the staining could be achieved by further optimisation of the coating protocol for cell staining. Nonetheless, live cell imaging was still possible as there was less manipulation to the cells and therefore it was possible to determine the generation of ROS with the application of all metabolites. Unlike in chapter 5 where there was an increase in ROS generation with HCy-T, this was not apparent with chronic application. Here the only increased in ROS was detected with 100µM HCA at 4 weeks. ROS generation may be predominantly an acute event, or a smaller, more gradual occurrence with the application of these metabolites. Therefore, a fuller time series of imaging may elucidate more information on ROS generation *per se*, and moving forward, the analysis of oxidatively damaged cellular components in biochemical rather than immunocytochemical assays may prove an easier method of investigating the effects of HCy, HCy-T and HA in cell-based models of ageing.

There was no significant increase in any of the AD-linked biomarkers examined within this culture system. However, all concentrations of all metabolites showed a tendency towards an increase in the expression of APP, pTau and PS1. Although there were 5 sets of protein extracted for this set of experiments, 2 were lost because the extracted sample was too dilute to gain information for experimentation. Furthermore, this could only be repeated twice

because only a small volume of extract that could be gathered from the remaining samples, this was due to the reduction in cell number. To enhance this for future experiments, cells should be grown in larger dishes to gather more cells or a coating applied to all dishes to enhance the chance of continued cell adhesion. Due to the lack of protein generated, examination of other proteins associated with cell ageing could not be conducted. Therefore, this data should be viewed as a pilot study of these metabolites and again warrants further repetition, adjusting the empirical conditions to improve yield.

A key feature of neuronal cell ageing, and an initiating factor in the development of neurodegenerative disorders, is the reduction in neuronal cell function and synapse loss. Therefore, future experiments examining electrophysiological recordings to determine if there was a reduction in action potential generation within these cells when treated with all the metabolites would be interesting. The presence of synapsin as determined by ELISA or immunofluorescence would also be interesting but could not be done as outlined in the reasons above.

To continue these experiments for future research, some optimisation to increase the adherence of the cells to the coverslips and the dishes must be carried out. More than half of the cells generated for these, and staining experiments, were lost due to cells detaching when all culture media was removed for the final experiments. This was not observed to this degree in the culture system as outlined in chapter 3 and as per the controls in these experiments, therefore it is likely due to the application of the toxic metabolites causing a reduction in adherence making experimentation problematic. Therefore, this system may not be effective for the study of cell neurotoxins in ageing. However, this system may be effective to look at neuroprotection. The addition of these metabolites to this system was too toxic to these cells making consistent results difficult to obtain.

CONCLUSIONS

This thesis aimed to examine the role of HCy and metabolites in neuronal cell death and establish a culture system that would be capable of supporting long term exposure to HCy and metabolites. In results 1 it was shown that using a novel differentiation protocol whilst forgoing expensive neurotrophic factors it was possible to maintain SH-SH5Y cells for 1 month. These cells remained viable and were identified as functional neurons as they were capable of spontaneously firing action potentials and displayed synaptic marker synapsin. For future work, further investigation to determine post-synaptic markers such as PSD95 should be examined. Additionally, markers for astrocytes and further determination of the culture population would have been beneficial. These cells also displayed signs of neuronal ageing in the form of oxidative damage to lipids and proteins. Therefore, this protocol gives rise to cells which are valuable for neurodegenerative and neuroprotective research, further benefit could be gained from transfecting these cells to further study the effects of specific neurodegenerative disease.

The second part of my thesis focussed on determining the mechanism by which HCy and HCy-T are neurotoxic. This found that unlike HCy, HCy-T toxicity could not be blocked with the addition of NMDA receptor antagonists to the same extent as HCy, this may be a result of the cyclic structure of HCy-T. However, the pattern of ERK signalling was the same as that of HCy, this may be because of the conversion to HCy-T back to HCy. Upon further examination in results 3 it is more likely that HCy-T is responsible for the increase in oxidative stress. Whilst neither HCy or HCy-T caused any alterations in NO release however this was very variable, and a higher throughput measurement of generation may reveal more. However, HCy-T shows a large increase in ROS generation and the mitochondria shows abnormal morphology, the mitochondria became highly interconnected which implies an impairment in the balance of mitochondrial fusion and fission. Furthermore, both metabolites showed both acute and chronic

impairment of mitochondrial membrane potential. Attempts were made to extract the mitochondria and examine the alterations of mitochondrial fusion and fission proteins such as FIS1 and Mfn, not enough was generated from the mitochondrial protein extraction methods to complete this.

The final results section aimed to examine the long term effects of subtoxic concentrations of HCy, HCy-T and HCA. However, this was unsuccessful as the cells generated from results 1 were too delicate for this type of experiment. Whilst widespread cell death was observed from phase contrast micrographs, this could not be quantified as the extent of cell death was below the limits of detection. Furthermore, determination of the cell stress markers was not successful as upon fixation, cells became detached. However, this did indicate that subtoxic concentrations of HCy, HCy-T and HCA were more neurotoxic over a period of 2 to 1 month and that ageing cells appear more susceptible to insult from these metabolites. As the cell death was so severe, the variability obtained from the cell death assays was too much to gain any significant results from. Furthermore, protein which was extracted to examine AD markers, APP, PS1 and pTau was in varied quantities and therefore results here were too varied to obtain significant results from. However, all metabolites appear to increase these markers and possibly with more samples this may be an interesting finding. This chapter highlighted that the protocol established in results 1 may be more effective for the study of neuroprotective agents than neurotoxic as the cells are too delicate for experiments of this nature.

REFERENCES

1. Lee M, Hong K-S, Chang S-C, Saver JL. Efficacy of homocysteine-lowering therapy with folic Acid in stroke prevention: a meta-analysis. Stroke. 2010 Jun;41(6):1205–12.

2. Selhub J. Homocysteine metabolism. Annu Rev Nutr. 1999 Jan;19:217–46.

3. Sharma P, Senthilkumar RD, Brahmachari V, Sundaramoorthy E, Mahajan A, Sharma A, et al. Mining literature for a comprehensive pathway analysis: a case study for retrieval of homocysteine related genes for genetic and epigenetic studies. Lipids Health Dis. 2006 Jan;5:1.

4. Coppedè F. One-carbon metabolism and Alzheimer's disease: focus on epigenetics. Curr Genomics. 2010;1:246–60.

5. Marker M, Schalinske KL, Smazal AL. Homocysteine Imbalance : a Pathological. 2012;755–62.

6. Bearden SE, Beard RS, Pfau JC. Extracellular transsulfuration generates hydrogen sulfide from homocysteine and protects endothelium from redox stress. Am J Physiol Heart Circ Physiol. 2010 Nov;299(5):H1568-76.

7. Coppedè F, Grossi E, Buscema M, Migliore L. Application of artificial neural networks to investigate one-carbon metabolism in Alzheimer's disease and healthy matched individuals. PLoS One. 2013 Jan;8(8):e74012.

8. Brattström L, Lindgren A, Israelsson B, Andersson A, Hultberg B. Homocysteine and cysteine: determinants of plasma levels in middle-aged and elderly subjects. J Intern Med. 1994 Dec ;236(6):633–41.

9. Mato JM, Luz Martínez-Chantar M, Lu SC. S-adenosylmethionine metabolism and liver disease.

10. Di Rosa G, Attinà S, Spanò M, Ingegneri G, Sgrò DL, Pustorino G, et al. Efficacy of folic acid in children with migraine, hyperhomocysteinemia and MTHFR polymorphisms. Headache. 2007 Oct;47(9):1342–4.

11. Liu C, Yang Y, Peng D, Chen L, Luo J. Hyperhomocysteinemia as a metabolic disorder parameter is independently associated with the severity of coronary heart disease. Saudi Med J. 2015 Jul;36(7):839–46.

12. Maron B, Loscalzo J. The Treatment of Hyperhomocysteinemia. Annu Rev Med. 2009;60:39–54.

13. Obeid R, Herrmann W. Mechanisms of homocysteine neurotoxicity in neurodegenerative diseases with special reference to dementia. FEBS Lett. 2006 May 29;580(13):2994–3005.

14. Ramsaransing GSM, Fokkema MR, Teelken a, Arutjunyan a V, Koch M, De Keyser J. Plasma homocysteine levels in multiple sclerosis. J Neurol Neurosurg Psychiatry. 2006 Feb;77(2):189–92.

15. Ganguly P, Alam SF. Role of homocysteine in the development of cardiovascular disease. Nutr J. 2015 Jan 10;14(1):6.

16. Verhoef P, Meleady R, Daly LE, Graham IM, Robinson K, Boers and the European COMAC Group GHJ. Homocysteine, vitamin status and risk of vascular disease; effects of gender and menopausal status. Eur Heart J. 1999 Sep;20(17):1234–44.

17. Zmuda JM, Bausserman LL, Maceroni D, Thompson PD. The effect of supraphysiologic doses of testosterone on fasting total homocysteine levels in normal men. Atherosclerosis. 1997 Apr 1;130(1–2):199–202.

18. Nakhai Pour HR, Grobbee DE, Muller M, Emmelot-Vonk M, van der Schouw YT. Serum sex hormone and plasma homocysteine levels in middle-aged and elderly men. Eur J Endocrinol . 2006 Dec 1;155(6):887–93.

19. Friso S, Lamon-Fava S, Jang H, Schaefer EJ, Corrocher R, Choi S-W. Oestrogen replacement therapy reduces total plasma homocysteine and enhances genomic DNA methylation in postmenopausal women. Br J Nutr. 2007 Apr;97(4):617–21.

20. Zhang Y, He Y, Zong Y, Guo J, Sun L, Ma Y, et al. 17β-estradiol attenuates homocysteine-induced oxidative stress and inflammatory response as well as MAPKs cascade via activating PI3-K/Akt signal transduction pathway in Raw 264.7 cells. Acta Biochim Biophys Sin (Shanghai). 2015 Feb 1;47(2):65–72.

21. Seghieri G, Breschi MC, Anichini R, De Bellis A, Alviggi L, Maida I, et al. Serum homocysteine levels are increased in women with gestational diabetes mellitus. Metabolism. 2003 Jun 1 ;52(6):720–3.

22. Gong T, Wang J, Yang M, Shao Y, Liu J, Wu Q, et al. Serum homocysteine level and gestational diabetes mellitus: A meta-analysis. J Diabetes Investig. 2016 Jul;7(4):622–8.

23. Alatab S, Fakhrzadeh H, Sharifi F, Mirarefin M, Badamchizadeh Z, Ghaderpanahi M, et al. Correlation of serum homocysteine and previous history of gestational diabetes mellitus. J Diabetes Metab Disord. 2013;12(1):34.

24. Lai JS, Pang WW, Cai S, Lee YS, Chan JKY, Shek LPC, et al. High folate and low vitamin B12 status during pregnancy is associated with gestational diabetes mellitus. Clin Nutr. 2018 Jun 1 ;37(3):940–7.

25. Bansal S, Kapoor S, Singh GP, Yadav S. Serum Homocysteine Levels in Type 2 Diabetes Mellitus Patients. Vol. 3, International Journal of Contemporary Medical Research ISSN. Online; 2015

26. Najib S, Sánchez-Margalet V. Homocysteine thiolactone inhibits insulin signaling, and glutathione has a protective effect. Vol. 27, Journal of Molecular Endocrinology. 2001

27. Li Y, Jiang C, Xu G, Wang N, Zhu Y, Tang C, et al. Homocysteine upregulates resistin production from adipocytes in vivo and in vitro. Diabetes. 2008 Apr 1;57(4):817–27.

28. A. V. S, P. A. Z, G. R. Changes in homocysteine levels during normal pregnancy and preeclampsia and its relation with oxidative stress. Int J Res Med Sci. 2016 Dec 19;5(1):330.

29. Walker MC, Smith GN, Perkins SL, Keely EJ, Garner PR. Changes in homocysteine levels during normal pregnancy. Am J Obstet Gynecol. 1999 Mar;180(3 Pt 1):660–4.

30. Hekmatdoost A, Vahid F, Yari Z, Sadeghi M, Eini-Zinab H, Lakpour N, et al. Methyltetrahydrofolate vs Folic Acid Supplementation in Idiopathic Recurrent Miscarriage with Respect to Methylenetetrahydrofolate Reductase C677T and A1298C Polymorphisms: A Randomized Controlled Trial. PLoS One. 2015 Jan;10(12):e0143569.

31. Solé-Navais P, Cavallé-Busquets P, Fernandez-Ballart JD, Murphy MM. Early pregnancy B vitamin status, one carbon metabolism, pregnancy outcome and child development. Biochimie. 2015 Dec 15

32. Puig-Alcaraz C, Fuentes-Albero M, Calderón J, Garrote D, Cauli O. Increased homocysteine levels correlate with the communication deficit in children with autism spectrum disorder. Psychiatry Res 2015 Oct 30;229(3):1031–7.

33. Semmler A, Heese P, Stoffel-Wagner B, Muschler M, Heberlein A, Bigler L, et al. Alcohol abuse and cigarette smoking are associated with global DNA hypermethylation: results

from the German Investigation on Neurobiology in Alcoholism (GINA). Alcohol. 2015 Mar;49(2):97–101.

34. Seghieri G, Breschi MC, Anichini R, De Bellis A, Alviggi L, Maida I, et al. Serum homocysteine levels are increased in women with gestational diabetes mellitus. Metabolism. 2003 Jun;52(6):720–3.

35. Kalhan SC, Marczewski SE. Methionine, homocysteine, one carbon metabolism and fetal growth. 2012;

36. Straßburg A, Krems C, Lührmann PM, Hartmann B, Neuhäuser-Berthold M. Effect of Age on Plasma Homocysteine Concentrations in Young and Elderly Subjects Considering Serum Vitamin Concentrations and Different Lifestyle Factors. Int J Vitam Nutr Res . 2004 Mar;74(2):129–36.

37. Dankner R, Chetrit A, Lubin F, Sela B-A. Life-style habits and homocysteine levels in an elderly population. Aging Clin Exp Res . 2004 Dec 10;16(6):437–42.

38. Cave AJ, Cox DW, Vicaruddin O. Loss of taste with clopidogrel. Can Fam Physician . 2008 Feb;54(2):195–6.

39. Shiraishi M, Haruna M, Matsuzaki M, Ota E, Murayama R, Sasaki S, et al. Relationship between plasma total homocysteine level and dietary caffeine and vitamin B6 intakes in pregnant women. Nurs Health Sci . 2014 Jun;16(2):164–70.

40. Panagiotakos DB, Pitsavos C, Zampelas A, Zeimbekis A, Chrysohoou C, Papademetriou L, et al. The association between coffee consumption and plasma total homocysteine levels: the "ATTICA" study. Heart Vessels . 2004 Nov;19(6):280–6.

41. Verhoef P, Pasman WJ, Van Vliet T, Urgert R, Katan MB. Contribution of caffeine to the homocysteine-raising effect of coffee: a randomized controlled trial in humans. Am J Clin Nutr . 2002 Dec;76(6):1244–8.

42. Vercambre M-N, Berr C, Ritchie K, Kang JH. Caffeine and cognitive decline in elderly women at high vascular risk. J Alzheimers Dis . 2013;35(2):413–21.

43. Miranda AM, Steluti J, Fisberg RM, Marchioni DM. Association between Coffee Consumption and Its Polyphenols with Cardiovascular Risk Factors: A Population-Based Study. Nutrients . 2017 Mar 14;9(3).

44. Monente C, Ludwig IA, Irigoyen A, De Peña M-P, Cid C. Assessment of Total (Free and Bound) Phenolic Compounds in Spent Coffee Extracts. J Agric Food Chem . 2015 May 6;63(17):4327–34.

45. Hultberg M, Isaksson A, Andersson A, Hultberg B. The polyphenol quercetin strongly increases homocysteine production in a human hepatoma (Hep G2) cell line. Clin Biochem . 2006 Feb;39(2):160–3.

46. Hodgson JM, Burke V, Beilin LJ, Croft KD, Puddey IB. Can black tea influence plasma total homocysteine concentrations? Am J Clin Nutr . 2003 Apr 1;77(4):907–11.

47. Olthof MR, Hollman PC, Zock PL, Katan MB. Consumption of high doses of chlorogenic acid, present in coffee, or of black tea increases plasma total homocysteine concentrations in humans. Am J Clin Nutr . 2001 Mar 1;73(3):532–8.

48. Ataie a, Sabetkasaei M, Haghparast a, Hajizadeh Moghaddam a, Ataie R, Nasiraei Moghaddam S. An investigation of the neuroprotective effects of Curcumin in a model of Homocysteine - induced oxidative stress in the rat's brain. Daru . 2010 Jan;18(2):128–36.

49. Verhoef P, Pasman WJ, Van Vliet T, Urgert R, Katan MB. Contribution of caffeine to the homocysteine-raising effect of coffee: a randomized controlled trial in humans. Am J Clin Nutr . 2002 Dec 1;76(6):1244–8.

50. González-Ortiz M, Pascoe-González S, Kam-Ramos AM, Martínez-Abundis E. Effect of tequila on homocysteine, insulin secretion, insulin sensitivity, and metabolic profile in healthy men. J Diabetes Complications . 2005;19(3):155–9.

51. Gibson A, Woodside J V, Young IS, Sharpe PC, Mercer C, Patterson CC, et al. Alcohol increases homocysteine and reduces B vitamin concentration in healthy male volunteers--a randomized, crossover intervention study. QJM . 2008 Nov 1;101(11):881–7.

52. Dixon JB, Dixon ME, O'Brien PE. Reduced plasma homocysteine in obese red wine consumers: a potential contributor to reduced cardiovascular risk status. Eur J Clin Nutr . 2002 Jun 25;56(7):608–14.

53. Sakuta H, Suzuki T. Alcohol consumption and plasma homocysteine. Alcohol . 2005 Oct;37(2):73–7.

54. Choi S-H, Choi-Kwon S, Kim M-S, Kim J-S. Poor nutrition and alcohol consumption are related to high serum homocysteine level at post-stroke. Nutr Res Pract . 2015 Oct;9(5):503–10.

55. Harper C, Dixon G, Sheedy D, Garrick T. Neuropathological alterations in alcoholic brains. Studies arising from the New South Wales Tissue Resource Centre. Prog Neuropsychopharmacol Biol Psychiatry . 2003 Sep;27(6):951–61.

56. Stickel F, Choi S-W, Kim Y-I, Bagley PJ, Seitz HK, Russell RM, et al. Effect of Chronic Alcohol Consumption on Total Plasma Homocysteine Level in Rats. Alcohol Clin Exp Res . 2000 Mar;24(3):259–64.

57. Shenoy V, Mehendale V, Prabhu K, Shetty R, Rao P. Correlation of Serum Homocysteine Levels with the Severity of Coronary Artery Disease. Indian J Clin Biochem . 2014 Jul 31;29(3):339–44.

58. Veeranna V, Zalawadiya SK, Niraj A, Pradhan J, Ference B, Burack RC, et al. Homocysteine and Reclassification of Cardiovascular Disease Risk. J Am Coll Cardiol . 2011 Aug 30;58(10):1025–33.

59. Okura T, Miyoshi K-I, Irita J, Enomoto D, Nagao T, Kukida M, et al. Hyperhomocysteinemia is one of the risk factors associated with cerebrovascular stiffness in hypertensive patients, especially elderly males.

60. Marcus J, Sarnak MJ, Menon V. Homocysteine lowering and cardiovascular disease risk: lost in translation. Can J Cardiol . 2007 Jul;23(9):707–10.

61. BOERS GHJ. Mild Hyperhomocysteinemia is an Independent Risk Factor of Arterial Vascular Disease. Semin Thromb Hemost . 2000;Volume 26(Number 03):291–6.

62. Moustafa AA, Hewedi DH, Eissa AM, Frydecka D, Misiak B. Homocysteine levels in schizophrenia and affective disorders-focus on cognition. Front Behav Neurosci . 2014 Jan;8:343.

63. Bhatia P, Singh N. Homocysteine excess: delineating the possible mechanism of neurotoxicity and depression. Fundam Clin Pharmacol . 2015 Aug 27

64. Kennedy SH. Core symptoms of major depressive disorder: relevance to diagnosis and treatment. Dialogues Clin Neurosci . 2008;10(3):271–7.

65. White DJ, Cox KHM, Peters R, Pipingas A, Scholey AB. Effects of Four-Week Supplementation with a Multi-Vitamin/Mineral Preparation on Mood and Blood Biomarkers

in Young Adults: A Randomised, Double-Blind, Placebo-Controlled Trial. Nutrients . 2015 Jan;7(11):9005–17.

66. Peerbooms OLJ, van Os J, Drukker M, Kenis G, Hoogveld L, de Hert M, et al. Meta-analysis of MTHFR gene variants in schizophrenia, bipolar disorder and unipolar depressive disorder: Evidence for a common genetic vulnerability? Brain Behav Immun . 2011 Nov 12;25(8):1530–43.

67. Kevere L, Purvina S, Bauze D, Zeibarts M, Andrezina R, Rizevs A, et al. Elevated Serum Levels of Homocysteine as an Early Prognostic Factor of Psychiatric Disorders in Children and Adolescents. Schizophr Res Treatment . 2012 Oct 2;2012:1–7.

68. Türksoy N, Bilici R, Yalçıner A, Ozdemir YÖ, Ornek I, Tufan AE, et al. Vitamin B12, folate, and homocysteine levels in patients with obsessive-compulsive disorder. Neuropsychiatr Dis Treat . 2014;10:1671–5.

69. Gariballa S. Testing homocysteine-induced neurotransmitter deficiency, and depression of mood hypothesis in clinical practice. Age Ageing . 2011 Nov 1;40(6):702–5.

70. Lakhan SE, Vieira KF. Nutritional therapies for mental disorders. Nutr J . 2008 Jan 21;7(1):2.

71. Patrick RP, Ames BN. Vitamin D and the omega-3 fatty acids control serotonin synthesis and action, part 2: relevance for ADHD, bipolar disorder, schizophrenia, and impulsive behavior. FASEB J . 2015 Jun;29(6):2207–22.

72. Goodman WK, Price LH, Delgado PL, Palumbo J, Krystal JH, Nagy LM, et al. Specificity of Serotonin Reuptake Inhibitors in the Treatment of Obsessive-Compulsive Disorder. Arch Gen Psychiatry . 1990 Jun 1;47(6):577.

73. Bystritsky A, Khalsa SS, Cameron ME, Schiffman J. Current diagnosis and treatment of anxiety disorders. P T . 2013 Jan;38(1):30–57.

74. Mesripour A, Hajhashemi V, Kuchak A. Effect of concomitant administration of three different antidepressants with vitamin B6 on depression and obsessive compulsive disorder in mice models. Res Pharm Sci . 2017 Feb;12(1):46–52.

75. Folstein M, Liu T, Peter I, Buel J, Arsenault L, Scott T, et al. The Homocysteine Hypothesis of Depression. Am J Psychiatry . 2007 Jun;164(6):861–7.

76. Mattson MP, Shea TB. Folate and homocysteine metabolism in neural plasticity and neurodegenerative disorders. Trends Neurosci . 2003 Mar;26(3):137–46.

77. Dietrich-Muszalska A, Malinowska J, Olas B, Głowacki R, Bald E, Wachowicz B, et al. The oxidative stress may be induced by the elevated homocysteine in schizophrenic patients. Neurochem Res . 2012 May;37(5):1057–62.

78. Brown AS, Bottiglieri T, Schaefer CA, Quesenberry CP, Liu L, Bresnahan M, et al. Elevated Prenatal Homocysteine Levels as a Risk Factor for Schizophrenia. Arch Gen Psychiatry . 2007 Jan 1 ;64(1):31.

79. Kristiansen L V, Bakir B, Haroutunian V, Meador-Woodruff JH. Expression of the NR2B-NMDA receptor trafficking complex in prefrontal cortex from a group of elderly patients with schizophrenia. Schizophr Res . 2010 Jun;119(1–3):198–209.

80. Misiak B, Frydecka D, Slezak R, Piotrowski P, Kiejna A. Elevated homocysteine level in first-episode schizophrenia patients—the relevance of family history of schizophrenia and lifetime diagnosis of cannabis abuse. Metab Brain Dis . 2014 Sep 30;29(3):661–70.

81. Remington G, Foussias G, Fervaha G, Agid O, Takeuchi H, Lee J, et al. Treating Negative Symptoms in Schizophrenia: an Update. Curr Treat options psychiatry . 2016;3:133–50.

82. Araújo JR, Martel F, Borges N, Araújo JM, Keating E. Folates and aging: Role in mild cognitive impairment, dementia and depression. Ageing Res Rev . 2015 Jul;22:9–19.

83. Stewart R, Asonganyi B, Sherwood R. Plasma Homocysteine and Cognitive Impairment in an Older British African-Caribbean Population. J Am Geriatr Soc . 2002 Jul 1;50(7):1227–32.

84. Moustafa A a, Hewedi DH, Eissa AM, Myers CE, Sadek H a. The relationship between associative learning, transfer generalization, and homocysteine levels in mild cognitive impairment. PLoS One . 2012 Jan;7(9):e46496.

85. Kruger WD, Gupta S. The effect of dietary modulation of sulfur amino acids on cystathionine β synthase-deficient mice. Ann N Y Acad Sci . 2015 Nov 24;

86. Algaidi SA, Christie LA, Jenkinson AM, Whalley L, Riedel G, Platt B. Long-term homocysteine exposure induces alterations in spatial learning, hippocampal signalling and synaptic plasticity. Exp Neurol . 2006 Jan;197(1):8–21.

87. Moore BD, Chakrabarty P, Levites Y, Kukar TL, Baine A-M, Moroni T, et al. Overlapping profiles of Aβ peptides in the Alzheimer's disease and pathological aging brains. Alzheimers Res Ther . 2012 Jan;4(3):18.

88. Martin L, Latypova X, Terro F. Post-translational modifications of tau protein: implications for Alzheimer's disease. Neurochem Int . 2011 Mar;58(4):458–71.

89. Blasko I, Jellinger K, Kemmler G, Krampla W, Jungwirth S, Wichart I, et al. Conversion from cognitive health to mild cognitive impairment and Alzheimer's disease:

prediction by plasma amyloid beta 42, medial temporal lobe atrophy and homocysteine. Neurobiol Aging . 2008 Jan;29(1):1–11.

90. Smith AD, Smith SM, de Jager CA, Whitbread P, Johnston C, Agacinski G, et al. Homocysteine-Lowering by B Vitamins Slows the Rate of Accelerated Brain Atrophy in Mild Cognitive Impairment: A Randomized Controlled Trial. Bush AI, editor. PLoS One . 2010 Sep 8;5(9):e12244.

91. Coppedè F, Tannorella P, Pezzini I, Migheli F, Ricci G, Caldarazzo lenco E, et al. Folate, Homocysteine, Vitamin B12, and Polymorphisms of Genes Participating in One-Carbon Metabolism in Late-Onset Alzheimer's Disease Patients and Healthy Controls. Antioxid Redox Signal . 2012 Jul 15;17(2):195–204.

92. Ho PI, Collins SC, Dhitavat S, Ortiz D, Ashline D, Rogers E, et al. Homocysteine potentiates beta-amyloid neurotoxicity: role of oxidative stress. J Neurochem . 2001 Jul;78(2):249–53.

93. Zhang C-E, Wei W, Liu Y-H, Peng J-H, Tian Q, Liu G-P, et al. Hyperhomocysteinemia increases beta-amyloid by enhancing expression of gamma-secretase and phosphorylation of amyloid precursor protein in rat brain. Am J Pathol . 2009 Apr;174(4):1481–91.

94. Scarpa S, Fuso A, D'Anselmi F, Cavallaro R a. Presenilin 1 gene silencing by S-adenosylmethionine: a treatment for Alzheimer disease? FEBS Lett . 2003 Apr;541(1–3):145–8.

95. Chan AY, Alsaraby A, Shea TB. Folate deprivation increases tau phosphorylation by homocysteine-induced calcium influx and by inhibition of phosphatase activity: Alleviation by S-adenosyl methionine. Brain Res . 2008 Mar 14;1199:133–7.

96. Kuszczyk M, Gordon-Krajcer W, Lazarewicz JW. Homocysteine-induced acute excitotoxicity in cerebellar granule cells in vitro is accompanied by PP2A-mediated dephosphorylation of tau. Neurochem Int . 2009;55(1–3):174–80.

97. Moore DJ, West AB, Dawson VL, Dawson TM. Molecular pathophysiology of Parkinson's disease. Annu Rev Neurosci . 2005 Jan;28:57–87.

98. Broderick G, Rajfer SI. The use of levodopa, an oral dopamine precursor, in congestive heart failure. Basic Res Cardiol . 1989;84 Suppl 1:187–90.

99. Cunha AS, Matheus FC, Moretti M, Sampaio TB, Poli A, Santos DB, et al. Agmatine attenuates reserpine-induced oral dyskinesia in mice: Role of oxidative stress, nitric oxide and glutamate NMDA receptors. Behav Brain Res. 2016;

100. Cheng H, Gomes-Trolin C, Aquilonius SM, Steinberg A, Löfberg C, Ekblom J, et al. Levels of L-methionine S-adenosyltransferase activity in erythrocytes and concentrations of S-adenosylmethionine and S-adenosylhomocysteine in whole blood of patients with Parkinson's disease. Exp Neurol . 1997 Jun;145(2 Pt 1):580–5.

101. Shin JY, Ahn Y-H, Paik M-J, Park HJ, Sohn YH, Lee PH. Elevated homocysteine by levodopa is detrimental to neurogenesis in parkinsonian model. PLoS One . 2012 Jan;7(11):e50496.

102. Romero JR, Pikula A, Nguyen TN, Nien YL, Norbash A, Babikian VL. Cerebral collateral circulation in carotid artery disease. Curr Cardiol Rev . 2009 Nov;5(4):279–88.

103. Krishnamurthi R V, Feigin VL, Forouzanfar MH, Mensah GA, Connor M, Bennett DA, et al. Global and regional burden of first-ever ischaemic and haemorrhagic stroke during 1990-2010: findings from the Global Burden of Disease Study 2010. Lancet Glob Heal . 2013 Nov;1(5):e259-81.

104. Sims NR, Muyderman H. Mitochondria, oxidative metabolism and cell death in stroke. Biochim Biophys Acta . 2010 Jan;1802(1):80–91.

105. Wu X-Q, Ding J, Ge A-Y, Liu F-F, Wang X, Fan W. Acute phase homocysteine related to severity and outcome of atherothrombotic stroke. Eur J Intern Med . 2013 Jun;24(4):362–7.

106. Saposnik G, Ray JG, Sheridan P, McQueen M, Lonn E. Homocysteine-Lowering Therapy and Stroke Risk, Severity, and Disability Additional Findings From the HOPE 2 Trial the HOPE 2 Investigators*.

107. Shi Z, Guan Y, Huo YR, Liu S, Zhang M, Lu H, et al. Elevated Total Homocysteine Levels in Acute Ischemic Stroke Are Associated With Long-Term Mortality. Stroke . 2015 Sep;46(9):2419–25.

108. Weston RM, Lin B, Dusting GJ, Roulston CL. Targeting oxidative stress injury after ischemic stroke in conscious rats: limited benefits with apocynin highlight the need to incorporate long term recovery. Stroke Res Treat . 2013 Jan 14;2013:648061.

109. Yu G, Wu F, Wang E-S. BQ-869, a novel NMDA receptor antagonist, protects against excitotoxicity and attenuates cerebral ischemic injury in stroke. Int J Clin Exp Pathol . 2015 Jan;8(2):1213–25.

110. Castillo J, Davalos A, Naveiro J, Noya M. Neuroexcitatory Amino Acids and Their Relation to Infarct Size and Neurological Deficit in Ischemic Stroke. Stroke . 1996 Jun 1;27(6):1060–5.

111. Lai TW, Zhang S, Wang YT. Excitotoxicity and stroke: Identifying novel targets for neuroprotection. Prog Neurobiol . 2014 Apr;115:157–88.

112. Lipton S a, Kim WK, Choi YB, Kumar S, D'Emilia DM, Rayudu P V, et al. Neurotoxicity associated with dual actions of homocysteine at the N-methyl-D-aspartate receptor. Proc Natl Acad Sci U S A . 1997 May 27;94(11):5923–8.

113. White AR, Huang X, Jobling MF, Barrow CJ, Beyreuther K, Masters CL, et al. Homocysteine potentiates copper- and amyloid beta peptide-mediated toxicity in primary neuronal cultures: possible risk factors in the Alzheimer's-type neurodegenerative pathways. J Neurochem . 2001 Dec 20;76(5):1509–20.

114. Kruman II, Kumaravel TS, Lohani A, Pedersen WA, Cutler RG, Kruman Y, et al. Folic Acid Deficiency and Homocysteine Impair DNA Repair in Hippocampal Neurons and Sensitize Them to Amyloid Toxicity in Experimental Models of Alzheimer ' s Disease. 2002;22(5):1752–62.

115. Garcia A, Zanibbi K. Homocysteine and cognitive function in elderly people. CMAJ . 2004 Oct 12;171(8):897–904.

116. Sachdev PS. Homocysteine and brain atrophy. Prog Neuropsychopharmacol Biol Psychiatry . 2005 Sep;29(7):1152–61.

117. Hansson O, Zetterberg H, Buchhave P, Londos E, Blennow K, Minthon L. Association between CSF biomarkers and incipient Alzheimer's disease in patients with mild cognitive impairment: a follow-up study. Lancet Neurol . 2006 Mar;5(3):228–34.

118. Ho PI, Ortiz D, Rogers E, Shea TB. Multiple aspects of homocysteine neurotoxicity: glutamate excitotoxicity, kinase hyperactivation and DNA damage. J Neurosci Res . 2002 Dec 1;70(5):694–702.

119. Perez-de-Arce K, Foncea R, Leighton F. Reactive oxygen species mediates homocysteine-induced mitochondrial biogenesis in human endothelial cells: modulation by antioxidants. Biochem Biophys Res Commun . 2005 Dec 16;338(2):1103–9.

120. Zhou J, Werstuck GH, Lhoták S, de Koning a BL, Sood SK, Hossain GS, et al. Association of multiple cellular stress pathways with accelerated atherosclerosis in hyperhomocysteinemic apolipoprotein E-deficient mice. Circulation . 2004 Jul 13;110(2):207–13.

121. Zieminska E, Matyja E, Kozlowska H, Stafiej A, Lazarewicz JW. Excitotoxic neuronal injury in acute homocysteine neurotoxicity: role of calcium and mitochondrial alterations. Neurochem Int . 2006;48(6–7):491–7.

122. Tang X-Q, Chen R-Q, Ren Y-K, Soldato P Del, Sparatore A, Zhuang Y-Y, et al. ACS6, a Hydrogen sulfide-donating derivative of sildenafil, inhibits homocysteine-induced apoptosis by preservation of mitochondrial function. Med Gas Res . 2011 Jan;1(1):20.

123. Foster GA, Roberts PJ. Neurochemical and pharmacological correlates of inferior olive destruction in the rat: Attenuation of the events mediated by an endogenous glutamate-like substance. Neuroscience . 1983 Feb;8(2):277–84.

124. Oldreive CE, Doherty GH. Neurotoxic effects of homocysteine on cerebellar Purkinje neurons in vitro. Neurosci Lett . 2007 Feb 8;413(1):52–7.

125. Ganapathy PS, Moister B, Roon P, Mysona BA, Dun Y, Moister TKVE, et al. Endogenous Elevation of Homocysteine Induces Retinal Neuron Death in the Cystathionine-beta-Synthase Mutant Mouse. Invest Ophthalmol Vis Sci. 2009;50(9):4460–70.

126. Zhou J, Portugal G, Kruger W, Wang H, Gould T, Pratico D. Diet-Induced Hyperhomocysteineemia Increases Amyloid-Beta Formation and Deposition in a Mouse Model of Alzheimer's Disease. 2010;7(2):140–9.

127. Jakubowski H, Głowacki R. CHEMICAL BIOLOGY OF HOMOCYSTEINE THIOLACTONE AND RELATED METABOLITES Institute of Bioorganic Chemistry , Polish Academy of Sciences , Department of Biochemistry and Biotechnology , Life Sciences Hcy- Protein N- linked Hcy tHcy. 2011;55:81–103.

128. Borowczyk K, Shih DM, Jakubowski H. Metabolism and Neurotoxicity of Homocysteine Thiolactone in Mice: Evidence for a Protective Role of Paraoxonase. J Alzheimer's Dis. 2012;30(2):225–31.

129. Yilmaz N. Relationship between paraoxonase and homocysteine: crossroads of oxidative diseases. Arch Med Sci . 2012 Feb 29;8(1):138–53.

130. Arvanitakis Z, Wilson RS, Bienias JL, Evans D a, Bennett D a. Diabetes mellitus and risk of Alzheimer disease and decline in cognitive function. Arch Neurol . 2004 May;61(5):661–6.

131. Patterson S, Flatt PR, McClenaghan NH. Major metabolic homocysteine-derivative, homocysteine thiolactone, exerts changes in pancreatic beta-cell glucose-sensing, cellular signal transduction and integrity. Arch Biochem Biophys . 2007 May 15;461(2):287–93.

132. Akchiche N, Bossenmeyer-Pourié C, Kerek R, Martin N, Pourié G, Koziel V, et al. Homocysteinylation of neuronal proteins contributes to folate deficiency-associated alterations of differentiation, vesicular transport, and plasticity in hippocampal neuronal cells. FASEB J . 2012 Oct;26(10):3980–92.

133. Suszynska J, Tisonczyk J, Lee H, Smith MA, Jakubowski H. Reduced Homocysteine-Thiolactonase Activity in Alzheimer's Disease. J Alzheimer's Dis. 2010;19(4):1177–83.

134. Goswami B, Tayal D, Gupta N, Mallika V. Paraoxonase: a multifaceted biomolecule. Clin Chim Acta . 2009 Dec;410(1–2):1–12.

135. Perla-Kaján J, Jakubowski H. Paraoxonase 1 protects against protein N-homocysteinylation in humans. FASEB J . 2010 Mar;24(3):931–6.

136. Perła-Kaján J, Jakubowski H. Paraoxonase 1 and homocysteine metabolism. Amino Acids . 2012 Oct 29;43(4):1405–17.

137. Hu N-W, Ondrejcak T, Rowan MJ. Glutamate receptors in preclinical research on Alzheimer's disease: update on recent advances. Pharmacol Biochem Behav . 2012 Feb;100(4):855–62.

138. Yao Y, Mayer ML. Characterization of a soluble ligand binding domain of the NMDA receptor regulatory subunit NR3A. J Neurosci . 2006 Apr 26;26(17):4559–66.

139. Furukawa H, Singh SK, Mancusso R, Gouaux E. Subunit arrangement and function in NMDA receptors. Nature . 2005 Nov 10;438(7065):185–92.

140. Rybakova Y, Akkuratov E, Kulebyakin K, Brodskaya O, Dizhevskaya A, Boldyrev A. Receptor-mediated oxidative stress in murine cerebellar neurons is accompanied by phosphorylation of MAP (ERK 1/2) kinase. Curr Aging Sci . 2012 Dec;5(3):225–30.

141. Groc L, Bard L, Choquet D. Surface trafficking of N-methyl-D-aspartate receptors: physiological and pathological perspectives. Neuroscience . 2009 Jan 12;158(1):4–18.

142. Vieira MM, Schmidt J, Ferreira JS, She K, Oku S, Mele M, et al. Multiple domains in the C-terminus of NMDA receptor GluN2B subunit contribute to neuronal death following in vitro ischemia. Neurobiol Dis . 2015 Nov 12;

143. Conti F. Neuronal and Glial Localization of NR1 and NR2A/B Subunits of the NMDA Receptor in the Human Cerebral Cortex. Cereb Cortex . 1999 Mar 1;9(2):110–20.

144. Hardingham GE, Bading H. Synaptic versus extrasynaptic NMDA receptor signalling: implications for neurodegenerative disorders. Nat Rev Neurosci . 2010 Oct;11(10):682–96.

145. Thomas CG, Miller AJ, Westbrook GL. Synaptic and extrasynaptic NMDA receptor NR2 subunits in cultured hippocampal neurons. J Neurophysiol . 2006 Mar 1;95(3):1727–34.

146. Massey P V, Johnson BE, Moult PR, Auberson YP, Brown MW, Molnar E, et al. Differential roles of NR2A and NR2B-containing NMDA receptors in cortical long-term potentiation and long-term depression. J Neurosci . 2004 Sep 8;24(36):7821–8.

147. Wyllie DJA, Livesey MR, Hardingham GE. Influence of GluN2 subunit identity on NMDA receptor function. Neuropharmacology . 2013 Nov;74:4–17.

148. Doronzo G, Russo I, Del Mese P, Viretto M, Mattiello L, Trovati M, et al. Role of NMDA receptor in homocysteine-induced activation of mitogen-activated protein kinase and phosphatidyl inositol 3-kinase pathways in cultured human vascular smooth muscle cells. Thromb Res . 2010 Feb;125(2):e23-32.

149. Ganapathy PS, White RE, Ha Y, Bozard BR, McNeil PL, Caldwell RW, et al. The role of N-methyl-D-aspartate receptor activation in homocysteine-induced death of retinal ganglion cells. Invest Ophthalmol Vis Sci . 2011 Jul;52(8):5515–24.

150. Ziemińska E, Stafiej A, Łazarewicz JW. Role of group I metabotropic glutamate receptors and NMDA receptors in homocysteine-evoked acute neurodegeneration of cultured cerebellar granule neurones. Neurochem Int . 2003 Sep;43(4–5):481–92.

151. Poddar R, Paul S. Novel crosstalk between ERK MAPK and p38 MAPK leads to homocysteine-NMDA receptor-mediated neuronal cell death. J Neurochem . 2013 Feb;124(4):558–70.

152. McCully KS. Chemical pathology of homocysteine. IV. Excitotoxicity, oxidative stress, endothelial dysfunction, and inflammation. Ann Clin Lab Sci . 2009 Jan;39(3):219–32.

153. Poddar R, Paul S. Homocysteine-NMDA receptor-mediated activation of extracellular signal-regulated kinase leads to neuronal cell death. J Neurochem . 2009 Aug 26;110(3):1095–106.

154. Cai B, Li X, Wang Y, Liu Y, Yang F, Chen H, et al. Apoptosis of bone marrow mesenchymal stem cells caused by homocysteine via activating JNK signal. PLoS One . 2013 Jan;8(5):e63561.

155. Poddar R, Paul S. Homocysteine-NMDA receptor mediated activation of extracellular-signal regulated kinase leads to neuronal cell death. J Neurochem. 2009;110(3):1095–106.

156. Chaffey H, Chazot PL. NMDA receptor subtypes: Structure, function and therapeutics. Curr Anaesth Crit Care . 2008 Aug;19(4):183–201.

157. Abushik P a, Niittykoski M, Giniatullina R, Shakirzyanova A, Bart G, Fayuk D, et al. The role of NMDA and mGluR5 receptors in calcium mobilization and neurotoxicity of homocysteine in trigeminal and cortical neurons and glial cells. J Neurochem . 2014 Apr;129(2):264–74.

158. Wang X, Cui L, Joseph J, Jiang B, Pimental D, Handy DDE, et al. Homocysteine Induces Cardiomyocyte Dysfunction and Apoptosis though p38 MAPK-Mediated Increase in Oxidant Stress. J Mol cell Cardiol. 2012;52(3):753–60.

159. Mayo JN, Beard RS, Price TO, Chen C-H, Erickson M a, Ercal N, et al. Nitrative stress in cerebral endothelium is mediated by mGluR5 in hyperhomocysteinemia. J Cereb Blood Flow Metab . 2012 May;32(5):825–34.

160. Hajnóczky G, Csordás G, Das S, Garcia-Perez C, Saotome M, Sinha Roy S, et al. Mitochondrial calcium signalling and cell death: Approaches for assessing the role of mitochondrial Ca2+ uptake in apoptosis. Cell Calcium . 2006 Nov;40(5–6):553–60.

161. Förstermann U, Sessa WC. Nitric oxide synthases: regulation and function. Eur Heart J . 2012 Apr;33(7):829–37, 837a–837d.

162. Law A, Gauthier S, Quirion R, Centre M. Neuroprotective and neurorescuing e € ects of isoform-speci ® c nitric oxide synthase inhibitors , nitric oxide scavenger , and antioxidant against beta-amyloid toxicity. 2001;1114–24.

163. Pacher P, Beckman JS, Liadet L. Nitric Oxide and Peroxynitrite in Health and Disease. Physiol Rev. 2007;87(1):315–424.

164. Guix FX, Uribesalgo I, Coma M, Muñoz FJ. The physiology and pathophysiology of nitric oxide in the brain. Prog Neurobiol . 2005 Jun;76(2):126–52.

165. Pieper AA, Blackshaw S, Clements EE, Brat DJ, Krug DK, White AJ, et al. Poly(ADP-ribosyl)ation basally activated by DNA strand breaks reflects glutamate-nitric oxide neurotransmission. Proc Natl Acad Sci U S A . 2000 Feb 15;97(4):1845–50.

166. Martin PM, Ola MS, Agarwal N, Ganapathy V. The Sigma Receptor Ligand (+)-Pentazocine Prevents Apoptotic Retinal Ganglion Cell Death induced in vitro by Homocysteine and Glutamate. Brain Res Mol brain Res Res Mol brain Res. 2004;123(0):66–75.

167. Stuhlinger MC, Tsao PS, Her J-H, Kimoto M, Balint RF, Cooke JP. Homocysteine Impairs the Nitric Oxide Synthase Pathway: Role of Asymmetric Dimethylarginine. Circulation . 2001 Nov 20;104(21):2569–75.

168. Li M, Wang L, Peng Y, Wang J-C, Zhou L-H. Knockdown of the neuronal nitric oxide synthase gene retard the development of the cerebellar granule neurons in vitro. Dev Dyn . 2010 Feb;239(2):474–81.

169. Glushchenko A, Jacobsen D. Molecular Targeting of Proteins by -Homocysteine : Mechanistic Implications for Vascular Disease. Antioxid Redox Signal. 2007;9(11):1883–98.

170. Zhu X, Smith MA, Honda K, Aliev G, Moreira PI, Nunomura A, et al. Vascular oxidative stress in Alzheimer Disease. J Neurol Sci. 2007;257:240–6.

171. FEINSTEIN DL, GALEA E, REIS DJ. Suppression of Glial iNOS Expression by Tyrosine Kinase Inhibitorsa. Ann N Y Acad Sci . 2006 Dec 17;738(1):325–8.

172. Endoh M, Maiese K, Wagner J. Expression of the inducible form of nitric oxide synthase by reactive astrocytes after transient global ischemia. Brain Res . 1994 Jul 18;651(1–2):92–100.

173. Heneka MT, Feinstein DL. Expression and function of inducible nitric oxide synthase in neurons. J Neuroimmunol . 2001 Mar 1;114(1–2):8–18.

174. Su JH, Deng G, Cotman CW. Neuronal DNA damage precedes tangle formation and is associated with up-regulation of nitrotyrosine in Alzheimer's disease brain. Brain Res . 1997 Nov 7;774(1–2):193–9.

175. Good PF, Hsu A, Werner P, Perl DP, Olanow CW. Protein nitration in Parkinson's disease. J Neuropathol Exp Neurol . 1998 Apr;57(4):338–42.

176. Tohgi H, Abe T, Yamazaki K, Murata T, Ishizaki E, Isobe C. Remarkable increase in cerebrospinal fluid 3-nitrotyrosine in patients with sporadic amyotrophic lateral sclerosis. Ann Neurol . 1999 Jul;46(1):129–31.

177. Dietrich-Muszalska A, Malinowska J, Olas B, Głowacki R, Bald E, Wachowicz B, et al. The Oxidative Stress May be Induced by the Elevated Homocysteine in Schizophrenic Patients. Neurochem Res . 2012 May 24;37(5):1057–62.

178. Choi YB, Tenneti L, Le DA, Ortiz J, Bai G, Chen HS, et al. Molecular basis of NMDA receptor-coupled ion channel modulation by S-nitrosylation. Nat Neurosci . 2000 Jan;3(1):15–21.

179. Safiulina D, Kaasik A, Abeliovich H, Abraham R, Acevedo-Arozena A. Energetic and Dynamic: How Mitochondria Meet Neuronal Energy Demands. PLoS Biol . 2013 Dec 31;11(12):e1001755.

180. Amadou CKS, Lesnefsky EJ, Stowe DF. Potential Therapeutic Benefits of Strategies Directed to Mitochondria. Antioxid Redox Signal. 2010;13(3).

181. Kühlbrandt W. Structure and function of mitochondrial membrane protein complexes. BMC Biol . 2015 Oct 29;13:89.

182. Van Laar VS, Roy N, Liu A, Rajprohat S, Arnold B, Dukes AA, et al. Glutamate excitotoxicity in neurons triggers mitochondrial and endoplasmic reticulum accumulation of Parkin, and, in the presence of N-acetyl cysteine, mitophagy. Neurobiol Dis. 2015 Feb;74:180–93.

183. MacAskill AF, Kittler JT. Control of mitochondrial transport and localization in neurons. Trends Cell Biol . 2010 Feb;20(2):102–12.

184. Yi M, Weaver D, Hajnóczky G. Control of mitochondrial motility and distribution by the calcium signal: a homeostatic circuit. J Cell Biol . 2004 Nov 22;167(4):661–72.

185. Chernyak B V, Bernardi P. The mitochondrial permeability transition pore is modulated by oxidative agents through both pyridine nucleotides and glutathione at two separate sites. Eur J Biochem . 1996 Jun 15;238(3):623–30.

186. Bezprozvanny I, Mattson MP. Neuronal Calcium Mishandling and the Pathogenesis of Alzheimer's Disease. Trends Neurosci. 2008;31(9):454–63.

187. Van Laar VS, Roy N, Liu A, Rajprohat S, Arnold B, Dukes AA, et al. Glutamate excitotoxicity in neurons triggers mitochondrial and endoplasmic reticulum accumulation of Parkin, and, in the presence of N-acetyl cysteine, mitophagy. Neurobiol Dis . 2015 Feb;74:180–93.

188. Du H, Yan SS. Mitochondrial permeability transition pore in Alzheimer's disease: cyclophilin D and amyloid beta. Biochim Biophys Acta . 2010 Jan;1802(1):198–204.

189. Mnatsakanyan N, Beutner G, Porter GA, Alavian KN, Jonas EA. Physiological roles of the mitochondrial permeability transition pore. J Bioenerg Biomembr . 2016 Feb 11

190. Ganapathy PS, Perry RL, Tawfik A, Smith RM, Perry E, Roon P, et al. Homocysteine-mediated modulation of mitochondrial dynamics in retinal ganglion cells. Invest Ophthalmol Vis Sci . 2011 Jul;52(8):5551–8.

191. Nguyen D, Alavi M V, Kim K-Y, Kang T, Scott RT, Noh YH, et al. A new vicious cycle involving glutamate excitotoxicity, oxidative stress and mitochondrial dynamics. Cell Death Dis . 2011 Jan;2:e240.

192. Drew B, Leeuwenburgh C. Method for measuring ATP production in isolated mitochondria: ATP production in brain and liver mitochondria of Fischer-344 rats with age and caloric restriction. Am J Physiol Regul Integr Comp Physiol . 2003 Nov;285(5):R1259-67.

193. Moreira PI, Carvalho C, Zhu X, Smith MA, Perry G. Mitochondrial dysfunction is a trigger of Alzheimer's disease pathophysiology. Biochim Biophys Acta - Mol Basis Dis . 2010 Jan;1802(1):2–10.

194. Hirashima Y, Seshimo S, Fujiki Y, Okabe M, Nishiyama K, Matsumoto M, et al. Homocysteine and copper induce cellular apoptosis via caspase activation and nuclear translocation of apoptosis-inducing factor in neuronal cell line SH-SY5Y. Neurosci Res . 2010 Aug;67(4):300–6.

195. Jin Y, Brennan L. Effects of homocysteine on metabolic pathways in cultured astrocytes. Neurochem Int . 2008 Jun;52(8):1410–5.

196. Galluzzi L, Aaronson S a, Abrams J, Alnemri ES, Andrews DW, Baehrecke EH, et al. Guidelines for the use and interpretation of assays for monitoring cell death in higher eukaryotes. Cell Death Differ . 2009 Aug;16(8):1093–107.

197. Kepp O, Galluzzi L, Lipinski M, Yuan J, Kroemer G. Cell death assays for drug discovery. Nat Rev Drug Discov . 2011 Mar;10(3):221–37.

198. Wappler EA, Institoris A, Dutta S, Katakam PVG, Busija DW. Mitochondrial Dynamics Associated with Oxygen-Glucose Deprivation in Rat Primary Neuronal Cultures. Strack S, editor. PLoS One . 2013 May 2;8(5):e63206.

199. Romero-Calvo I, Ocón B, Martínez-Moya P, Suárez MD, Zarzuelo A, Martínez-Augustin O, et al. Reversible Ponceau staining as a loading control alternative to actin in Western blots. Anal Biochem . 2010 Jun;401(2):318–20.

200. Antony PMA, Boyd O, Trefois C, Ammerlaan W, Ostaszewski M, Baumuratov AS, et al. Platelet mitochondrial membrane potential in Parkinson's disease. Ann Clin Transl Neurol . 2015 Jan;2(1):67–73.

201. Jin YN, Johnson GVW. The interrelationship between mitochondrial dysfunction and transcriptional dysregulation in Huntington disease. J Bioenerg Biomembr . 2010 Jun;42(3):199–205.

202. Perry SW, Norman JP, Barbieri J, Brown EB, Gelbard HA. Mitochondrial membrane potential probes and the proton gradient: a practical usage guide. Biotechniques . 2011 Feb;50(2):98–115.

203. Gerencser AA, Chinopoulos C, Birket MJ, Jastroch M, Vitelli C, Nicholls DG, et al. Quantitative measurement of mitochondrial membrane potential in cultured cells: calcium-induced de- and hyperpolarization of neuronal mitochondria. J Physiol . 2012 Jun 15;590(12):2845–71.

204. Jakubowski W, Bartosz G. 2,7-DICHLOROFLUORESCIN OXIDATION AND REACTIVE OXYGEN SPECIES: WHAT DOES IT MEASURE? Cell Biol Int . 2000 Oct;24(10):757–60.

205. Agholme L, Lindström T, Kågedal K, Marcusson J, Hallbeck M. An in vitro model for neuroscience: differentiation of SH-SY5Y cells into cells with morphological and biochemical characteristics of mature neurons. J Alzheimers Dis . 2010 Jan 1;20(4):1069–82.

206. Kovalevich J, Langford D. Considerations for the Use of SH-SY5Y Neuroblastoma Cells in Neurobiology HHS Public Access. Methods Mol Biol. 2013;1078:9–21.

207. Simpson PB, Bacha JI, Palfreyman EL, Woollacott a J, McKernan RM, Kerby J. Retinoic acid evoked-differentiation of neuroblastoma cells predominates over growth factor

stimulation: an automated image capture and quantitation approach to neuritogenesis. Anal Biochem . 2001 Nov 15;298(2):163–9.

208. Guzhova I, Hultquist A, Cetinkaya C, Nilsson K, Påhlman S, Larsson LG. Interferon-gamma cooperates with retinoic acid and phorbol ester to induce differentiation and growth inhibition of human neuroblastoma cells. Int J cancer . 2001 Oct 1;94(1):97–108.

209. Filograna R, Civiero L, Ferrari V, Codolo G, Greggio E, Bubacco L, et al. Analysis of the Catecholaminergic Phenotype in Human SH-SY5Y and BE(2)-M17 Neuroblastoma Cell Lines upon Differentiation. Castresana JS, editor. PLoS One . 2015 Aug 28;10(8):e0136769.

210. Di X, Yan J, Zhao Y, Zhang J, Shi Z, Chang Y, et al. L-theanine protects the APP (Swedish mutation) transgenic SH-SY5Y cell against glutamate-induced excitotoxicity via inhibition of the NMDA receptor pathway. Neuroscience . 2010 Jul 14;168(3):778–86.

211. Zhao Z, Lu R, Zhang B, Shen J, Yang L, Xiao S, et al. Differentiation of HT22 neurons induces expression of NMDA receptor that mediates homocysteine cytotoxicity. Neurol Res . 2012 Jan;34(1):38–43.

212. Fenwick N, Griffin G, Gauthier C. The welfare of animals used in science: how the "Three Rs" ethic guides improvements. Can Vet J = La Rev Vet Can . 2009 May;50(5):523–30.

213. Encinas M, Iglesias M, Liu Y, Wang H, Muhaisen A, Ceña V, et al. Sequential treatment of SH-SY5Y cells with retinoic acid and brain-derived neurotrophic factor gives rise to fully differentiated, neurotrophic factor-dependent, human neuron-like cells. J Neurochem . 2000 Sep;75(3):991–1003.

214. Constantinescu R, Constantinescu a T, Reichmann H, Janetzky B. Neuronal differentiation and long-term culture of the human neuroblastoma line SH-SY5Y. J Neural Transm Suppl . 2007 Jan;(72):17–28.

215. Agholme L, Lindström T, Kågedal K, Marcusson J, Hallbeck M. An in vitro model for neuroscience: differentiation of SH-SY5Y cells into cells with morphological and biochemical characteristics of mature neurons. J Alzheimers Dis . 2010 Jan;20(4):1069–82.

216. Constantinescu R, Constantinescu AT, Reichmann H, Janetzky B. Neuronal differentiation and long-term culture of the human neuroblastoma line SH-SY5Y. 2007;17–28.

217. Xicoy H, Wieringa B, Martens GJM. The SH-SY5Y cell line in Parkinson's disease research: a systematic review. Mol Neurodegener . 2017 Dec 24;12(1):10.

218. Påhlman S, Ruusala A-I, Abrahamsson L, Mattsson MEK, Esscher T. Retinoic acid-induced differentiation of cultured human neuroblastoma cells: a comparison with phorbolester-induced differentiation. Cell Differ . 1984 Jun;14(2):135–44.

219. Encinas M, Iglesias M, Liu Y, Wang H, Muhaisen a, Ceña V, et al. Sequential treatment of SH-SY5Y cells with retinoic acid and brain-derived neurotrophic factor gives rise to fully differentiated, neurotrophic factor-dependent, human neuron-like cells. J Neurochem . 2000 Sep;75(3):991–1003.

220. Xun Z, Lee D, Lim J, Canaria CA, Barnebey A, Yanonne SM, et al. Retinoic acid-induced differentiation increases the rate of oxygen consumption and enhances spare respiratory capacity of mitochondria in SH-SY5Y. Mech Aging Dev. 2012;133(4):176–85.

221. Jämsä A, Hasslund K, Cowburn RF, Bäckström A, Vasänge M. The retinoic acid and brain-derived neurotrophic factor differentiated SH-SY5Y cell line as a model for Alzheimer's

disease-like tau phosphorylation. Biochem Biophys Res Commun . 2004 Jul 2;319(3):993–1000.

222. Dwane S, Durack E, Kiely P a. Optimising parameters for the differentiation of SH-SY5Y cells to study cell adhesion and cell migration. BMC Res Notes . 2013 Jan;6(1):366.

223. Dwane S, Durack E, Kiely PA. Optimising parameters for the differentiation of SH-SY5Y cells to study cell adhesion and cell migration. BMC Res Notes . 2013 Sep 11;6:366.

224. Abe K. Therapeutic potential of neurotrophic factors and neural stem cells against ischemic brain injury. J Cereb Blood Flow Metab . 2000 Oct 1;20(10):1393–408.

225. Zhu X, Yao H, Peng F, Callen S, Buch S. PDGF-mediated protection of SH-SY5Y cells against Tat toxin involves regulation of extracellular glutamate and intracellular calcium. Toxicol Appl Pharmacol . 2009 Oct 15;240(2):286–91.

226. Nishida Y, Adati N, Ozawa R, Maeda A, Sakaki Y, Takeda T. Identification and classification of genes regulated by phosphatidylinositol 3-kinase- and TRKB-mediated signalling pathways during neuronal differentiation in two subtypes of the human neuroblastoma cell line SH-SY5Y. BMC Res Notes . 2008 Jan;1(1):95.

227. Salmon AB, Richardson A, Pérez VI. Update on the oxidative stress theory of aging: does oxidative stress play a role in aging or healthy aging? Free Radic Biol Med . 2010 Mar 1;48(5):642–55.

228. Dröge W. Oxidative stress and ageing: is ageing a cysteine deficiency syndrome? Philos Trans R Soc Lond B Biol Sci . 2005 Dec 29;360(1464):2355–72.

229. Lopes FM, Schröder R, Júnior MLC da F, Zanotto-Filho A, Müller CB, Pires AS, et al. Comparison between proliferative and neuron-like SH-SY5Y cells as an in vitro model for Parkinson disease studies. Brain Res . 2010 Jun;1337:85–94.

230. Fotakis G, Timbrell JA. In vitro cytotoxicity assays: Comparison of LDH, neutral red, MTT and protein assay in hepatoma cell lines following exposure to cadmium chloride. Toxicol Lett . 2006 Jan;160(2):171–7.

231. Joshi HC, Cleveland DW. Differential utilization of beta-tubulin isotypes in differentiating neurites. J Cell Biol . 1989;109(2).

232. Korecka JA, van Kesteren RE, Blaas E, Spitzer SO, Kamstra JH, Smit AB, et al. Phenotypic Characterization of Retinoic Acid Differentiated SH-SY5Y Cells by Transcriptional Profiling. Lim K-L, editor. PLoS One . 2013 May 28;8(5):e63862.

33. Daubner SC, Le T, Wang S. Tyrosine hydroxylase and regulation of dopamine synthesis. Arch Biochem Biophys . 2011 Apr 1;508(1):1–12.

234. Iyer R, Menon V, Buice M, Koch C, Mihalas S. The Influence of Synaptic Weight Distribution on Neuronal Population Dynamics. Sporns O, editor. PLoS Comput Biol . 2013 Oct 24;9(10):e1003248.

235. Raman IM, Gustafson AE, Padgett D. Ionic Currents and Spontaneous Firing in Neurons Isolated from the Cerebellar Nuclei.

236. Gella A, Bolea I. Oxidative Stress in Alzheimer's Disease : Pathogenesis , Biomarkers and Therapy. In: Alzheimer's Disease Pathogenesis-Core Concepts, Shifting Paradigms and Therapeutic Targets. 2002.

237. Morel Y, Barouki R. Repression of gene expression by oxidative stress. Biochem J. 1999;342:481–96.

238. Dias IHK, Mistry J, Fell S, Reis A, Spickett CM, Polidori MC, et al. Oxidized LDL lipids increase β-amyloid production by SH-SY5Y cells through glutathione depletion and lipid raft formation. Free Radic Biol Med . 2014 Oct;75:48–59.

239. Liochev SI. Reactive oxygen species and the free radical theory of aging. Free Radic Biol Med . 2013 Jul;60:1–4.

240. Murphy MP. How mitochondria produce reactive oxygen species. Biochem J . 2009 Jan 1;417(1):1–13.

241. Cheung Y-T, Lau WK-W, Yu M-S, Lai CS-W, Yeung S-C, So K-F, et al. Effects of all-trans-retinoic acid on human SH-SY5Y neuroblastoma as in vitro model in neurotoxicity research. Neurotoxicology . 2009 Jan;30(1):127–35.

242. Zhang L, Yu H, Zhao X, Lin X, Tan C, Cao G, et al. Neuroprotective effects of salidroside against beta-amyloid-induced oxidative stress in SH-SY5Y human neuroblastoma cells. Neurochem Int . 2010 Nov;57(5):547–55.

243. Prince JA, Oreland L. Staurosporine Differentiated Human SH-SY5Y Neuroblastoma Cultures Exhibit Transient Apoptosis and Trophic Factor Independence. Brain Res Bull . 1997 Jan;43(6):515–23.

244. Liberio MS, Sadowski MC, Soekmadji C, Davis RA, Nelson CC, Languino LR. Differential Effects of Tissue Culture Coating Substrates on Prostate Cancer Cell Adherence, Morphology and Behavior. PLoS One . 2014;9(11).

245. Jones OR, Scheuerlein A, Salguero-Gómez R, Camarda CG, Schaible R, Casper BB, et al. Diversity of ageing across the tree of life. Nature . 2014 Jan 9;505(7482):169–73.

246. Schneider L, Giordano S, Zelickson BR, S Johnson M, A Benavides G, Ouyang X, et al. Differentiation of SH-SY5Y cells to a neuronal phenotype changes cellular bioenergetics and the response to oxidative stress. Free Radic Biol Med . 2011 Dec 1;51(11):2007–17.

247. Afriyie-Gyawu E, Ifebi E, Ampofo-Yeboah A, Kyte B, Shrestha S, Zhang J. Serum folate levels and fatality among diabetic adults: A 15-y follow-up study of a national cohort. Nutrition . 2015 Dec 7

248. Seshadria S, Beiser A, Selhub J, Jaques P, Rosenberg I, D'Agostino R, et al. Plasma Homocysteine as a risk factor for dementia and Alzheimer's disease. N Engl J Med. 2002;346(7):476–83.

249. Jakubowski H, Zhang L, Bardeguez a., Aviv a. Homocysteine Thiolactone and Protein Homocysteinylation in Human Endothelial Cells : Implications for Atherosclerosis. Circ Res . 2000 Jul 7;87(1):45–51.

250. Morris M. Homocysteine and Alzheimer's disease. Lancet Neurol . 2003;2(July):425–8.

251. Roybal CN, Yang S, Sun C-W, Hurtado D, Vander Jagt DL, Townes TM, et al. Homocysteine increases the expression of vascular endothelial growth factor by a mechanism involving endoplasmic reticulum stress and transcription factor ATF4. J Biol Chem . 2004 Apr 9;279(15):14844–52.

252. Jakubowski H. Pathophysiological Consequences of Homocysteine Excess. J Nutr . 2006 Jun 1;136(6):1741S–1749.

253. Hrnčić D, Rašić-Marković A, Krstić D. The role of nitric oxide in homocysteine thiolactone-induced seizures in adult rats. Cell Mol. 2010;219–31.

254. Hrnčić D, Rašić-Marković a, Macut D, Šušić V, Djuric D, Stanojlović O. Homocysteine thiolactone-induced seizures in adult rats are aggravated by inhibition of inducible nitric oxide synthase. Hum Exp Toxicol . 2014 May;33(5):496–503.

255. Lominadze D, Tyagi N, Sen U, Ovechkin A, Tyagi SC. Homocysteine alters cerebral microvascular integrity and causes remodeling by antagonizing GABA-A receptor. Mol Cell Biochem . 2012 Dec;371(1–2):89–96.

256. Kulikov A V, Rzhaninova AA, Goldshtein D V, Boldyrev AA. Expression of NMDA receptors in multipotent stromal cells of human adipose tissue under conditions of retinoic acid-induced differentiation. Bull Exp Biol Med . 2007 Oct;144(4):626–9.

257. Treiman DM. GABAergic mechanisms in epilepsy. Epilepsia . 2001 Jan;42 Suppl 3:8–12.

258. Tyagi N, Gillespie W, Vacek JC, Sen U, Tyagi SC, Lominadze D. Activation of GABA-A receptor ameliorates homocysteine-induced MMP-9 activation by ERK pathway. J Cell Physiol . 2009 Jul;220(1):257–66.

259. Chang H-H, Lin DP-C, Chen Y-S, Liu H-J, Lin W, Tsao Z-J, et al. Intravitreal homocysteine-thiolactone injection leads to the degeneration of multiple retinal cells, including photoreceptors. Mol Vis . 2011 Jan;17(July):1946–56.

260. Jakubowski H. Homocysteine Thiolactone : Metabolic Origin and Protein Homocysteinylation in Humans. J Nutr. 2000;377–81.

261. Rao R V, Bredesen DE. Misfolded proteins, endoplasmic reticulum stress and neurodegeneration. Curr Opin Cell Biol . 2004 Dec;16(6):653–62.

262. Doronzo G, Russo I, Del Mese P, Viretto M, Mattiello L, Trovati M, et al. Role of NMDA receptor in homocysteine-induced activation of mitogen-activated protein kinase and phosphatidyl inositol 3-kinase pathways in cultured human vascular smooth muscle cells. Thromb Res . 2010 Feb 2;125(2):e23-32.

263. Zieminska E, Lazarewicz JW. Excitotoxic neuronal injury in chronic homocysteine neurotoxicity studied in vitro: the role of NMDA and group I metabotropic glutamate receptors. Acta Neurobiol Exp (Wars) . 2006 Jan;66(4):301–9.

264. Robert K, Pagès C, Ledru a, Delabar J, Caboche J, Janel N. Regulation of extracellular signal-regulated kinase by homocysteine in hippocampus. Neuroscience . 2005 Jan;133(4):925–35.

265. Rašić-Marković A, Hrnčić D, Djurić D, Macut D, Lončar-Stevanović H, Stanojlović O. The effect of N-methyl-D-aspartate receptor antagonists on D,L-homocysteine thiolactone induced seizures in adult rats. Acta Physiol Hung . 2011 Mar;98(1):17–26.

266. Henneberger C, Papouin T, Oliet SHR, Rusakov DA. Long-term potentiation depends on release of d-serine from astrocytes. Nature . 2010 Jan 14;463(7278):232–6.

267. Doronzo G, Russo I, Del Mese P, Viretto M, Mattiello L, Trovati M, et al. Role of NMDA receptor in homocysteine-induced activation of mitogen-activated protein kinase and phosphatidyl inositol 3-kinase pathways in cultured human vascular smooth muscle cells. Thromb Res . 2010 Feb;125(2):e23-32.

268. Jara-Prado A, Ortega-Vazquez A, Martinez-Ruano L, Rios C, Santamaria A. Homocysteine-induced brain lipid peroxidation: effects of NMDA receptor blockade, antioxidant treatment, and nitric oxide synthase inhibition. Neurotox Res . 2003 Jan;5(4):237–43.

269. Obeid R, Herrmann W. Mechanisms of homocysteine neurotoxicity in neurodegenerative diseases with special reference to dementia. 2006;

270. Di X, Yan J, Zhao Y, Zhang J, Shi Z, Chang Y, et al. L-theanine protects the APP (Swedish mutation) transgenic SH-SY5Y cell against glutamate-induced excitotoxicity via inhibition of the NMDA receptor pathway. Neuroscience . 2010 Jul 14;168(3):778–86.

271. Srejovic I, Jakovljevic V, Zivkovic V, Barudzic N, Radovanovic A, Stanojlovic O, et al. The effects of the modulation of NMDA receptors by homocysteine thiolactone and dizocilpine on cardiodynamics and oxidative stress in isolated rat heart. Mol Cell Biochem . 2015 Mar 3;401(1–2):97–105.

272. Kann O, Kovács R. Mitochondria and neuronal activity. Am J Physiol Cell Physiol . 2007 Feb 1;292(2):C641-57.

273. Zorov DB, Juhaszova M, Sollott SJ. Mitochondrial reactive oxygen species (ROS) and ROS-induced ROS release. Physiol Rev . 2014 Jul;94(3):909–50.

274. Feng Y, Wang X. Antioxidant therapies for Alzheimer's disease. Oxid Med Cell Longev . 2012 Jan;2012:472932.

275. Bonda DJ, Wang X, Perry G, Nunomura A, Tabaton M, Zhu X, et al. Oxidative stress in Alzheimer disease: a possibility for prevention. Neuropharmacology . 2010;59(4–5):290–4.

276. Westermann B. Mitochondrial fusion and fission in cell life and death. Nat Rev Mol Cell Biol . 2010 Dec;11(12):872–84.

277. Martin LJ. Biology of Mitochondria in Neurodegenerative Diseases. Prog Mol Biol Transl Sci. 2012;107:1–57.

278. Pan L-L, Wang J, Jia Y-L, Zheng H-M, Wang Y, Zhu Y-Z. Asymmetric synthesis and evaluation of danshensu-cysteine conjugates as novel potential anti-apoptotic drug candidates. Int J Mol Sci . 2014 Jan;16(1):628–44.

279. Lacza Z, Pankotai E, Busija DW. Mitochondrial nitric oxide synthase: current concepts and controversies. Front Biosci (Landmark Ed . 2009 Jan 1;14:4436–43.

280. Garthwaite J, Garthwaite G, Palmer RM, Moncada S. NMDA receptor activation induces nitric oxide synthesis from arginine in rat brain slices. Eur J Pharmacol . 1989 Oct 17;172(4–5):413–6.

281. Horn TFW, Wolf G, Duffy S, Weiss S, Keilhoff G, MacVicar BA. Nitric oxide promotes intracellular calcium release from mitochondria in striatal neurons. FASEB J . 2002 Oct 1;16(12):1611–22.

282. Landmesser U, Merten R, Spiekermann S, Büttner K, Drexler H, Hornig B, et al. Vascular extracellular superoxide dismutase activity in patients with coronary artery disease: relation to endothelium-dependent vasodilation. Circulation . 2000 May 16;101(19):2264–70.

283. Kingwell BA. Nitric oxide-mediated metabolic regulation during exercise: effects of training in health and cardiovascular disease. FASEB J . 2000 Sep 1;14(12):1685–96.

284. Kuhlencordt PJ, Gyurko R, Han F, Scherrer-Crosbie M, Aretz TH, Hajjar R, et al. Accelerated atherosclerosis, aortic aneurysm formation, and ischemic heart disease in apolipoprotein E/endothelial nitric oxide synthase double-knockout mice. Circulation . 2001 Jul 24;104(4):448–54.

285. Williams HM, Lippok H, Doherty GH. Nitric oxide and peroxynitrite signalling triggers homocysteine-mediated apoptosis in trigeminal sensory neurons in vitro. Neurosci Res . 2008 Apr;60(4):380–8.

286. Hrnčić D, Rašić-Marković A, Macut D, Šušić V, Djuric D, Stanojlović O. Homocysteine thiolactone-induced seizures in adult rats are aggravated by inhibition of inducible nitric oxide synthase. Hum Exp Toxicol . 2014 May 11;33(5):496–503.

287. Kuroda K, Suzumura K, Shirakawa T, Hiraishi T, Nakahara Y, Fushiki H, et al. Investigation of Mechanisms for MK-801-Induced Neurotoxicity Utilizing Metabolomic Approach. Toxicol Sci . 2015 Aug;146(2):344–53.

288. Suski JM, Lebiedzinska M, Bonora M, Pinton P, Duszynski J, Wieckowski MR. Relation Between Mitochondrial Membrane Potential and ROS Formation. In: Methods in molecular biology (Clifton, NJ) . 2012. p. 183–205.

289. Liang HL, Sedlic F, Bosnjak Z, Nilakantan V. SOD1 and MitoTEMPO partially prevent mitochondrial permeability transition pore opening, necrosis, and mitochondrial apoptosis after ATP depletion recovery. Free Radic Biol Med . 2010 Nov 30;49(10):1550–60.

290. Najib S, Sánchez-Margalet V. Homocysteine thiolactone inhibits insulin signaling, and glutathione has a protective effect. J Mol Endocrinol . 2001 Aug;27(1):85–91.

291. Welch GN, Upchurch GR, Farivar RS, Pigazzi A, Vu K, Brecher P, et al. Homocysteine-induced nitric oxide production in vascular smooth-muscle cells by NF-kappa B-dependent transcriptional activation of Nos2. Proc Assoc Am Physicians;110(1):22–31.

292. Jiang Y, Zhang J, Xiong J, Cao J, Li G, Wang S. Ligands of peroxisome proliferator-activated receptor inhibit homocysteine-induced DNA methylation of inducible nitric oxide synthase gene. Acta Biochim Biophys Sin (Shanghai) . 2007 May;39(5):366–76.

293. Hamon M, Vallet B, Bauters C, Wernert N, McFadden EP, Lablanche JM, et al. Long-term oral administration of L-arginine reduces intimal thickening and enhances neoendothelium-dependent acetylcholine-induced relaxation after arterial injury. Circulation . 1994 Sep 9;90(3):1357–62.

294. Martinez-Vicente M. Neuronal Mitophagy in Neurodegenerative Diseases. Front Mol Neurosci . 2017 Mar 8;10:64.

295. Han J-Y, Kang M-J, Kim K-H, Han P-L, Kim H-S, Ha J-Y, et al. Nitric Oxide Induction of Parkin Translocation in PTEN-induced Putative Kinase 1 (PINK1) Deficiency. J Biol Chem . 2015 Apr 17;290(16):10325–35.

296. Kovac S, Domijan A-M, Walker MC, Abramov AY. Seizure activity results in calcium- and mitochondria-independent ROS production via NADPH and xanthine oxidase activation. Cell Death Dis . 2014 Oct 2;5(10):e1442–e1442.

297. Yi F, Li P-L. Mechanisms of homocysteine-induced glomerular injury and sclerosis. Am J Nephrol . 2008 Jan;28(2):254–64.

298. Shen L, Ji H-F. Associations between Homocysteine, Folic Acid, Vitamin B12 and Alzheimer's Disease: Insights from Meta-Analyses. J Alzheimer's Dis . 2015 Jun 25;46(3):777–90.

299. Quadri P, Fragiacomo C, Pezzati R, Zanda E, Forloni G, Tettamanti M, et al. Homocysteine, folate, and vitamin B-12 in mild cognitive impairment, Alzheimer disease, and vascular dementia. Am J Clin Nutr . 2004 Jul 1;80(1):114–22.

300. Foister NSL, Oldreive CE, Mackie JB, Doherty GH. Embryonic cerebellar granule cells are resistant to necrosis induced by homocysteine. Brain Res Dev Brain Res . 2005 Nov 7;160(1):85–9.

301. Bern M, Saladino J, Sharp JS. Conversion of methionine into homocysteic acid in heavily oxidized proteomics samples. Rapid Commun Mass Spectrom . 2010 Mar 30;24(6):768–72.

302. Soto C. Plaque busters: strategies to inhibit amyloid formation in Alzheimer's disease. Mol Med Today . 1999;5(August).

303. Dauer W, Przedborski S. Parkinson ' s Disease : Mechanisms and Models. Neuron. 2003;39:889–909.

304. Meng S, Ciment S, Jan M, Tran T, Pham H, Cueto R, et al. Homocysteine induces inflammatory transcriptional signalling in monocytes. Front Biosci. 2013;18:685–95.

305. Meredith JE, Sankaranarayanan S, Guss V, Lanzetti AJ, Berisha F, Neely RJ, et al. Characterization of novel CSF Tau and ptau biomarkers for Alzheimer's disease. PLoS One . 2013;8(10):e76523.

306. Maler J., Seifert W, Hüther G, Wiltfang J, Rüther E, Kornhuber J, et al. Homocysteine induces cell death of rat astrocytes in vitro. Neurosci Lett . 2003 Aug;347(2):85–8.

307. Kruman II, Culmsee C, Chan SL, Kruman Y, Guo Z, Penix L, et al. Homocysteine elicits a DNA damage response in neurons that promotes apoptosis and hypersensitivity to excitotoxicity. J Neurosci . 2000 Sep 15;20(18):6920–6.